東海大学大学院平成 26 年度博士論文

インホイルモータを用いた小型電気自動車のスキッド制御

SKID CONTROL OF SMALL ELECTRIC VEHICLE WITH IN-WHEEL MOTORS

指導　山本　佳男　教授

東海大学大学院総合理工学研究科

総合理工学専攻

MOHAMAD HEERWAN BIN PEEIE

Contents

Nomenclatures

B_F	braking force (N)
b_T	width of the interacted tire surface (m)
C_R	regenerative brake coefficient
g	gravitational acceleration (m/s^2)
h	center gravity of the vehicle (m)
I	inertia moment of the vehicle (kgm^2)
I_ω	inertia moment of the tire (kgm^2)
K_x	the rigidness of the tire in longitudinal axis (N/m^3)
K_y	the rigidness of the tire in lateral axis (N/m^3)
L	length of the vehicle (m)
l_f	the length from the center of the vehicle to the center of the front tire (m)
l_r	the length from the center of the vehicle to the center of the rear tire (m)
l_T	length of the interacted tire surface (m)
m	vehicle mass (kg)
P	pressure (Pa)
R	radius of the brake shoe
r	wheel radius (m)
T	torque (Nm)
t	time (s)
u	vehicle velocity in the longitudinal direction (m/s)

v	vehicle velocity in the lateral direction (m/s)
W_z	wheel load (N)
X	the longitudinal force acting on the tire (N)
Y	the lateral force acting on the tire (N)
β	side slip angle (rad)
β_T	side slip angle of the tire (rad)
θ	steering angle (rad)
γ	yaw angular velocity of the vehicle (rad/s)
μ	friction coefficient
ρ	slip ratio
ω	tire angular velocity (rad/s)

Subscripts:

f	front
r	rear
fr	front right
fl	front left
rr	rear right
rl	rear left

Chapter 1

INTRODUCTION

1.1 Background

In recent years, due to the environmental problems and concern over increasing fuel prices have given interest to the automotive manufacturers to develop the electric vehicles (EVs), fuel cell electric vehicles (FCEVs) and hybrid electric vehicles (HEVs) [1-1], [1-2]. These vehicles use an electric motor for propulsion, and batteries as electrical storage devices. Compared with the internal combustion engine vehicles (ICEVs), electric motor has many advantages such as a fast torque response in milliseconds, easiness in obtaining accurate torque feedback, capable of generating both traction and braking forces and small size but powerful output [1-3] ~ [1-6].

Although EVs, FCEVs and HEVs offer the most promising solutions to reduce the emission, the cost of these vehicles always becomes the biggest hurdle for the people owning it [1-7]. To reduce the EVs cost, some of the car makers have introduced the compact EVs. For example, Toyota Auto Body Company has introduced "The Super-Compact Electric Vehicle (also known as Toyota COMS)" while Nissan has introduced "Choi Mobi Yokohama". Figure 1-1 shows the Toyota COMS while Figure 1-2 shows the Nissan Choi Mobi Yokohama. The capacity of the Toyota COMS is for one passenger while the capacity of the Nissan Choi Mobi Yokohama is for two passengers.

For urban areas and narrow space, due to the size and the propulsion system of the Toyota COMS and Nissan Choi Mobi Yokohama, these vehicles assume to be the best green technology vehicles. However, the Nissan Choi Mobi Yokohama is limited to Yokohama City and is not for sale to the public. On the other hand, the Toyota COMS can be used for many purposes and everyone in everywhere can buy and use it. Generally, the model of the Toyota COMS is divided into two categories, that is, for a personal and business. Figure 1-3 shows the Toyota COMS that has been used by Seven Eleven Corporation in Japan for deliveries. By using the Toyota COMS, it is easy to deliver the stuff and the environmental problem also can be decreased.

The propulsion system of the Toyota COMS is in-wheel motor. The in-wheel motor is an electric motor that is incorporated into the hub of a wheel and drives it directly. Figure 1-4 illustrates an in-wheel motor that was attached at the hub of a wheel. By applying the traction force directly to the wheel and simplifying the drivetrain, the energy efficiency of EVs is enhanced [1-8]. More importantly, the in-wheel motor technology provides the opportunity for superior motion control of the vehicle due to the fact that the electric motor can be

controlled precisely and significantly faster [1-9], [1-10]. Based on the specifications and the propulsion system of the Toyota COMS, it can be said that Toyota COMS is the best compact EVs to improve the environmental problem and also to facilitate our daily life.

Figure 1-1 Toyota COMS for a personal usage

Figure 1-2 Nissan Choi Mobi Yokohama

Figure 1-3 Toyota COMS for deliveries

Figure 1-4 In-wheel motor

1.2 Problem Statement

In general, the size of the tire for the small EVs is smaller than conventional vehicles. Figure 1-4 (a) shows the front view of the tire, while Figure 1-4 (b) shows the side view of the tire. As shown in Figure 1-4 (b), an in-wheel motor was attached at the tire and this tire is called the driving tire. Due to the space limitation at the driving tire, some of the small EVs employ a mechanical braking system rather than hydraulic braking system. Even though the mechanical braking system is compact, the rigidness and the response performance of the mechanical braking system is lower than a hydraulic braking system [1-11] ~ [1-13]. On the other hand, for a non-driving tire, there is no problem to install the hydraulic braking system. For this reason, some of the small two in-wheel EVs employ the hydraulic-mechanical hybrid brake system as a braking system. In this braking system, the hydraulic braking system is installed on the non-driving tire, while the mechanical braking system is installed on the driving tire.

The other braking system of the small EVs is the regenerative brake system. Regenerative brake is a braking method that utilizes the mechanical energy from the motor by converting kinetic energy into electrical energy, which is fed back into the battery source. In regenerative braking mode, when the driver applies force to the brake pedal, the electric motor works in reverse direction thus slowing the car. While running backwards, the motor acts as the generator and recharge the batteries [1-14]. Figure 1-5 shows the regenerative braking action during braking, while Figure 1-6 shows the car in the normal running condition, whereas the motor turning forward and taken energy from the battery. Based on the mechanism of the regenerative braking system, the regenerative braking force is proportional to the wheel speed. Generally, during braking on dry asphalt and in the normal condition, the braking torque required is much larger than the torque that an electric motor can produce. Therefore, the regenerative brake system must work together with the mechanical brake system [1-15].

During braking on the road with a low friction coefficient or in an emergency braking situation, hydraulic-mechanical hybrid brake system and regenerative brake system cannot perform equally well on dry asphalt. The hydraulic braking force and the regenerative braking force that was applied to the front and rear wheel to stop their rotation often exceeds the force that is making them rotate. This causes the tire to stop rotating gradually and begin skidding. Once in a skid, the tires no longer have the ability to provide directional control to the vehicle, no matter how much steering input is attempted by the driver [1-16].

An anti-lock braking system (ABS) which is a basic skid control method is very crucial on the icy road and under heavy braking because it can prevent tire from locking and vehicle from skidding [1-17]. Although ABS is very crucial, the space limitation on the driving tire always becomes the challenges for the researcher to install the hydraulic unit of ABS toward driving tire. On the other hand, the regenerative braking force produced from the in-wheel motor needs to be controlled to obtain the optimum braking force and prevent tire from locking [1-15]. Based on the braking system and safety system of the small EVs with hydraulic-mechanical hybrid brake system, it can be considered that it is not safe enough.

(a) Front view

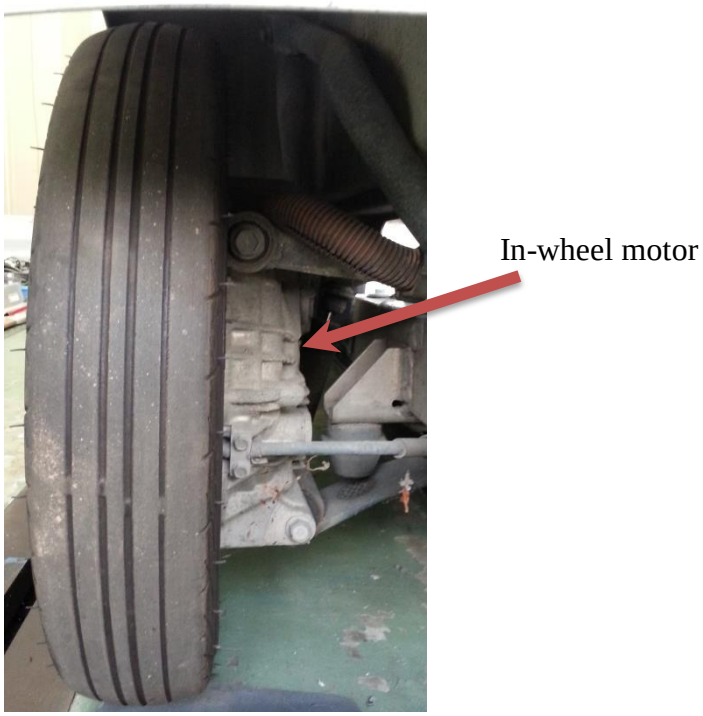

(b) Side view

Figure 1-5 Front view and side view of the tire

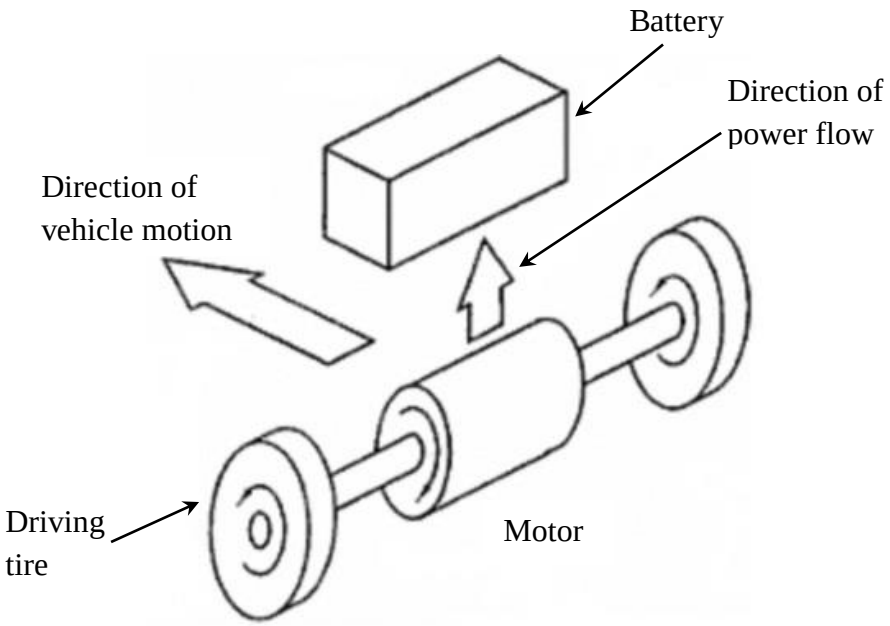

(a) Regenerative action during braking

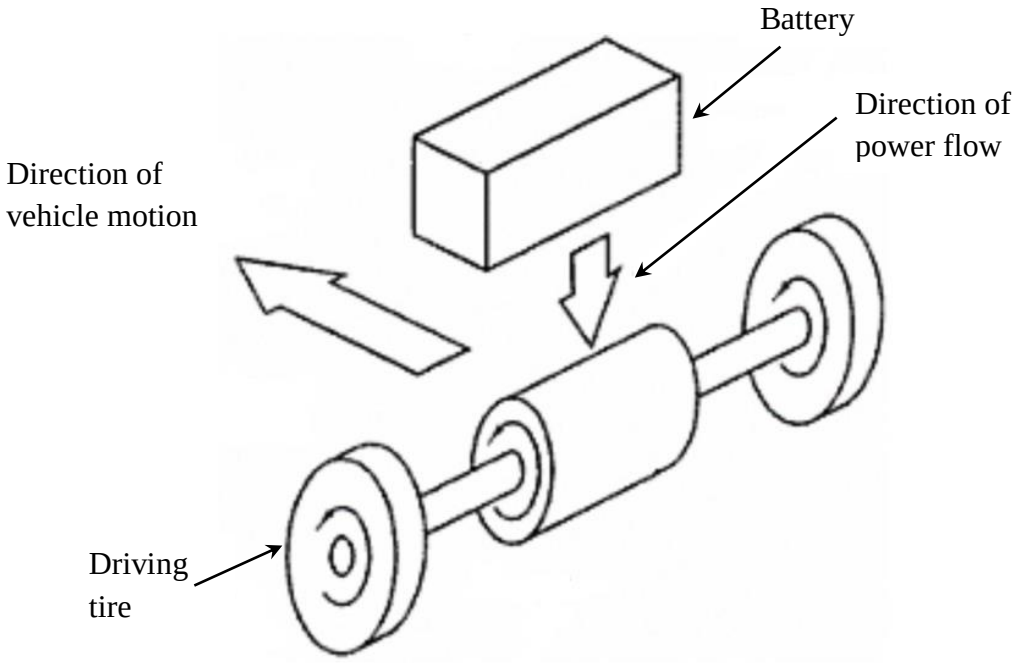

(b) Normal forward during driving

Figure 1-6 Mechanism of regenerative brake

1.3 Objective of Research

The objective of this research is to improve the safety and stability of the small EVs with hydraulic-mechanical hybrid brake system. A novel method of the ABS and regenerative brake timing control was proposed to prevent the tire lock and vehicle from skidding during braking on an icy road. A hydraulic unit of ABS is installed at the front tire to prevent the front tire from lock-up, while an in-wheel motor at the rear tire is operated as actuator of ABS to control the regenerative braking torque. During braking on an icy road, the combination of ABS and regenerative brake control can prevent tire lock and a vehicle from skidding. Finally, the safety and stability of the vehicle can be improved.

1.4 Past Research

Over the past year, there are many studies on improving EVs performance. These studies can be divided into two categories; study on battery technologies and study on EVs motion control. The objective of the studies of the battery technologies is to ensure EVs could travel the farthest with a single charge [1-18] ~ [1-28]. The main issue with electrical energy storage systems is their energy density. Energy density is defined as the amount of energy stored in a given system per unit mass [1-18]. The conventional lead acid battery has an energy density about 35 Wh/kg compared to a useful energy density of more than 2000 Wh/kg for gasoline [1-19]. For this reason, the electric drive range for EVs has always been limited by the size and mass of the energy storage system.

The main objective of the study of EVs motion control is to improve EVs stability and safety [1-29] ~ [1-67]. Based on the characteristics of the motor that has fast and accurate torque response, some researchers have controlled the tire force at each wheel to improve the stability of the EVs [1-29] ~ [1-35]. On the other hand, several studies on ABS to improve the safety of the EVs also have been done [1-36] ~ [1-56]. However, the studies of ABS for EVs are only focused for the conventional EVs, and not for the small EVs with in-wheel motor. The regenerative brake control also has been studied by several researchers to improve the safety and stability of the EVs [1-57] ~ [1-67]. They have used regenerative brake to improve the braking performance and to control the yaw motion of the EVs.

Based on the disadvantages of the braking system of the small EVs, this study is focused on to improve the braking performance of the small EVs. This study is related to the vehicle motion control. The most important part of this study is to apply the ABS at the small EVs and to control the regenerative braking torque. In the first step of this study, the characteristics and control strategy of the ABS and regenerative braking system have been reviewed.

1.4.1 Anti-lock brake system (ABS) review

In previous study, different control methods have been used to improve the performance of ABS. The model-based approach is applied to search for the optimum brake torque via sliding modes [1-68]. This approach requires the tire force, hence, a sliding observer is used to estimate it. Sliding mode control has been tested in a hardware-in-the-loop (HIL) simulator and also in a vehicle [1-69]. A derivative part depending on the rotational acceleration is introduced in order to reduce the chattering of the sliding controller. Choi and Cho (1998), have proposed the sliding controller to show the advantage of a PWM controller actuator [1-70].

Another theoretical approach is adaptive Lyapunov-based nonlinear wheel slip controller [1-71]. This controller has been extended by introducing speed dependence of the Lyapunov function and also including a model of the hydraulic circuit dynamics [1-72]. Another Lyapunov based nonlinear adaptive tire slip controller is using Sontag's formula [1-73]. No actuator dynamics have been included in this analysis.

Liu and Sun (1995) have proposed feedback linearization to design a slip controller. In their model, gain scheduling is used to handle the variation of the tire friction curve with respect to speed [1-74]. Tsiotras and Canudas de Wit (2000) have proposed a maximum tire and road friction approach using optimal control theory. The model is based on a static friction model [1-75].

A conventional ABS controller as a piecewise linear controller including analysis of the switching cycles has been proposed by Wellstead and Pettit (1997) [1-76]. A simple PD wheel slip controller by the Ziegler-Nichols rule has been designed by Taheri and Law (1991) [1-77]. The model focusing on the desired slip value and the desired slip value is estimated by evaluating the switching of a conventional ABS.

1.4.2 Regenerative brake control review

Regenerative braking is one of the most important and most widely used technologies in EVs [1-53]. The most common regenerative braking system in EVs today uses an electric motor, capable of providing both propulsion and braking forces [1-54]. This technology can afford fuel savings by converting the kinetic energy of a moving vehicle into electric energy during deceleration [1-55], [1-61]. On the other hand, due to the fast torque response of the electric motor, it can benefit the wheel slip control in an emergency braking maneuver or during braking on an icy road [1-62]. Based on the characteristics of the electric motor, the study of regenerative braking can be divided into two categories, which is to improve the energy recapture and to control the regenerative braking torque.

Cikanek and Bailey (2002), have proposed a detailed description of the regenerative braking algorithm. The proposed model was presented along with simulation results from a dynamic model of the parallel hybrid EV (HEV) [1-78]. A vehicle model, a slip ratio model and a vehicle speed observer were developed to control the anti-lock performance of an HEV during braking. Through an iterative learning process, the motor torque was optimized to keep the tire slip ratio corresponding to the peak traction coefficient during braking, and simulations were performed on a compact size vehicle [1-79]. Paterson and Ramsay (1993) have designed a fuzzy controller algorithm to accurately switch off the regenerative braking and at the same time to switch on the physical brakes [1-80]. Gao et. al. (2001), have developed the simulation to maximize the regenerative braking force [1-81].

Furthermore, Yeo and Kim (2002), have developed the experiments to improve energy recovering efficiency [1-82]. The method of energy regenerative braking was analyzed for a brushless direct current (DC) motor, and the drive and control circuit were realized by digital signal processing (DSP) and EXB841 [1-83]. In [1-84] , they have presented the effect of rotating inertias on the power and energy for each component during regenerative braking of a vehicle. The results showed that the rotating inertias can contribute a significant fraction (8 – 13%) of the energy recovered during deceleration because of the relatively lower losses of rotating components compared with vehicle inertia. It can be concluded that the energy recovering efficiency can be improved by a good control method.

1.5 Organization of the Thesis

This thesis is organized into 5 chapters. A brief outline of the thesis is as follows:

Chapter 1 In this chapter, brief explanations on small EVs and the propulsion system of the small EVs are presented. The background of the study, problem statement, objectives of the study, past research and organization of the thesis are described.

Chapter 2 In this chapter, the analysis vehicle model is introduced. The main specifications and the braking system of the analysis vehicle are described. Then, a simulation model of the small EV has been developed using Matlab/Simulink. The hydraulic-mechanical hybrid brake system of the small EVs in the simulation model is constructed based on the analysis vehicle model. The focus will be on the braking performance of the analysis vehicle model without any control. The experiment and the numerical analysis have been done to examine the braking performance of the hydraulic-mechanical hybrid brake system. The method and the experiment apparatus involved are also described.

Chapter 3 In this chapter, a simulation model of hydraulic-mechanical hybrid brake system with ABS is constructed. 3 channel type of ABS has been used in the simulation model. Each channel contains IN valve and OUT valve. For the front tire, the IN valve and OUT valve are installed at each tire, and it is located between the master cylinder and the front wheel cylinder. However, for the rear tire, due to the space limitation at the rear tire, only one set of IN valve and OUT valve is installed, and it is located between the master cylinder and rear power cylinder. The combination of the hydraulic-mechanical hybrid brake system with ABS has been developed in Matlab/Simulink. The assumptions used during the simulations are also described.

Chapter 4 In this chapter, the regenerative brake control is introduced. The experiment and simulation have been done to measure the optimum value of the regenerative brake coefficient. The method and the experiment apparatus involved are also described. Then, the simulation model of the hydraulic-mechanical hybrid brake system with ABS and regenerative brake control is developed in Matlab/Simulink. The regenerative brake control operates similarly to ABS. The assumptions used during the simulation are also described.

Chapter 5 In this chapter, the overall conclusion of the study that has been done are discussed. The recommendations for future work for this study also presented.

Chapter 2

BRAKING PERFORMANCE OF THE ANALYSIS VEHICLE MODEL

2.1 Introduction

In this part, the experiments have been done to examine the braking performance of the analysis vehicle model. First, the theory of the vehicle dynamics is described. The theory will be focused on the vehicle motion during braking. Then, the analysis vehicle model, Toyota COMS, model AK 10E-PC is introduced. The main specifications and the braking system of the analysis vehicle model are examined. Next, the experiment of the vehicle braking performance is developed. The experimental apparatus and the experimental methods are described. In the last part of this chapter, the experimental results are presented and discussed.

2.2 Theory

2.2.1 Vehicle motion

In this study, the four wheel vehicle dynamics model has been used to obtain the fundamental knowledge of the vehicle dynamic motion. Figure 2-1 shows the force vector of the four wheel vehicle model [2-1]. This vehicle model has two wheels at the front and two wheels at the rear. All of the wheels are fitted to the rigid body of the vehicle. The two wheels at the front can be steered by the steering, but the other two wheels at the rear cannot be steered. In this model, the coordinate frame is fixed to the vehicle, which has the *x*-axis in the longitudinal direction, the *y*-axis in the lateral direction and the *z*-axis in the vertical direction, with the origin at the vehicle center of gravity (CG). With this coordinate system, during traction or braking, the vehicle will have longitudinal motion in *x* direction, lateral motion in *y* direction and yaw motion around *z* axis. Based on Figure 2-1, the equation of longitudinal motion, lateral motion and yaw motion are as below:

$$m\left(\frac{du}{dt} - v\Upsilon\right) = (-{}^{x}F_{fr} - {}^{x}F_{fl})\cos\theta + (-{}^{y}F_{fr} - {}^{y}F_{fl})\sin\theta - {}^{x}F_{rr} - {}^{x}F_{rl} \quad (2\text{-}1)$$

$$m\left(\frac{dv}{dt} + u\Upsilon\right) = ({}^{y}F_{fr} + {}^{y}F_{fl})\cos\theta + (-{}^{x}F_{fr} - {}^{x}F_{fl})\sin\theta + {}^{y}F_{rr} + {}^{y}F_{rl} \quad (2\text{-}2)$$

$$I\frac{d\gamma}{dt} = l_f({}^{y}F_{fr}\cos\theta + {}^{y}F_{fl}\cos\theta - {}^{x}F_{fr}\sin\theta - {}^{x}F_{fl}\sin\theta) - l_r({}^{y}F_{rr} + {}^{y}F_{rl}) + \frac{df}{2}(-{}^{x}F_{fr}\cos\theta + {}^{x}F_{fl}\cos\theta - {}^{y}F_{fr}\sin\theta + {}^{y}F_{fl}\sin\theta) + \frac{dr}{2}(-{}^{x}F_{rr} + {}^{x}F_{rl}) \quad (2\text{-}3)$$

where *u* and *v* is the velocity of the vehicle in longitudinal and lateral axis respectively, Υ is the vehicle yaw rotational speed, ${}^{x}F_{fr}$, ${}^{x}F_{fl}$, ${}^{x}F_{rr}$, ${}^{x}F_{rl}$ are the longitudinal force, while ${}^{y}F_{fr}$, ${}^{y}F_{fl}$, ${}^{y}F_{rr}$, ${}^{y}F_{rl}$ are the lateral force. Subscripts *fr*, *fl*, *rr* and *rl* shows front right, front left, rear right and rear left respectively. In this study, we used the brush tire model to understand theoretically the force generated by the tire. Figure 2-2 shows the brush tire model in longitudinal and lateral directions [2-2]. This tire model allows elastic deformation in both the longitudinal and lateral directions. The tread rubber is not a continuous circular body, but consists of a large number of independent springs around the tire circumference.

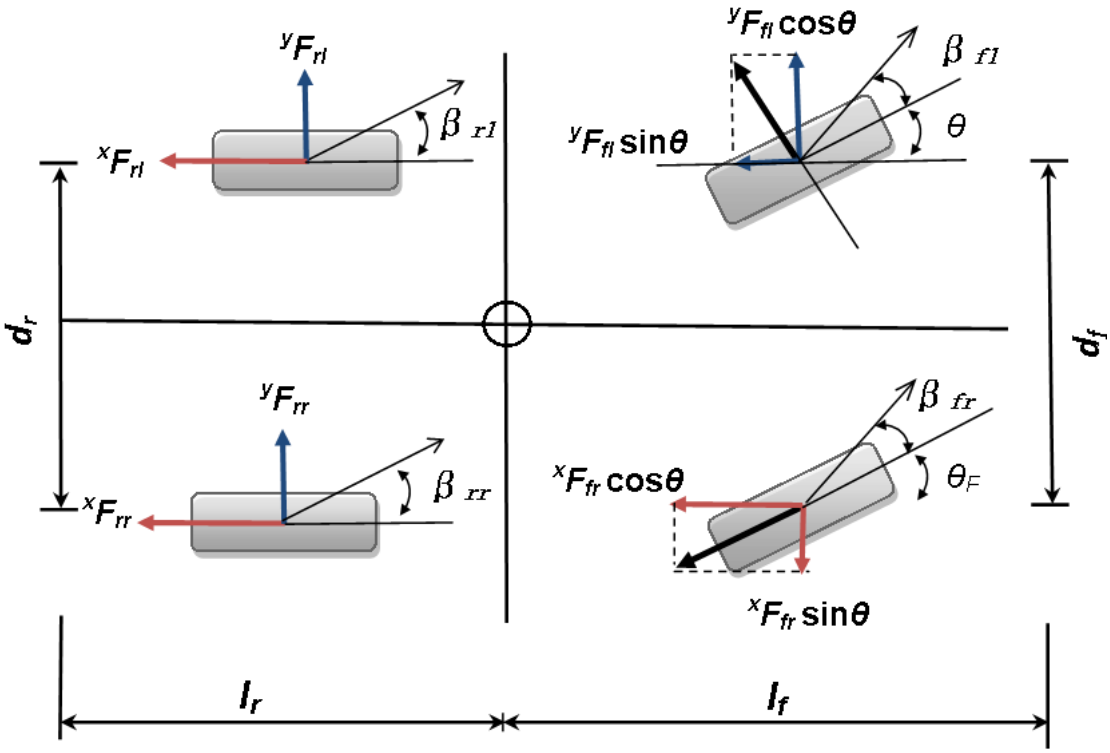

Figure 2-1 Force vectors of the four wheel vehicle model

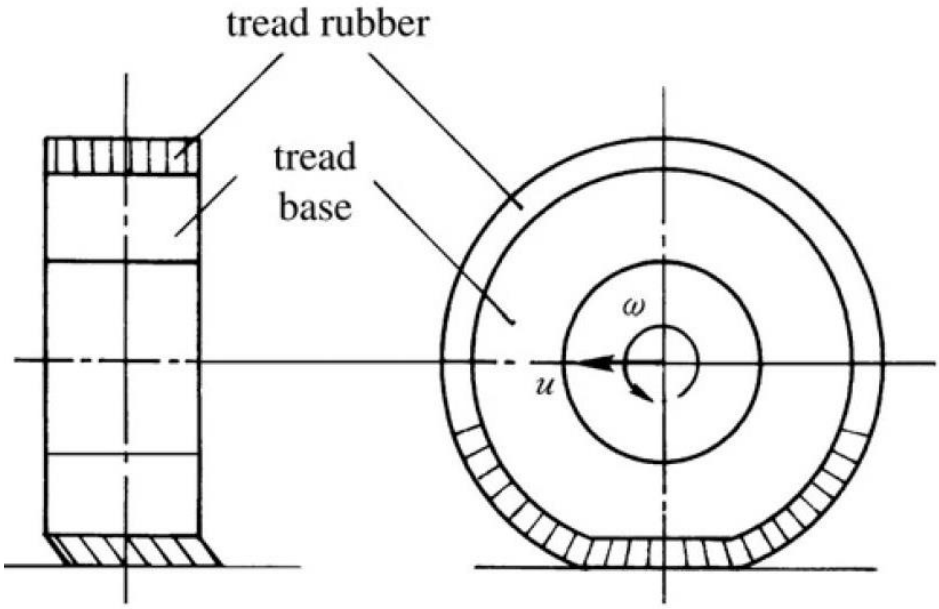

Figure 2-2 Brush tire model in longitudinal and lateral directions

2.2.2 Side slip angle

To study the lateral force acting on the tire, it is necessary to examine the side slip angle of the tire respectively. Figure 2-3 shows the tire forces in three directions, which are *x* direction, *y* direction and *z* direction. From this figure, the tire is rotating with an angular velocity, ω, while travelling in a direction that forms the side slip angle, β, to the rotation plane. The tire produce side slip angle, β, when the travelling direction of the tire is out of line with the rotational plane or the tire heading direction.

As shown in Figure 2-4, if the wheel has a side slip, a force that is perpendicular to its rotation plane is generated. This force could be regarded as a reaction force that prevents side slip when the wheel produces a side slip angle. Normally, this force is called the lateral force, while the component that is perpendicular to the wheel rotation plane, is called the cornering force. When the side slip angle is small, these two forces are treated as the same.

Figure 2-5 shows the velocity component in x and y directions for each tire. The heading direction of the rear wheel is same as the vehicle longitudinal direction. The rigid body vehicle has a velocity component of *u* in the longitudinal, *x* direction, and *v* in the lateral, *y* direction. The vehicle also has an angular velocity of γ around the center of gravity (CG). Consequently, each tire will has a translational or linear velocity component of the center of gravity, and an angular velocity component due to the rotation around the center of gravity. The heading direction of the front wheel has an angular displacement of δ with respect to the vehicle longitudinal direction. This is the actual steer angle of the front wheels. The heading direction of the rear wheels is the same as the vehicle longitudinal direction. Therefore, the side slip angle for each tire could be written as below:

$$\beta_{fr} = \beta + \frac{l_f \gamma}{u} - \delta \quad ; \quad \beta_{fl} = \beta + \frac{l_f \gamma}{u} - \delta$$

$$\beta_{rr} = \beta + \frac{l_r \gamma}{u} \quad ; \quad \beta_{rl} = \beta + \frac{l_r \gamma}{u} \tag{2-4}$$

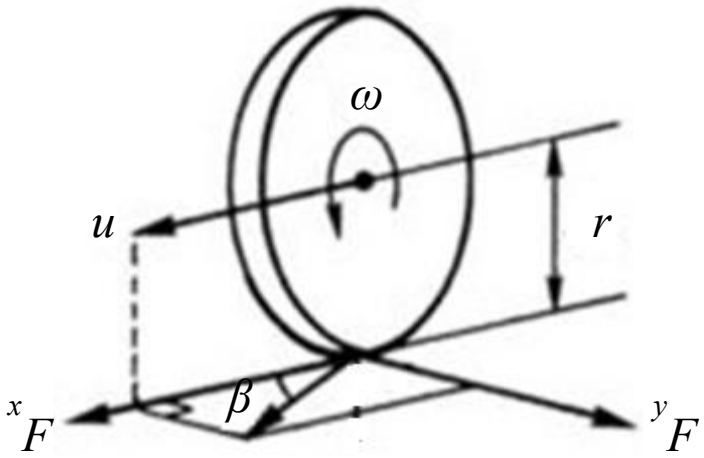

Figure 2-3 Tire forces in three directions

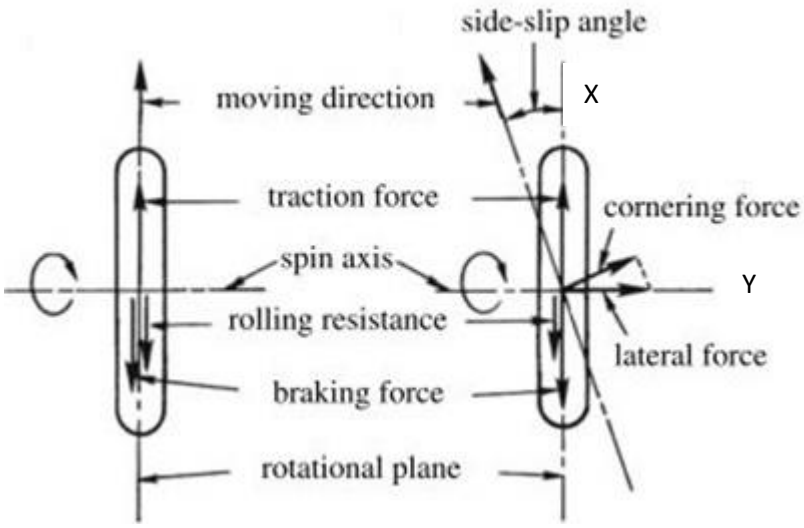

Figure 2-4 Vehicle tire motion

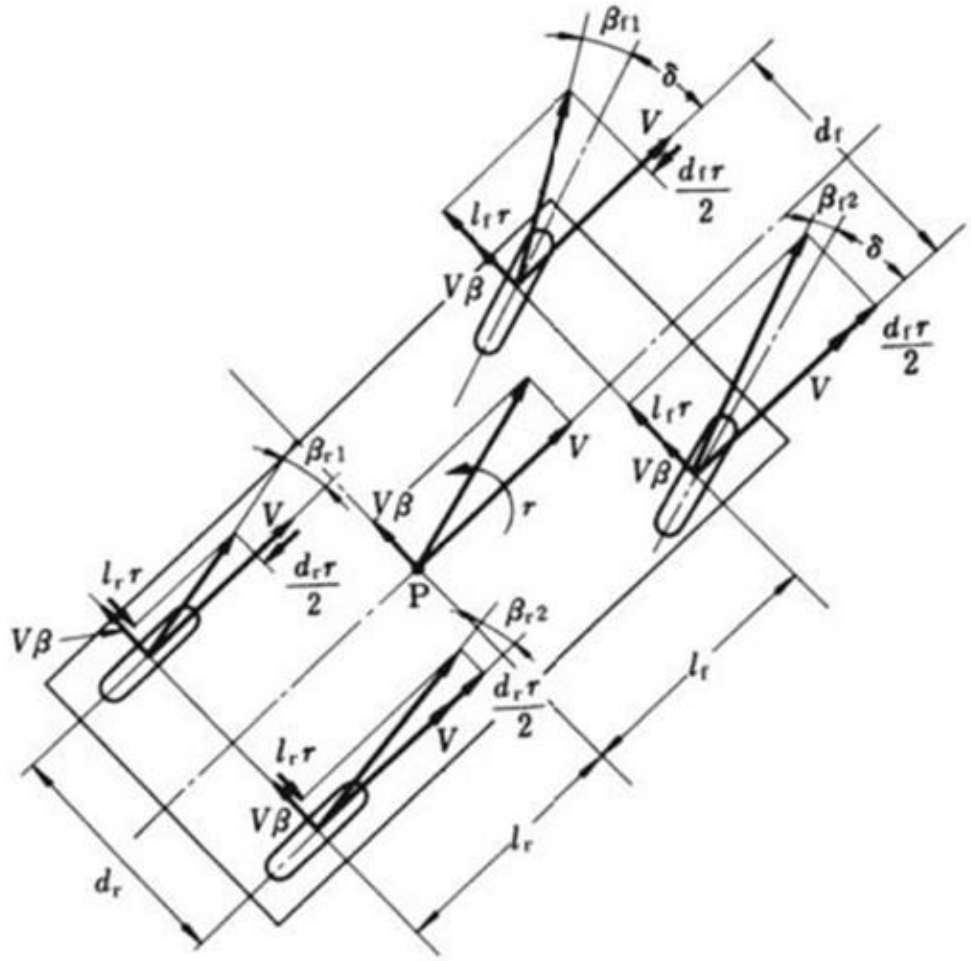

Figure 2-5 Side slip angle at each tire

2.2.3 Slip ratio

To study the longitudinal force acting on the tire, it is necessary to examine the slip ratio of the tire respectively. Slip ratio is defined as the difference between the vehicle actual longitudinal velocity and the rotational velocity of the tire, $r\omega$. The equations of slip ratio during braking and acceleration are as below [2-3]:

$$\rho = \frac{r\omega - u}{u} \quad \text{: during braking} \tag{2-5a}$$

$$\rho = \frac{r\omega - u}{rw} \quad \text{: during acceleration} \tag{2-5b}$$

A rough explanation of why the longitudinal tire force depends on the slip ratio can be seen from Figure 2-6. The lower portion of Figure 2-6 shows a schematic representation of deformation of the tread elements of the tire. As shown in Figure 2-6, the net velocity at the treads is $r\omega$-u. The tire on a vehicle deforms due to the normal load on it and makes contact with the road over the contact patch.

In case of acceleration, $r\omega > u$, the net velocity of the treads is in an opposite direction to the direction of the longitudinal velocity of the vehicle. Assume that the slip, $r\omega$-u is small. Then, there is a region of the contact patch where the tread elements do not slide with respect to the ground, called the static region. As the tire rotates and a tread element enters the contact patch, its tip which is in contact with the ground must have zero velocity. This is because there is no sliding in the static region of the contact patch. The top of the tread element moves with a velocity of $r\omega$-u. Hence, the tread element will bend forward as shown in Figure 2-6 and the bending will be in the direction of the longitudinal direction of motion of the vehicle. Thus, the net longitudinal force on the tires from the ground is in the forward direction.

In the case of braking, the longitudinal velocity is greater than the rotational velocity of tire, $u > r\omega$. In this case, the net velocity at the treads is in the forward direction and the bristles on the tire will bend backwards. Hence, the longitudinal force on the tire is in the opposite direction to the vehicle longitudinal direction.

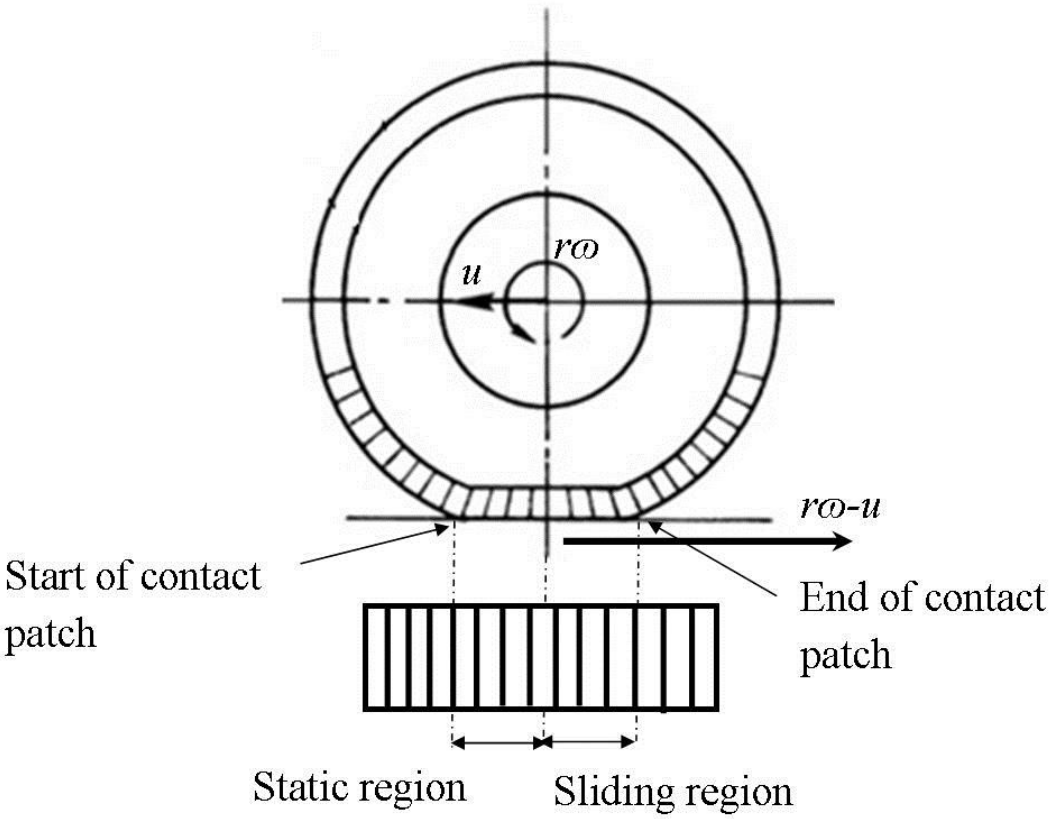

Figure 2-6 Longitudinal force on the tire

2.2.4 Wheel dynamics

In this study, the driving system of our analysis vehicle model is in-wheel motor. This motor was attached at the both rear tires. Then, the rear tire will be the driving tire, while the front tire will be non-driven tire. For the driving tire, the dynamic equation for the wheel rotational dynamics is shown in Eq. (2-6), while for the non-driven tire, the rotational dynamic equation is shown in Eq. (2-7).

$$I_{fr}\dot{\omega}_{fr} = -T_{Bfr} - r_{fr}\,{}^{x}F_{fr} \quad , \quad I_{fl}\dot{\omega}_{fl} = -T_{Bfl} - r_{fl}\,{}^{x}F_{fl} \tag{2-6}$$

$$I_{rr}\dot{\omega}_{rr} = T_{Drr} - T_{Brr} - r_{rr}\,{}^{x}F_{rr} \quad , \quad I_{rl}\dot{\omega}_{rl} = T_{Drl} - T_{Brl} - r_{rl}\,{}^{x}F_{rl} \tag{2-7}$$

where I is the inertia of the tire. M.H.Peeie et. al, (2013) has developed the experiment to measure the value of inertia for the driving tire and non-driven tire. In the numerical analysis, the value of I_f and I_r is set to 0.43 kgm^2 and 2.53 kgm^2, respectively. T_D is the driving torque, T_B is the braking torque, r is the radius of the tire and ${}^{x}F$ is the longitudinal force of the front/rear tire.

Generally, the brake torque at each wheel is a function of the brake pressure, P_b at that wheel, the brake area of the wheel A_w, the brake friction coefficient μ_b and the brake radius R_b. Then, the equation of the brake torque at each wheel can be written as below:

$$T_{Bfr} = A_w\mu_b R_{bfr} P_{bfr} \quad , T_{Bfl} = A_w\mu_b R_{bfl} P_{bfl}$$

$$T_{Brr} = A_w\mu_b R_{brr} P_{brr} \quad , \quad T_{Brl} = A_w\mu_b R_{brl} P_{brl} \tag{2-8}$$

2.3 Analysis Vehicle Model

2.3.1 Main specifications

In this study, Toyota COMS model AK10E-PC has been used as an analysis vehicle model. Figure 2-7 shows the Toyota COMS AK10E-PC on the dry asphalt road. The driving system of this vehicle uses two in-wheel motors and they were attached at the both rear tires. Based on the handbook from the Toyota Auto Body Company, the main specifications of this vehicle are as in Table 2-1 [2-4].

Table 2-1 Main Specifications of the Toyota COMS AK10E-PC

Vehicle Model		AK10E-PC
Weight	Vehicle Weight (kg)	270
	Vehicle Gross Weight (kg)	325
Type of fuel		Electricity
Maximum speed	Forward (km/h)	50
	Backward (km/h)	15
Mileage per 1 charge of battery (km)		80
Length (mm)		1935
Width (mm)		995
Height (mm)		1600
Wheelbase (mm)		1655
Distance from the center of gravity to the front tire (mm)		840
Distance from the center of gravity to the rear tire (mm)		815
Tire (Front and rear)		90/90-12 54J
Main battery		Lead Acid Battery 12V x 42Ah x 6 pieces (72V)
Braking System		4 Wheel Drum Brake (Front : Hydraulic Braking System, Rear : Mechanical Braking System)
Driving System		Rear Wheel Drive (In-Wheel Motor)
Charging time (h)		8

Figure 2-7 Toyota COMS AK10E-PC on the dry asphalt road

2.3.2 Braking system of the analysis vehicle model

As described in Table 2-1, our analysis vehicle model employed the hydraulic-mechanical hybrid brake system. The hydraulic brake system was installed at the front part, while the mechanical brake system was installed at the rear part. The hydraulic brake system consists of the front brake tube, brake hose, wheel cylinder and front drum brake, while the mechanical brake system consists of the rear brake tube, power cylinder, link, wire, and rear drum brake. Figure 2-8, Figure 2-9 and Figure 2-10 show the master cylinder, power cylinder and front drum brake of our analysis vehicle model, respectively. The power cylinder is located between the master cylinder and rear tire.

In past years, H.Ogino et al, have constructed 2 wheel model of the hydraulic-mechanical hybrid brake system [2-5]. This model is shown in Figure 2-11. However, the four wheel model of the hydraulic-mechanical hybrid brake system was not constructed yet. In this study, the braking system of the Toyota COMS AK10E-PC has been analyzed. Based on our measurement, the schematic figure of the brake line for the hydraulic-mechanical hybrid brake system is constructed. Figure 2-12 shows the brake line of the hydraulic-mechanical hybrid brake system. In this system, when a driver pushes a brake pedal, the braking pressure generated from the master cylinder is directed to the front wheel cylinder. However, for a mechanical brake system, the braking pressure generated from the master cylinder is directed to the power cylinder. Then, the piston in the power cylinder will pull the link lever and wire that were attached between the power cylinder and rear drum brake.

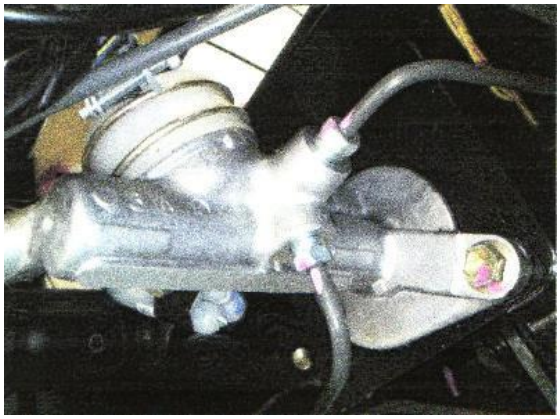

Figure 2-8 Master cylinder of Toyota COMS AK10E-PC

Figure 2-9 Power cylinder of Toyota COMS AK10E-PC

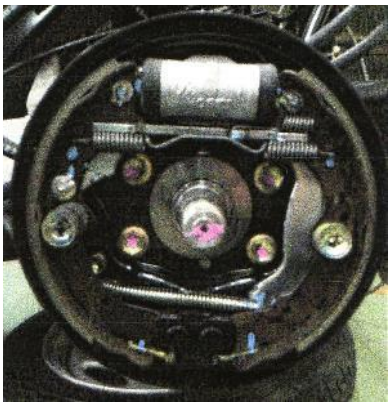

Figure 2-10 Front drum brake of Toyota COMS AK10E-PC

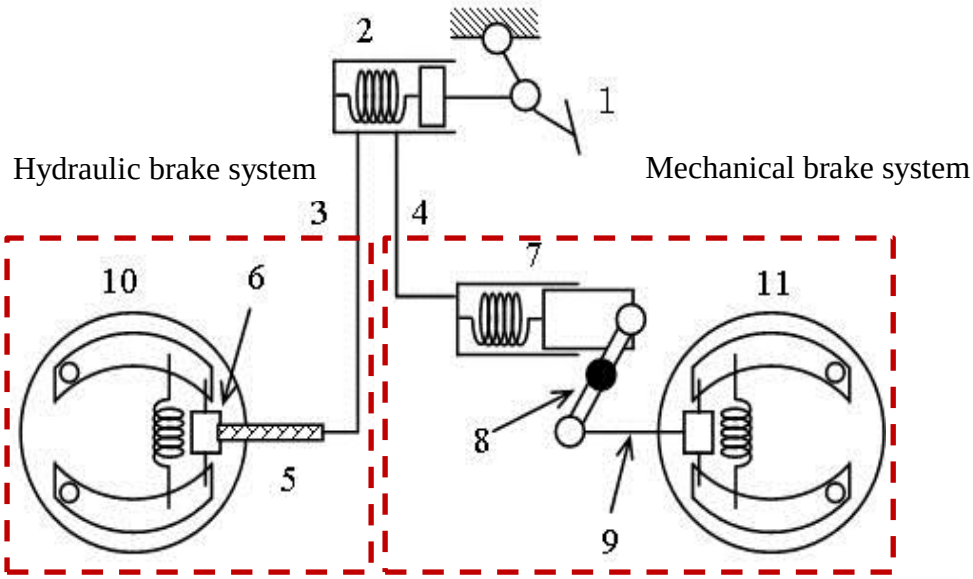

1:Brake Pedal; 2:Master Cylinder; 3:Front Brake Tube; 4:Rear Brake Tube;
5:Brake Hose; 6:Wheel Cylinder; 7:Power Cylinder; 8:Link ; 9:Wire;
10:Front Drum Brake; 11:Rear Drum Brake

Figure 2-11 Two wheel model of the hydraulic-mechanical hybrid brake system

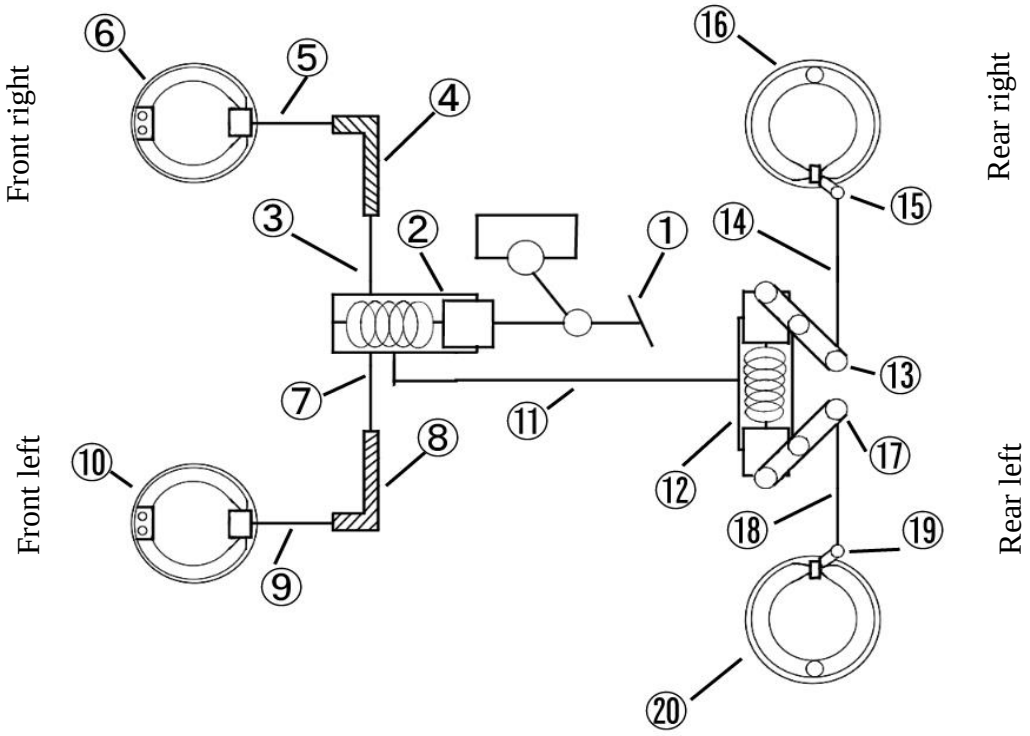

1: Brake pedal; 2: Master cylinder (Diameter 18mm); 3: Brake pipe (Length 380 mm, Diameter 3 mm); 4: Brake hose (Length 390 mm); 5: Brake pipe (Length 250 mm, Diameter 3 mm); 6: Drum brake (Drum radius 82 mm, Diameter of the wheel cylinder 18 mm); 7: Brake pipe (Length 755 mm, Diameter 3 mm); 8: Brake hose (Length 390 mm); 9: Brake pipe (Length 250 mm, Diameter 3 mm); 10: Drum brake (Drum radius 82 mm, Diameter of the wheel cylinder 18 mm); 11. Brake pipe (Length 2450 mm, Diameter 3 mm); 12: Power cylinder (Diameter 18 mm); 13: Link of the power cylinder (Length 60 mm); 14: Wire (Length 550 mm); 15: Link of the drum brake (Length 26 mm); 16: Drum brake (Drum radius 48 mm); 17: Link of the power cylinder (Length 60 mm); 18: Wire (550 mm); 19: Link of the drum brake (26 mm); 20: Drum brake (Drum radius 28 mm)

Figure 2-12 Brake line of the hydraulic-mechanical hybrid brake system

2.4 Experimental Equipment

2.4.1 Electronic devices

The experimental devices that have been used in the experiment are listed in Table 2-2, while the photos of the electronic devices are shown in Figure 2-13 through Figure 2-23.

Table 2-2 Electronic devices and their functions

No	Device	Model	Function
1	Data logger	KEYENCE NR-2000	Record all the data
2	Fluid pressure sensor	KYOWA PGM-500KD	Measure the brake pressure in the master cylinder
4	Digital displays	ONO SOKKI TM-3130	Display the rotation speed of the tire
6	Digital displays	ONO SOKKI	Display the velocity of the vehicle
5	Photoelectric rotation detector meter	ONO SOKKI LG-916	Measure the rotation speed of the tire
6	Spatial filter	ONO SOKKI LC-3110	Measure the longitudinal velocity of the vehicle
7	Acceleration sensor	KYOWA AS-10B	Measure the acceleration of the vehicle

Figure 2-13 Data logger (KEYENCE NR-2000)

Figure 2-14 Digital display for rotation speed of the tire (ONO SOKKI TM-3130)

Figure 2-15 Strain amplifier (KYOWA DPM-713B)

Figure 2-16 Strain amplifier (KYOWA DPM-601B)

Figure 2-17 Photoelectric rotation detector at the front tire (ONO SOKKI LG-916)

Figure 2-18 Photoelectric rotation detector at the rear tire (ONO SOKKI LG-916)

Figure 2-19 Spatial filter (ONO SOKKI LC-3110)

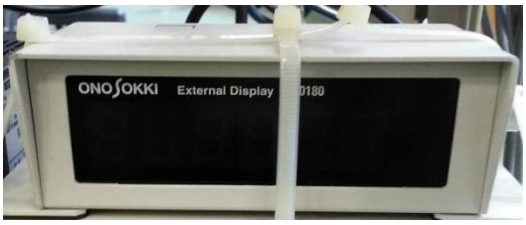

Figure 2-20 Digital display for vehicle velocity (ONO SOKKI)

Figure 2-21 Terminal box (ONO SOKKI LC-0110)

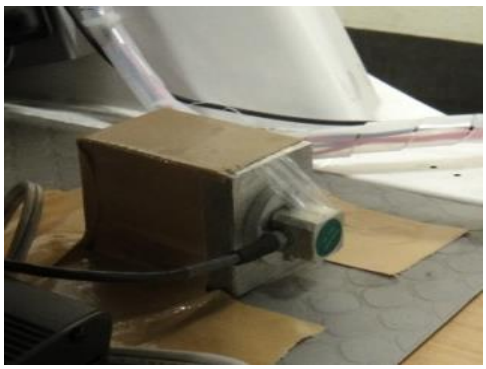

Figure 2-22 Acceleration sensor (KYOWA AS-10B)

Figure 2-23 Fluid pressure sensor (KYOWA PGM-500KD)

2.4.2 Anti-vibration device

During acceleration and braking, to prevent the electronic devices from vibrating, the anti-vibration devices have been used. Figure 2-24 shows the anti-vibration device that was installed in our experimental vehicle. By using an anti-vibration device, the electronic devices are more stable and the experimental data would be more precise.

Figure 2-24 Anti-vibration device

2.5 Experimental Methods

2.5.1 Installation of the electronic devices on the experimental vehicle

The first part in our experiment is to install all of the electronic devices on the experimental vehicle. Figure 2-25 shows the quarter model of the vehicle with the electronic devices. When the driver pushes a pedal brake, the fluid pressure sensor (2) will measure the braking pressure that was flowing from the master cylinder (1) to the wheel cylinder. At the same time, the spatial filter (10), photoelectric rotation detector (6) and the acceleration sensor (9) will measure the vehicle velocity, rotation speed of the tire and the acceleration of the vehicle. All of the data that were measured by the sensors will be recorded in the data logger.

2.5.2 Construction of the braking force generator

The next part in our experiment is to construct the braking force generator. The function of the braking force generator is to gain the constant braking pressure. In the experiment, the braking force generator will be used to examine the effect of the various values of braking pressure against the vehicle braking performance. The braking force generator consists of three components, which are brake lever, stopper and bolt. All of these components were shown in Figure 2-26, Figure 2-27 and Figure 2-28, respectively. 3 types of bolt have been used in the experiment and each type can obtain 1 MPa, 1.5 MPa and 2 MPa of the braking pressure.

In the experiment, when a driver pushes the brake lever (1), the brake level (2) will push the brake pedal (4) of the vehicle. The stopper (3) will stop the brake lever at the certain degrees and the constant braking force will be generated to the brake pedal. Then, the braking pressure in the master cylinder will be constant. By using this method, the driver's desired constant braking pressure can be obtained.

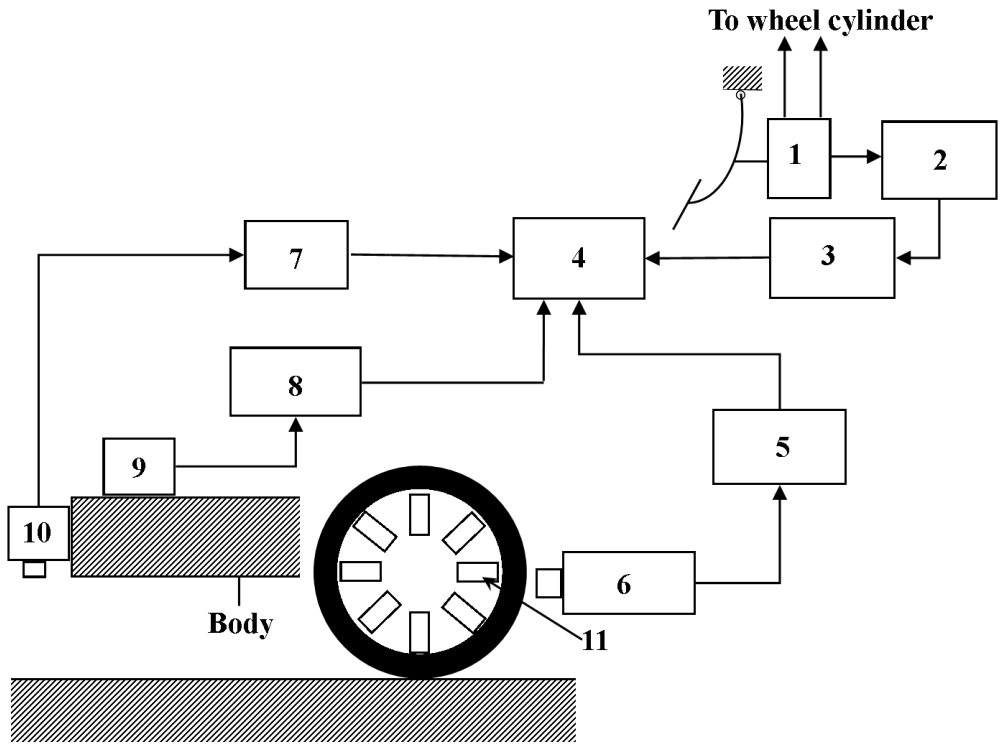

1: Master cylinder (NISSIN 11/16); 2: Fluid pressure sensor (KYOWA PGM-500KD); 3: Strain amplifier (KYOWA DPM-713B); 4: Data logger (KEYENCE NR-2000); 5: Digital display (ONO SOKKI TM-3130); 6: Photoelectric rotation detector (ONO SOKKI LG-916); 7: Terminal box; 8: Strain amplifier (KYOWA DPM-601B); 9: Acceleration sensor (KYOWA AS-10B); 10: Spatial filter (ONO SOKKI LC-3110); 11: Reflection tape

Figure 2-25 Electronic devices installed on the vehicle

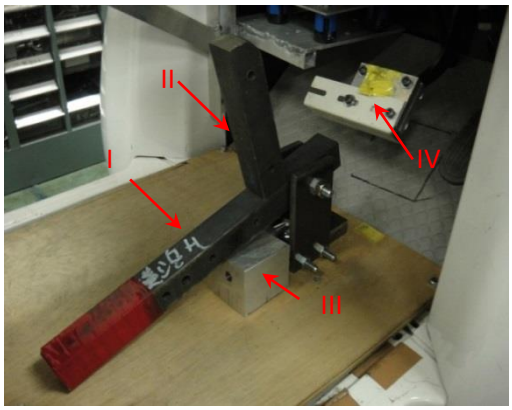

Figure 2-26 Brake lever and stopper

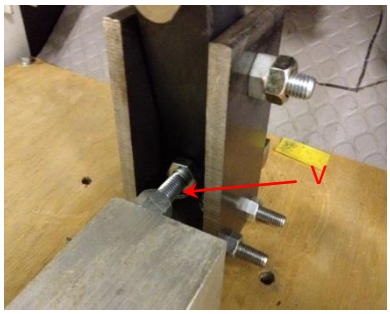

Figure 2-27 Bolt at the brake stopper

I: First lever

II:Second lever

III:Brake pedal force stopper

IV:Brake pedal

V: Bolt

Figure 2-28 Three types of bolts to obtain the constant braking pressure (1 MPa, 1.5 MPa and 2 MPa)

2.5.3 Experiment on the analysis vehicle

In the experiment to examine the braking performance of the vehicle, two types of the braking system have been used, which are hydraulic-mechanical hybrid brake system without regenerative brake and hydraulic-mechanical hybrid brake system with regenerative brake.

- Hydraulic-mechanical hybrid brake system without regenerative brake system

In this experiment, the regenerative brake is kept in a non-operational condition. The vehicle only uses hydraulic-mechanical hybrid brake system for braking. Figure 2-29 shows the experimental vehicle with a driver, while Figure 2-30 shows the shift switch for driving (D), neutral (N) and reverse (R). During braking, the driver will change the shift switch from driving (D) to neutral (N). In this situation, the electric current from the battery to the in-wheel motor was cut off and the in-wheel motor can not produce the regenerative braking force. The vehicle only has hydraulic-mechanical hybrid brake system as a braking system.

In the experiment, several conditions have been set as below:

1. Road condition: Dry asphalt
2. Steering angle: 0 degrees
3. Braking pressure: 1 MPa, 1.5 MPa, 2 MPa
4. Maximum speed of the vehicle velocity: 10 km/h, 15 k/h, 20 km/h

From the experimental conditions, we assumed that:

1. The vehicle is running on the straight line.
2. The braking pressure in the master cylinder is constant until the vehicle completely stops.

- ❖ Hydraulic-mechanical hybrid brake system with regenerative brake system

In this experiment, the regenerative brake is operational. During braking, the shift switch is still on the driving (D). In this situation, the in-wheel motor will produce the regenerative braking force. The braking force at the rear tire will be the mechanical braking force and the regenerative braking force. The experimental conditions and assumptions are same as the experiment without regenerative brake.

Experimental conditions:

1. Road condition: Dry asphalt
2. Steering angle: 0 degrees
3. Braking pressure: 1 MPa, 1.5 MPa, 2 MPa
4. Maximum speed of the vehicle velocity: 10 km/h, 15 k/h, 20 km/h

Experimental assumptions:

1. The vehicle is running on the straight line.
2. The braking pressure in the master cylinder is constant until the vehicle completely stops.

Figure 2-29 Experimental vehicle with a driver

Figure 2-30 Shift switch

2.6 Experimental Results and Discussion

2.6.1 Hydraulic-mechanical hybrid brake system without regenerative brake

In the experiment, the driver's desired braking pressure are 1 MPa, 1.5 MPa and 2MPa. Each experiment has been done in three times and the experimental data have been summarized into minimum, average and maximum values. In Figure 2-31, Figure 2-32 and Figure 2-33, the driver's desired braking pressure are 1 MPa, 1.5 MPa and 2 MPa, respectively. From Figure 2-31 to Figure 2-33, the average value of the braking pressure is close to the driver's desired constant braking pressure. However, due to the roughness of the road, the constant braking pressure cannot be obtained.

The effect of the hydraulic-mechanical hybrid brake system without regenerative brake to the vehicle velocity were shown from Figure 2-34 to Figure 2-36. In Figure 2-34, Figure 2-35 and Figure 2-36, the driver's desired braking pressure are 1 MPa, 1.5 MPa and 2 MPa, respectively. From Figure 2-34, in case of driver's desired braking pressure is 1 MPa, the stopping time of the vehicle is 6.3 seconds. The stopping time of the vehicle with the driver's desired braking pressure 1.5 MPa (Figure 2-35), the stopping time of the vehicle is around 4 seconds. In case of the driver's desired braking pressure is 2 MPa (Figure 2-36), the stopping time of the vehicle is around 3 seconds. From these results, the stopping time of the vehicle can be minimized if the braking pressure is increase.

The effect of the hydraulic-mechanical hybrid brake system without regenerative brake to the rotational speed of the front tire were shown in Figure 2-37 to Figure 2-39. In Figure 2-37, Figure 2-38 and Figure 2-39, the driver's desired braking pressure are 1 MPa, 1.5 MPa and 2 MPa, respectively. Similarly to the vehicle velocity, the rotational speed of the front tire in Figure 2-37 to Figure 2-39 were decreased gradually.

The effect of the hydraulic-mechanical hybrid brake system without regenerative brake to the rotational speed of the rear tire were shown in Figure 2-40 to Figure 2-42. In Figure 2-40, Figure 2-41 and Figure 2-42, the driver's desired braking pressure are 1 MPa, 1.5 MPa and 2 MPa, respectively. Similarly to the rotational speed of the front tire, the rotational speed of the rear tire in Figure 2-40 to Figure 2-42 were decreased gradually.

From the experimental results, on the dry asphalt road, without regenerative brake, although rear tire only employed mechanical braking force, the vehicle scan stop smoothly. The rotational speed of the front and rear tires were decreased gradually. This result verified

that hydraulic-mechanical hybrid brake system can stop the small EVs on the dry asphalt road smoothly.

In this study, to measure the performance of the hydraulic-mechanical hybrid brake system without regenerative brake, the stopping time of the hydraulic-mechanical hybrid brake system without regenerative brake is needed to compare with the hydraulic-mechanical hybrid brake system with regenerative brake activated.

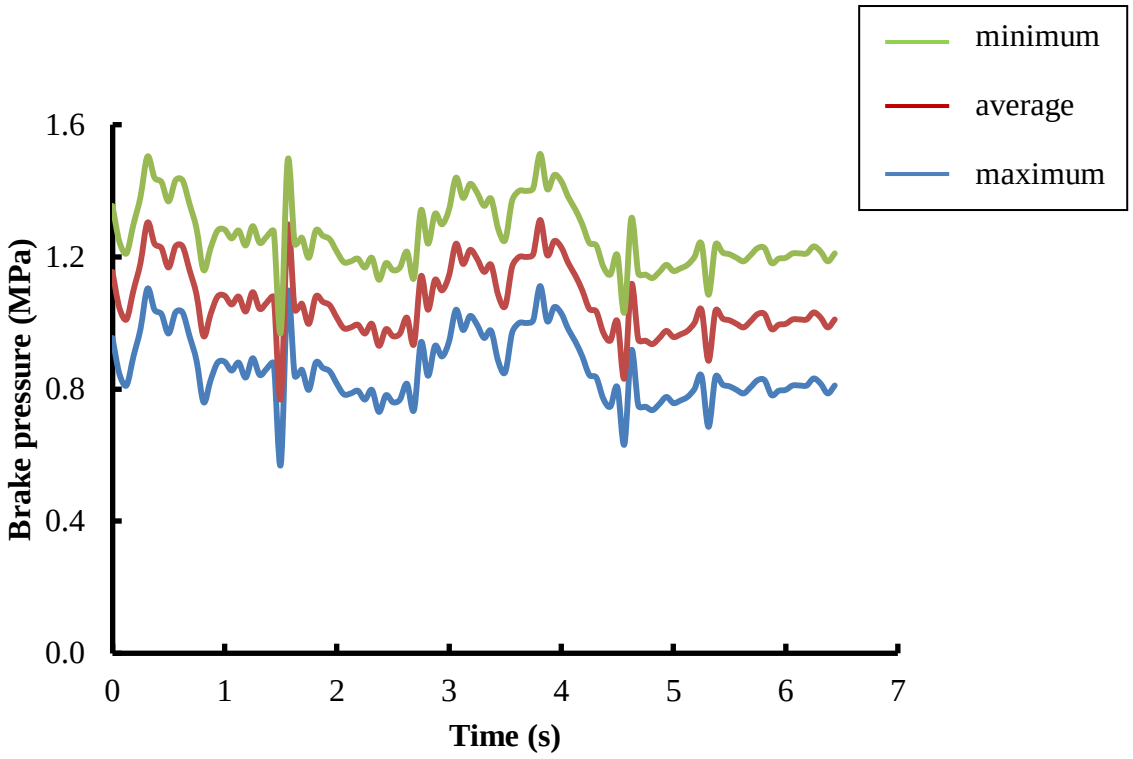

Figure 2-31 Braking pressure in the master cylinder

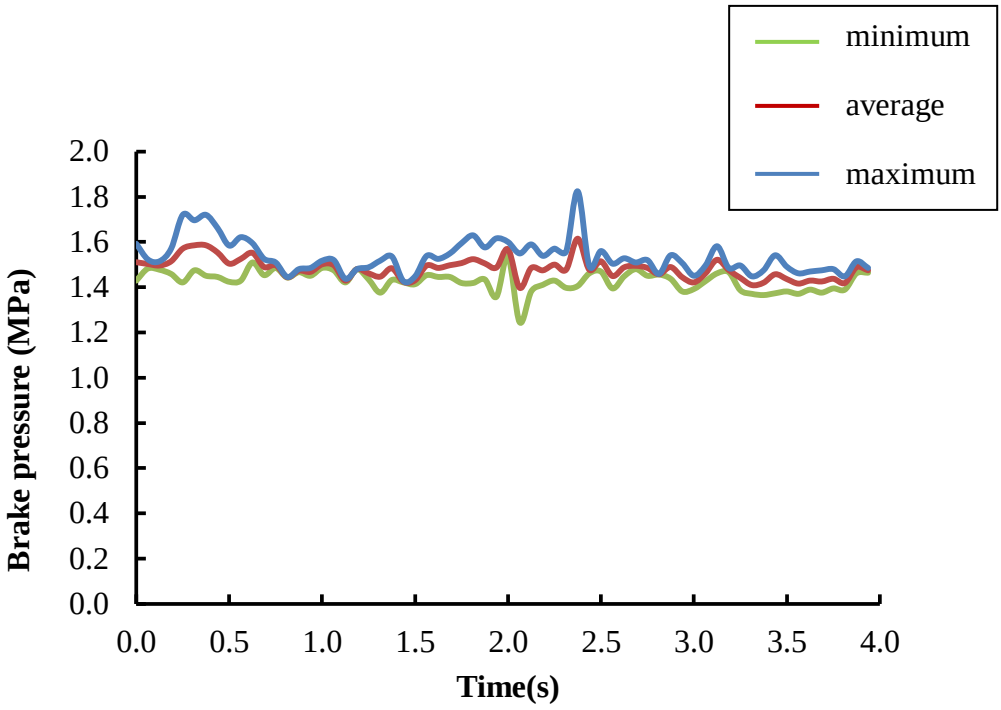

Figure 2-32 Braking pressure in the master cylinder

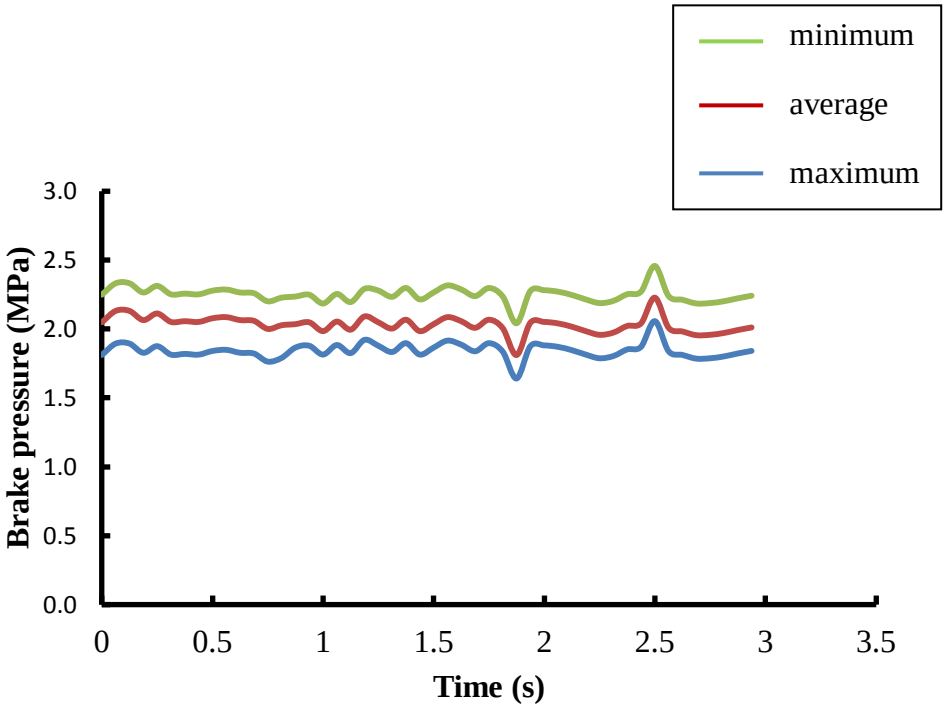

Figure 2-33 Braking pressure in the master cylinder

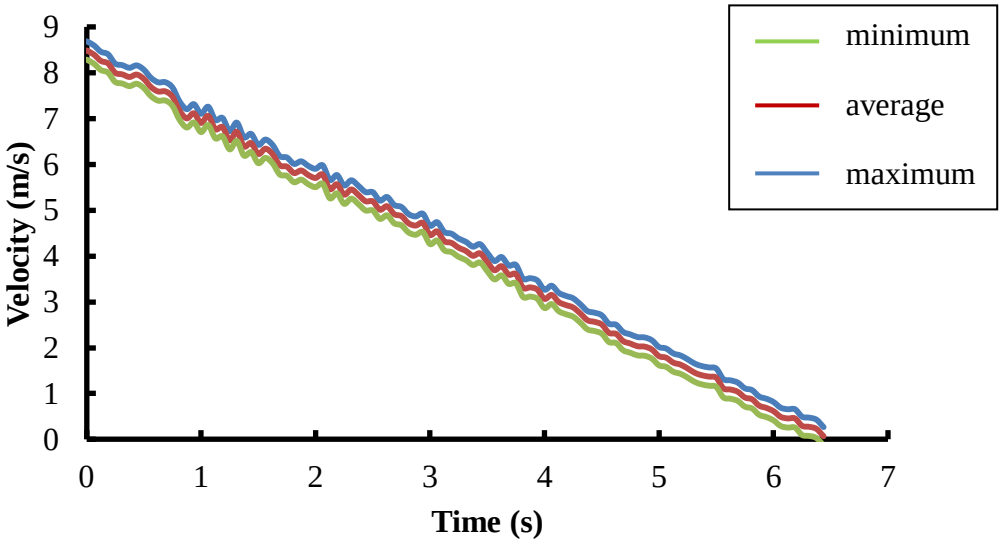

Figure 2-34 Change of vehicle velocity

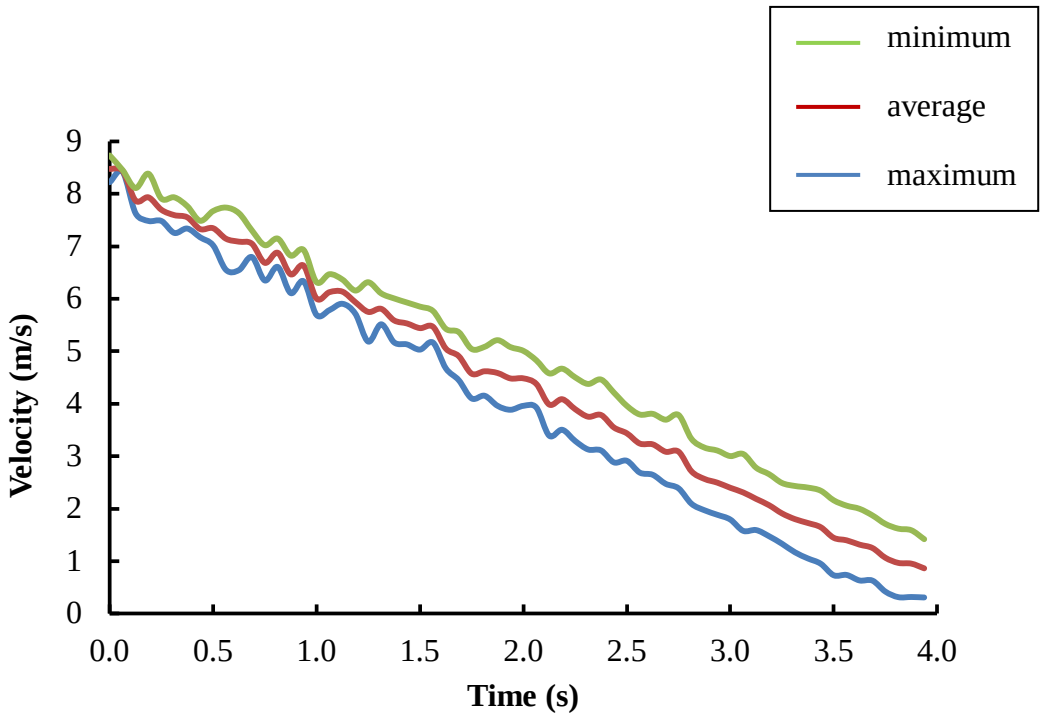

Figure 2-35 Change of vehicle velocity

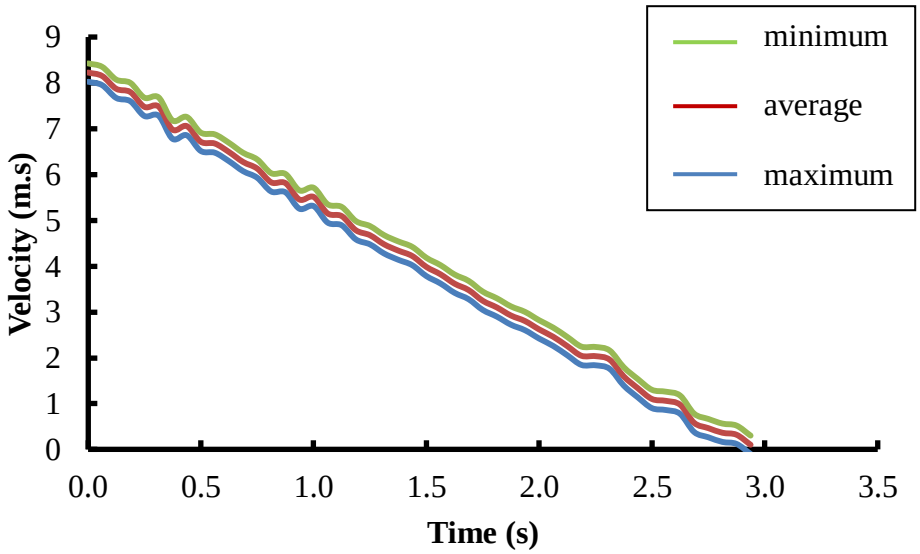

Figure 2-36 Change of vehicle velocity

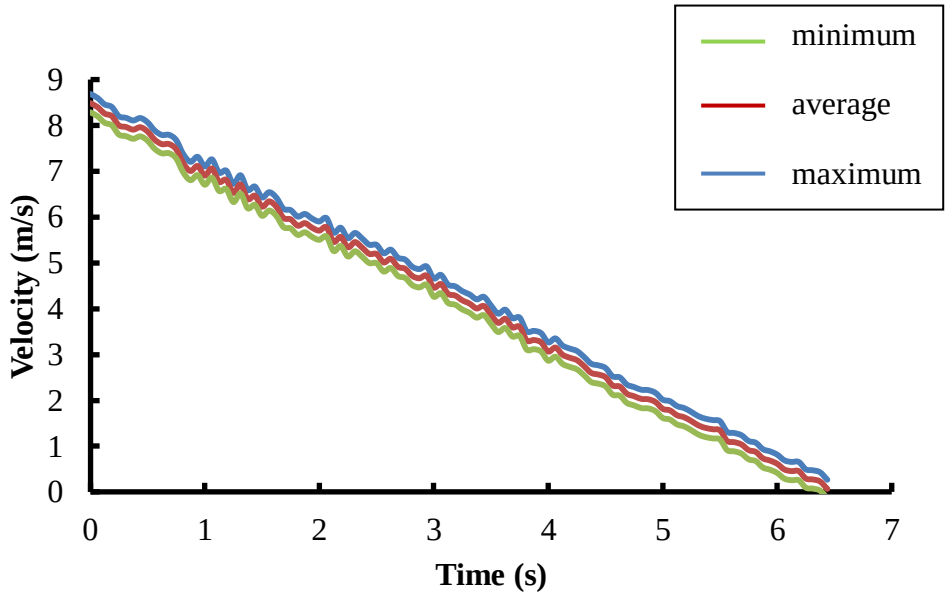

Figure 2-37 Change of rotational speed of the front tire

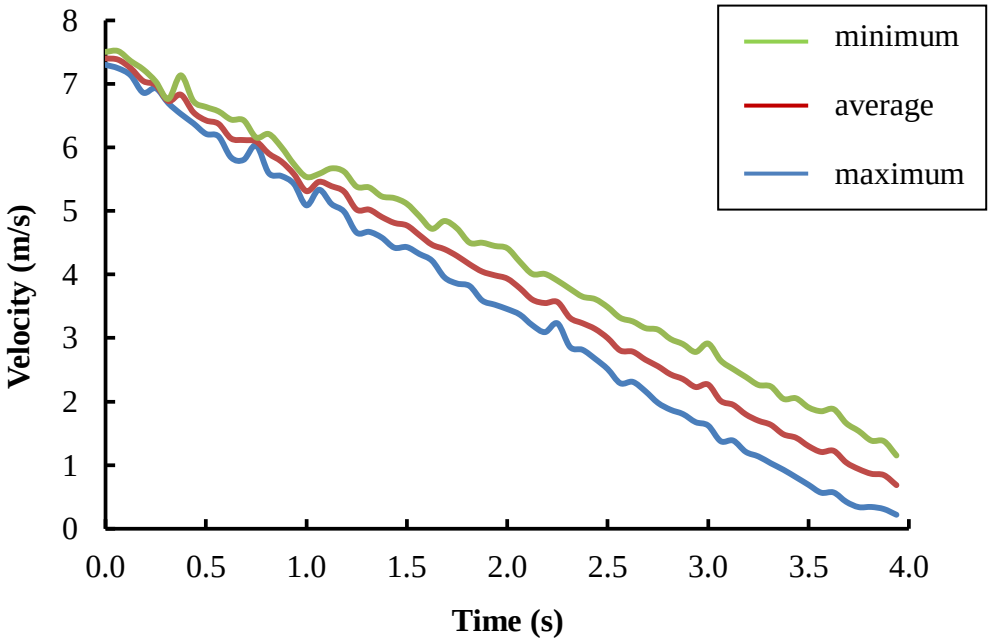

Figure 2-38 Change of rotational speed of the front tire

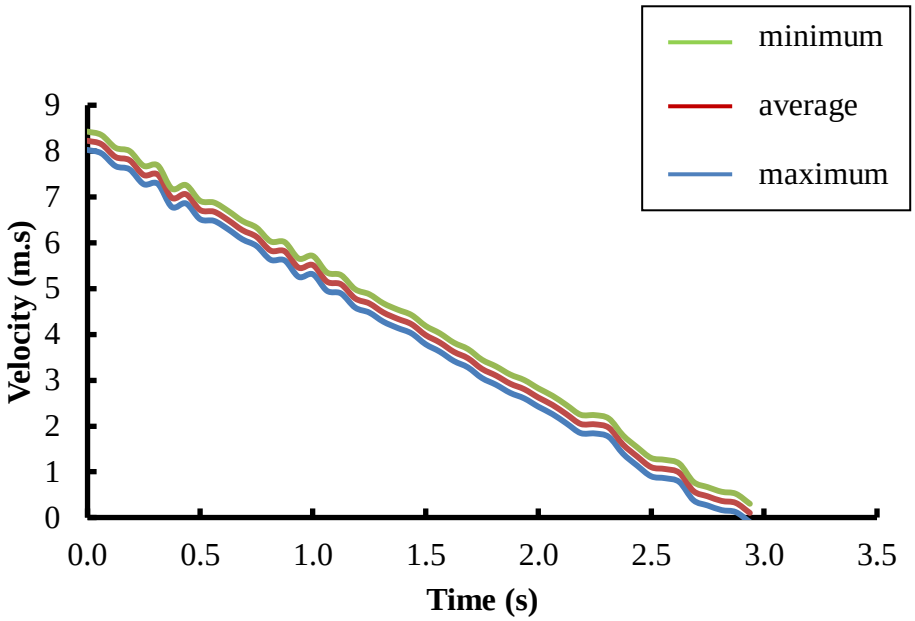

Figure 2-39 Change of rotational speed of the front tire

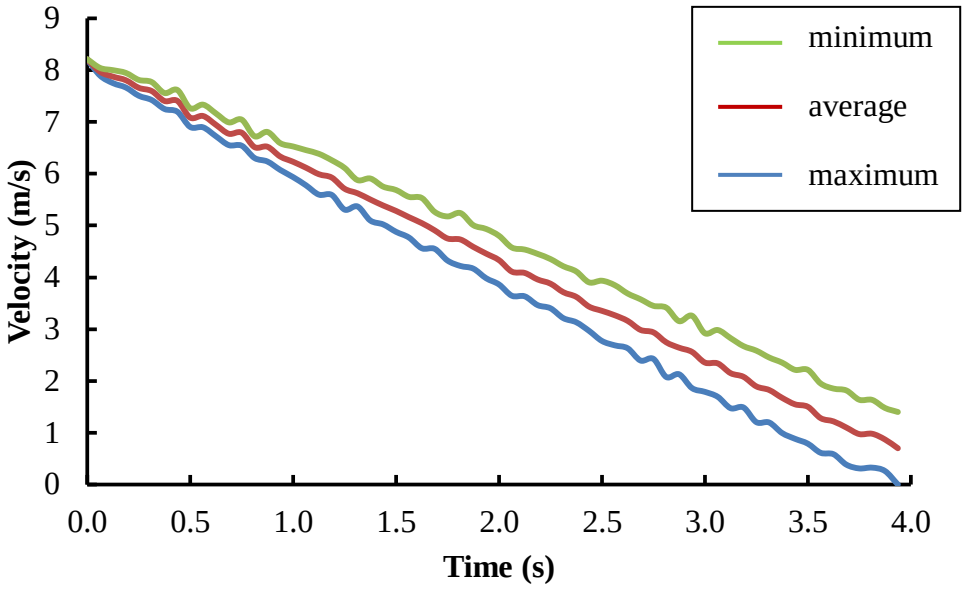

Figure 2-40 Change of rotational speed of the rear tire

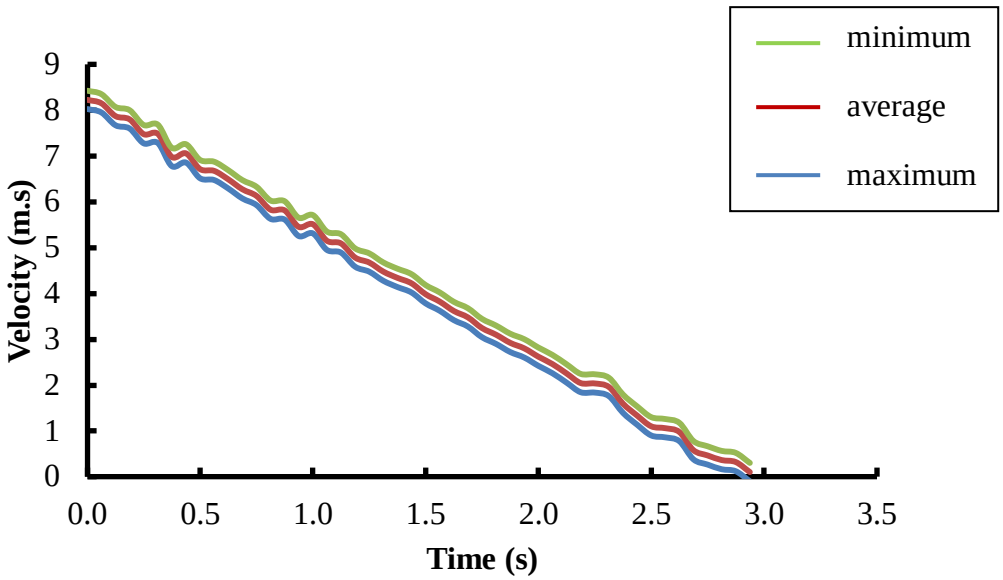

Figure 2-41 Change of rotational speed of the rear tire

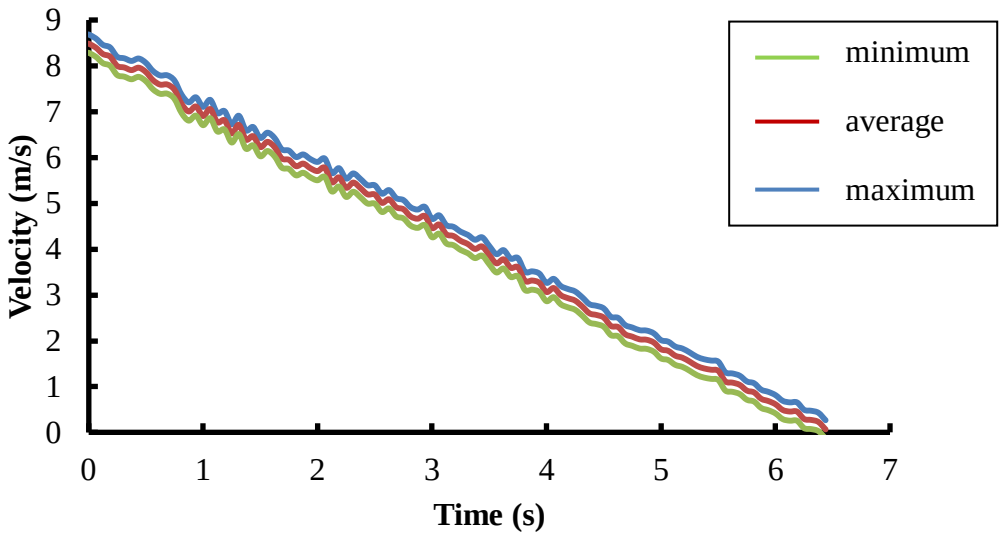

Figure 2-42 Change of rotational speed of the rear tire

2.6.2 Hydraulic-mechanical hybrid brake system with regenerative brake

In the experiment, the driver's desired braking pressure are 1 MPa, 1.5 MPa and 2MPa. Each experiment has been done in three times and the experimental data have been summarized into minimum, average and maximum values. In Figure 2-43, Figure 2-44 and Figure 2-45, the driver's desired braking pressure are 1 MPa, 1.5 MPa and 2 MPa, respectively. From Figure 2-43 to Figure 2-45, the average value of the braking pressure is close to the driver's desired constant braking pressure. However, due to the roughness of the road, the constant braking pressure cannot be obtained.

The effect of the hydraulic-mechanical hybrid brake system without regenerative brake to the vehicle velocity were shown from Figure 2-46 to Figure 2-48. In Figure 2-46, Figure 2-47 and Figure 2-48, the driver's desired braking pressure are 1 MPa, 1.5 MPa and 2 MPa, respectively. From Figure 2-46, in case of driver's desired braking pressure is 1 MPa, the stopping time of the vehicle is around 3 seconds. The stopping time of the vehicle with the driver's desired braking pressure 1.5 MPa (Figure 2-47), the stopping time of the vehicle is around 2.5 seconds. In case of the driver's desired braking pressure is 2 MPa (Figure 2-48), the stopping time of the vehicle is around 2.3 seconds. From these results, the stopping time of the vehicle can be minimized if the braking pressure is increase.

The effect of the hydraulic-mechanical hybrid brake system without regenerative brake to the rotational speed of the front tire were shown in Figure 2-49 to Figure 2-51. In Figure 2-49, Figure 2-50 and Figure 2-51, the driver's desired braking pressure are 1 MPa, 1.5 MPa and 2 MPa, respectively. Similarly to the vehicle velocity, the rotational speed of the front tire in Figure 2-49 to Figure 2-51 were decreased gradually.

The effect of the hydraulic-mechanical hybrid brake system without regenerative brake to the rotational speed of the rear tire were shown in Figure 2-52 to Figure 2-54. In Figure 2-52, Figure 2-53 and Figure 2-54, the driver's desired braking pressure are 1 MPa, 1.5 MPa and 2 MPa, respectively. Similarly to the rotational speed of the front tire, the rotational speed of the rear tire in Figure 2-52 to Figure 2-54 were decreased gradually.

From the experimental results, on the dry asphalt road, without regenerative brake, although rear tire only employed mechanical braking force, the vehicle scan stop smoothly. The rotational speed of the front and rear tires were decreased gradually. This result verified

that hydraulic-mechanical hybrid brake system can stop the small EVs on the dry asphalt road smoothly.

From these results, it is verified that hydraulic-mechanical hybrid brake system with regenerative brake can decrease the stopping time of the vehicle during braking and as the result the braking performance of the small electric vehicle can be increased.

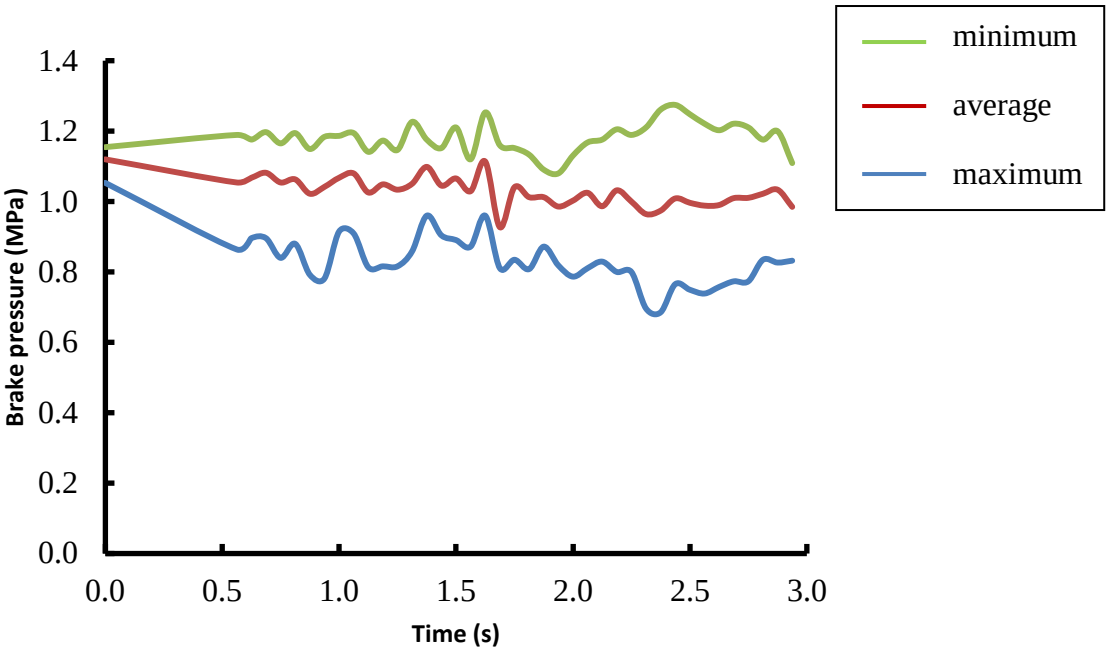

Figure 2-43 Braking pressure in the master cylinder

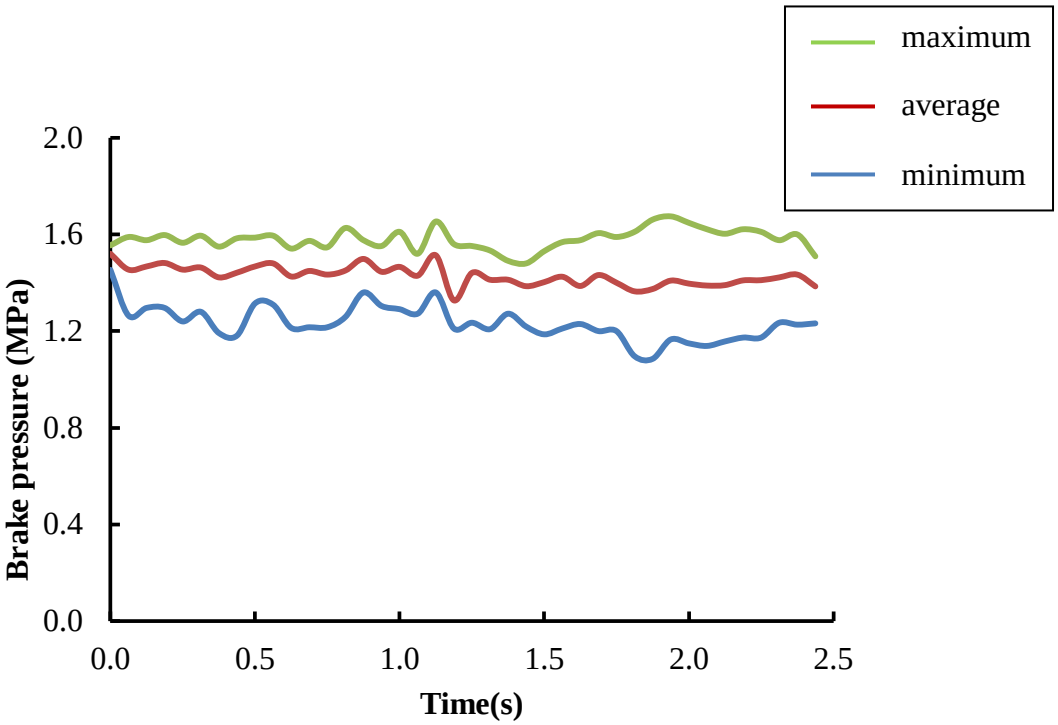

Figure 2-44 Braking pressure in the master cylinder

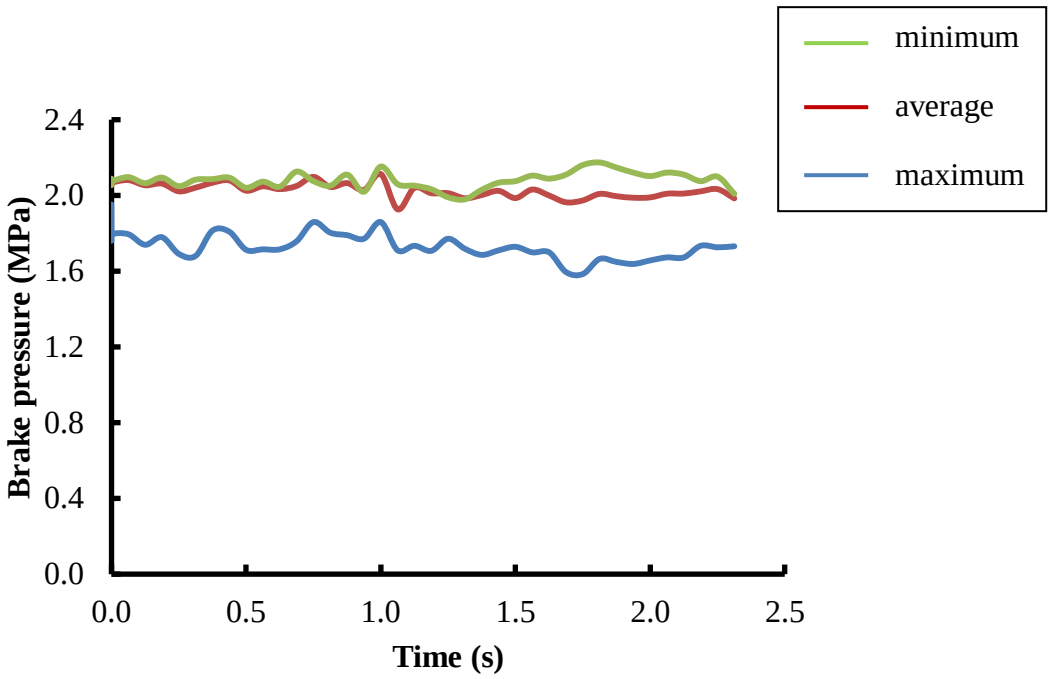

Figure 2-45 Braking pressure in the master cylinder

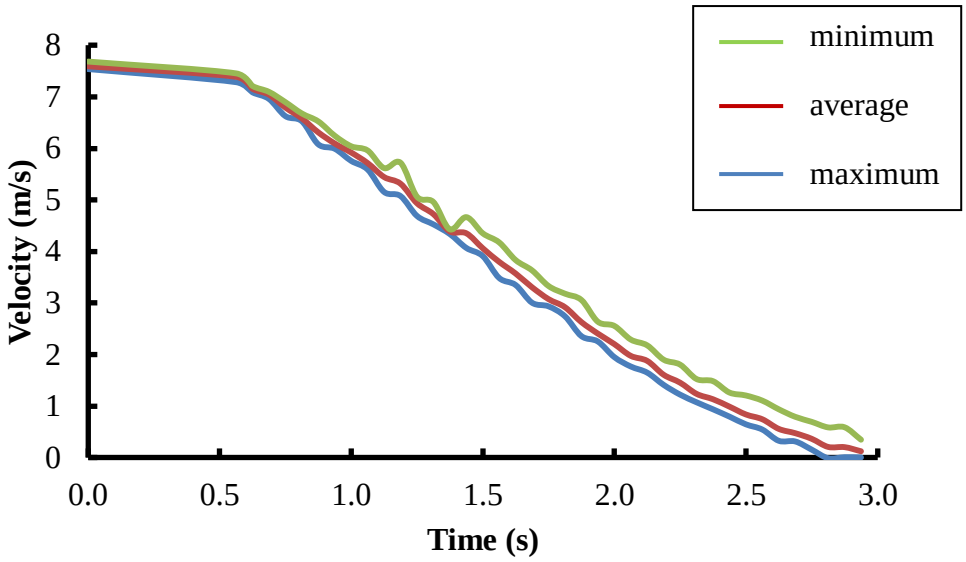

Figure 2-46 Change of vehicle velocity

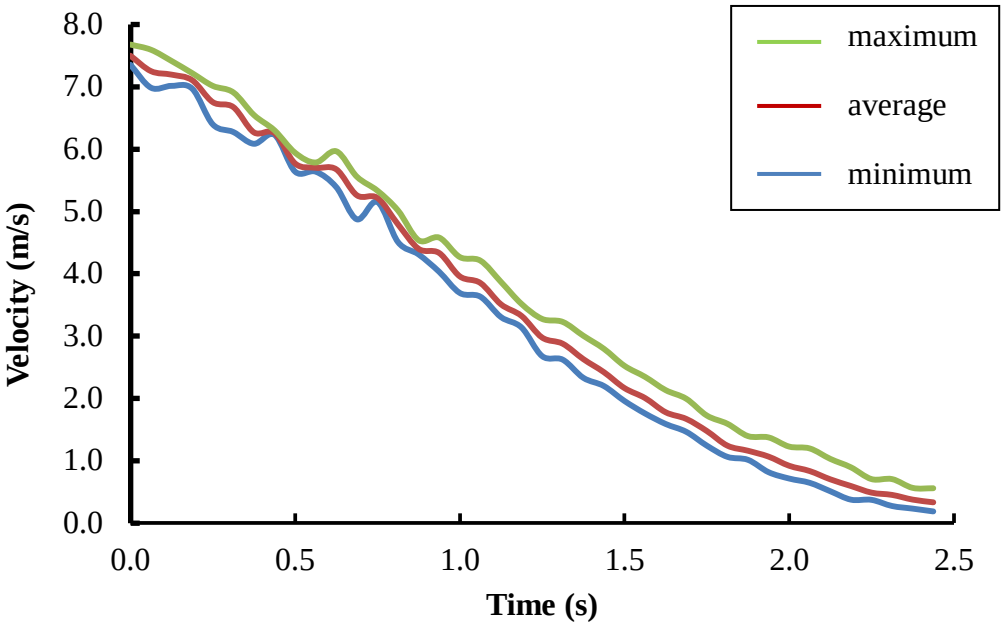

Figure 2-47 Change of vehicle velocity

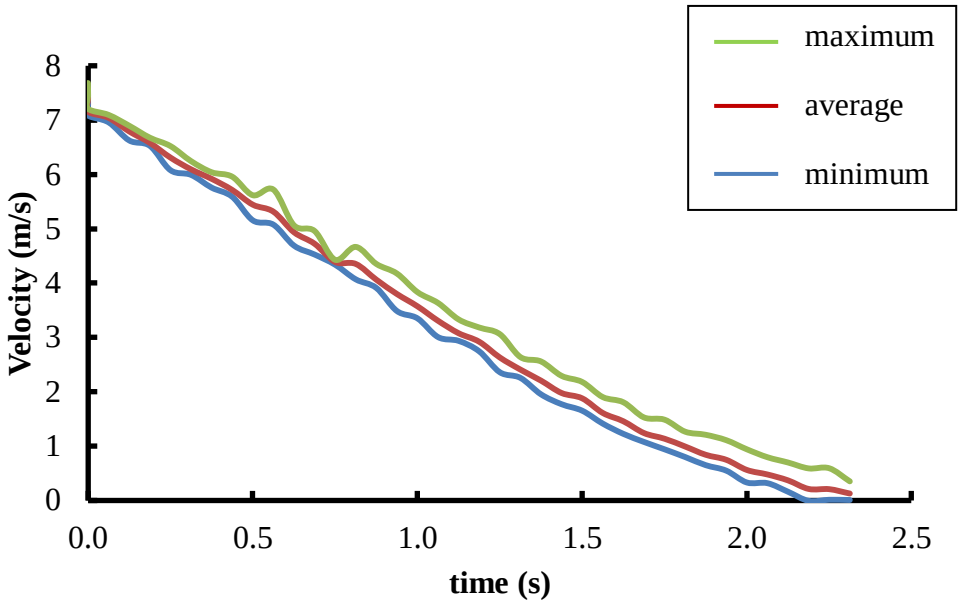

Figure 2-48 Change of vehicle velocity

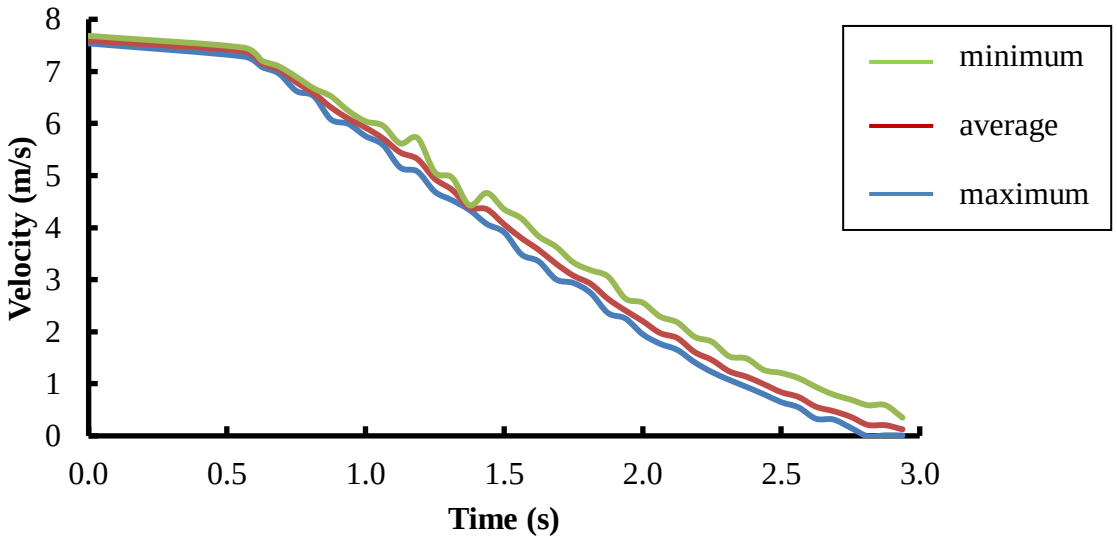

Figure 2-49 Change of rotational speed of the front tire

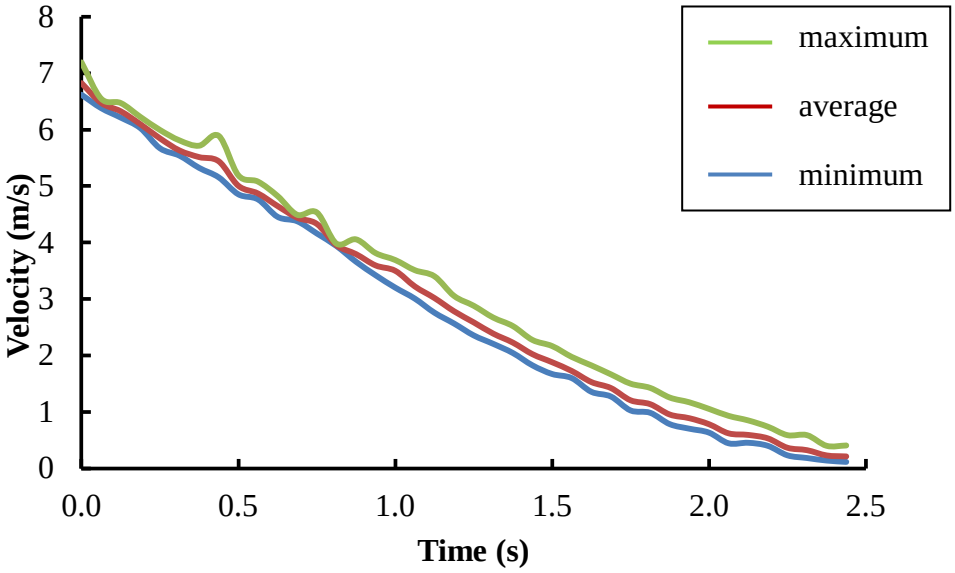

Figure 2-50 Change of rotational speed of the front tire

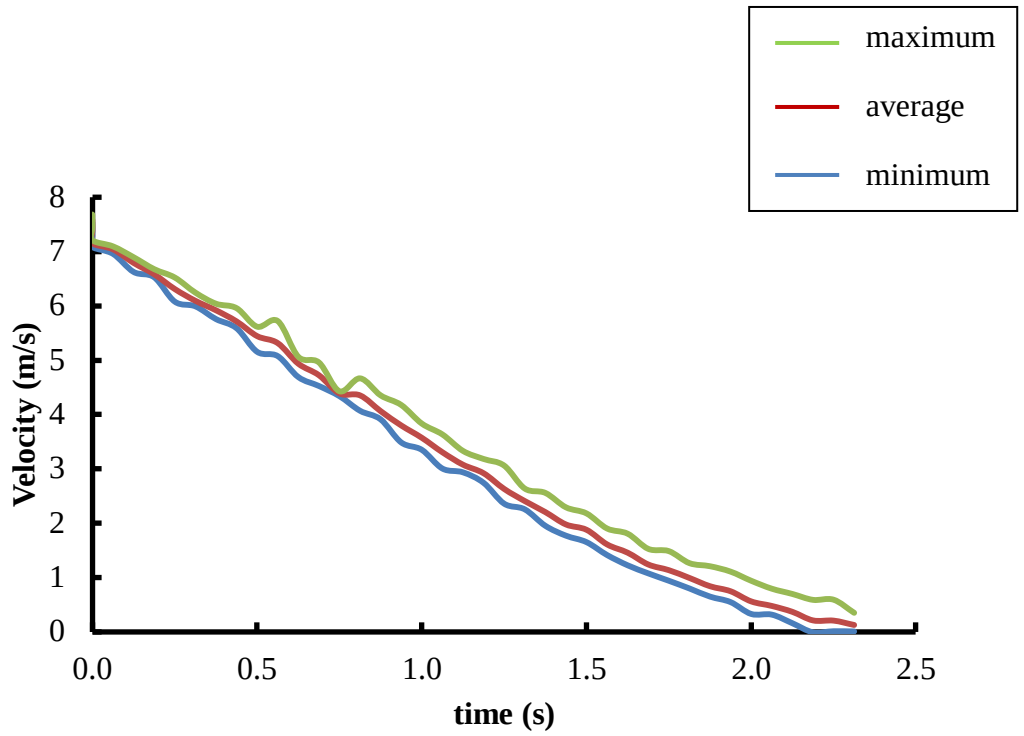

Figure 2-51 Change of rotational speed of the front tire

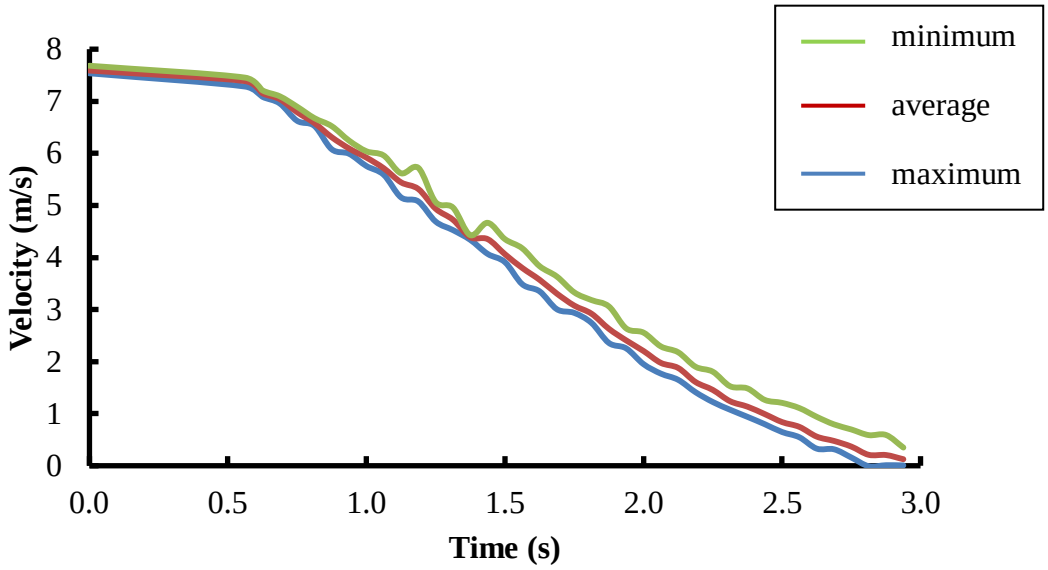

Figure 2-52 Change of rotational speed of the rear tire

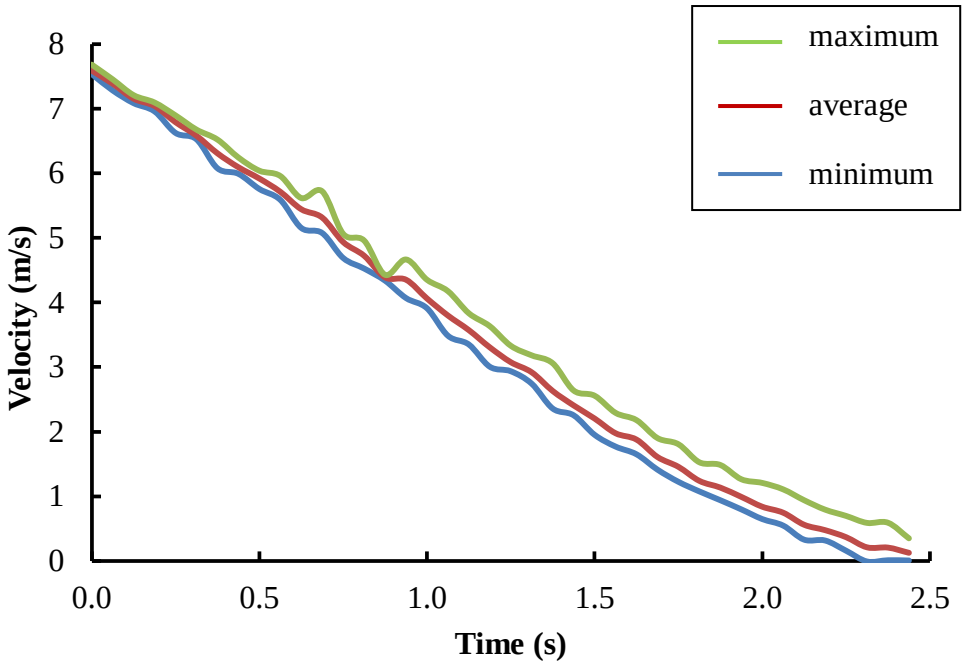

Figure 2-53 Change of rotational speed of the rear tire

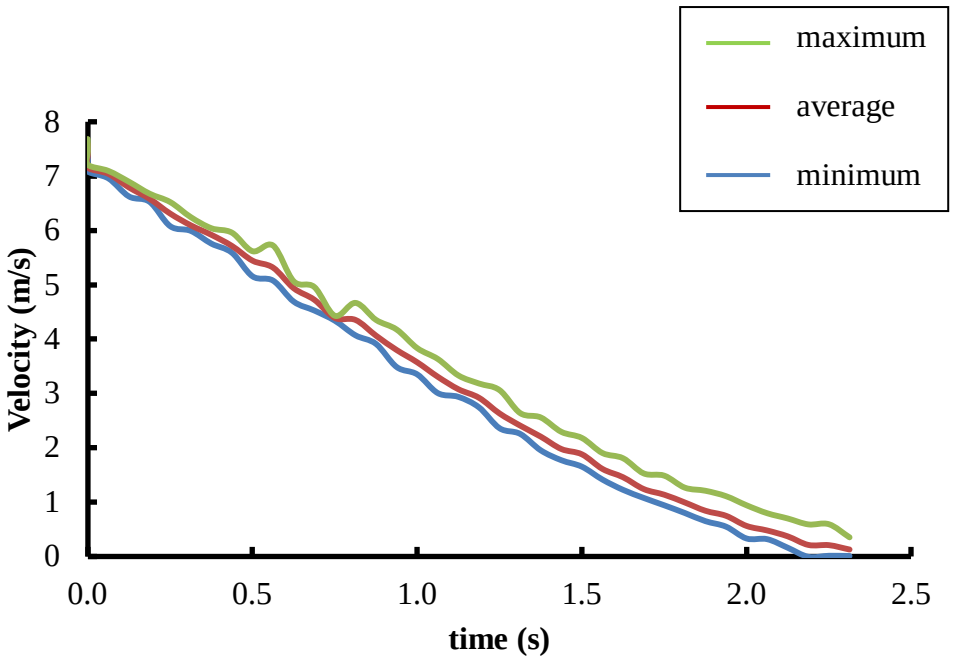

Figure 2-54 Change of rotational speed of the front tire

2.7 Summary

In this chapter, the experiments have been done to analysis the braking performance of the hydraulic-mechanical hybrid brake system. Two braking conditions have been set in the experiments, which are hydraulic-mechanical hybrid brake system without regenerative brake, and hydraulic-mechanical hybrid brake system with regenerative brake. The findings from the experimental results are summarized below:

1. Due to the roughness of the road, the constant braking pressure in the master cylinder is difficult to obtain.
2. During braking on dry asphalt road, without regenerative brake, the braking force from the hydraulic-mechanical hybrid brake system can stop the vehicle smoothly.
3. Although the hydraulic-mechanical hybrid brake system without regenerative brake can stop the vehicle smoothly, the stopping time is longer than hydraulic-mechanical hybrid brake system with regenerative brake.
4. To increase the braking performance of the small EVs with hydraulic-mechanical hybrid brake system, the regenerative brake system is necessary to work together with the mechanical brake system.

Chapter 3

HYDRAULIC-MECHANICAL HYBRID BRAKE SYSTEM WITH ABS

3.1 Introduction

In this chapter, to improve the braking performance of the small EVs with hydraulic-mechanical hybrid brake system, the anti-lock brake system (ABS), which is a basic skid control method, is combined with the hydraulic-mechanical hybrid brake system. First, the function and the composition of ABS are described. Then, the simulation model of the hydraulic-mechanical hybrid brake system with ABS is developed. The calculation procedures and the simulation conditions are presented. The effects of the hydraulic-mechanical hybrid brake system with ABS are analyzed by MATLAB/Simulink. In the last part of this chapter, the simulation results are presented and discussed. Finally, the findings from the simulation results are described in the summary.

3.2 Slip Phenomena

The prime function of an anti-lock brake system (ABS) is to prevent the tire from locking and to keep the skid of the tire within a desired range as shown in Figure 3-1 [3-1]. This will ensure that the tire can develop a sufficiently high braking force for stopping the vehicle, and at the same time it can retain an adequate cornering force for directional control and stability [3-2]. The equations of slip ratio are as below:

$\rho = \frac{u - r\omega}{u}$: accelerating wheel (3-1a)

$\rho = \frac{u - r\omega}{r\omega}$: decelerating wheel (3-1b)

where u is the wheel absolute velocity or vehicle chassis velocity in the longitudinal direction. r and ω are the wheel radius and tire angular velocity, respectively.

Wheel skid will occur when the large braking torque rapidly generated at the wheel or the driving torque suddenly drops with various road conditions. Based on Figure 3-1, during braking on an icy road, when the slip ratio rapidly increases towards 1.0, the braking force and the side force generation on the wheel will be disappeared. This causes unstable vehicle motion and could result in a dangerous spin motion.

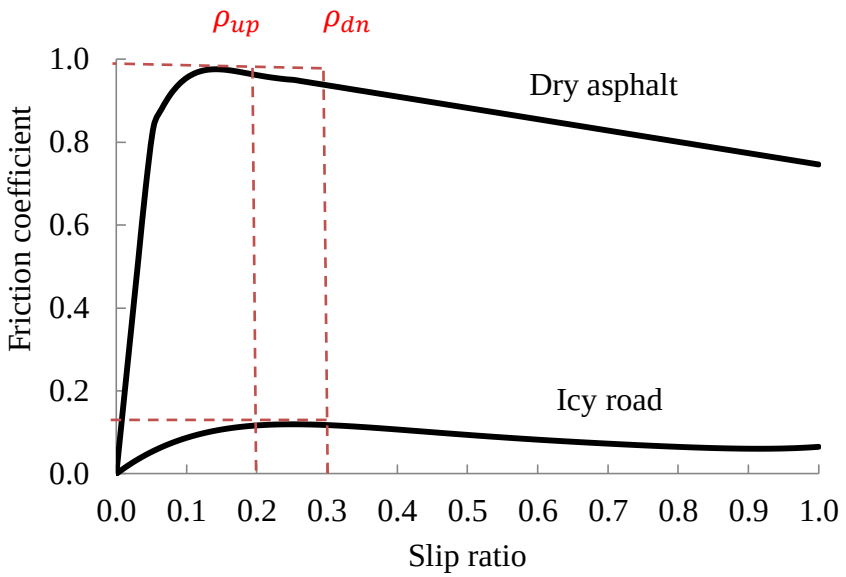

Figure 3-1 Typical friction coefficient and slip ratio curves for icy road and dry asphalt

3.3 Composition of ABS

In general, ABS consists of wheel sensor, electronic control unit (ECU) and hydraulic unit, as schematically shown in Figure 3-2. To monitor the rotation of the individual tires, wheel sensors are mounted directly to the wheeled hubs. They usually generate 90-100 pulses per wheel revolution. The angular speed and angular deceleration (or acceleration) of the tire is derived from these digital pulse signals by differentiation with respect to time. The signals generated by the sensors are transmitted to the electronic control unit for processing.

The control unit usually consists of three modules: a signal processing module, a control module and a monitor module. After the signals generated by the wheel sensors have been processed in the processing module, the measured parameters and/or those derived from them are compared with the corresponding predetermined threshold values. When certain conditions that indicate the impending lockup of the tire are met by the control module, a command signal is sent to the hydraulic unit.

As shown in Figure 3-2, the hydraulic unit is located between the master cylinder and wheel cylinder. It consists of solenoid valves, pump and pistons. There are two types of solenoid valve; IN valve and OUT valve. Generally, solenoid valves have three brake pressure modes, which are increase, hold and reduce. These solenoid valves will open or close based on the signal from the control module. For example, if the signal from control module showing the slip ratio is larger than the optimum range, the OUT valve will open, and the pump begins to operate. Then, the pressure in the wheel cylinder and the braking force at the tire will be decreased. As a result, the slip ratio becomes small, and the friction coefficient becomes large. On the other hand, when the signal from the control module is smaller than the optimum range, the IN valve will open and the OUT valve will close. The pressure in the wheel cylinder and the braking force will be increased, and the slip ratio then becomes large.

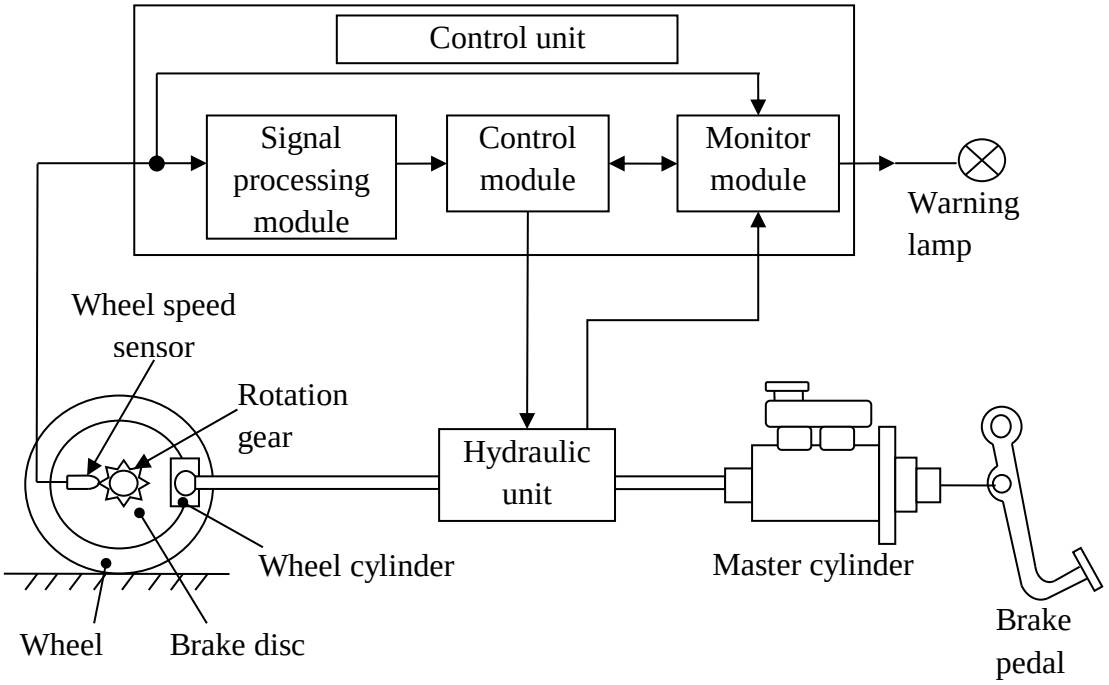

Figure 3-2 Compositions of ABS

3.4 Simulation

3.2.1 Simulation model

The most common layout of anti-lock braking system for passenger cars is the four-channel and four-sensor or three-channel and four-sensor configurations [3-3]. A channel refers to the portion of the brake system where the control unit controls independently of the rest of the brake system. For instance, the four-channel and four-sensor configuration has four hydraulic brake circuits with sensors for monitoring the operating conditions of the four tires separately. Each tire is controlled individually, based on the information obtained by the respective sensors. However, the three-channel and four-sensor configuration has three hydraulic brake circuits. The two front tires are controlled individually, while the two rear tires are jointly controlled.

In this study, the braking system of the analysis vehicle model is hydraulic-mechanical hybrid brake system. As shown in Figure 3-3, this braking system has three hydraulic brake circuit; two between the master cylinder and each front tire, and another one between the master cylinder and rear power cylinder. Due to the space limitation and the mechanical brake system at the rear tire, we choose three-channel and four-sensor configurations of ABS. Figure 3-4 shows the combination of the hydraulic-mechanical hybrid brake system with ABS. In this system, the hydraulic unit of ABS was installed at each front tire and between the master cylinder and rear power cylinder.

3.2.2 Mechanism of the simulation model

The mechanism of this ABS is similar to the commercial ABS, which is based on the slip ratio. By using Eq. (3-1a) and Eq. (3-1b), in case of ABS in action, if $\rho > \rho_{dn}$, the IN valve is closed, the OUT valve is opened, and the pump begins to operate. The pressure in the wheel cylinder and the braking force are decreased. As a result, the slip ratio becomes small, and the friction coefficient becomes large. When $\rho < \rho_{up}$, the IN valve opens and the OUT valve closes again. The pressures in the wheel cylinder and the braking force are increased, and the slip ratio then becomes large. This mechanism is repeated to ensure that the slip ratio is always in the optimum range.

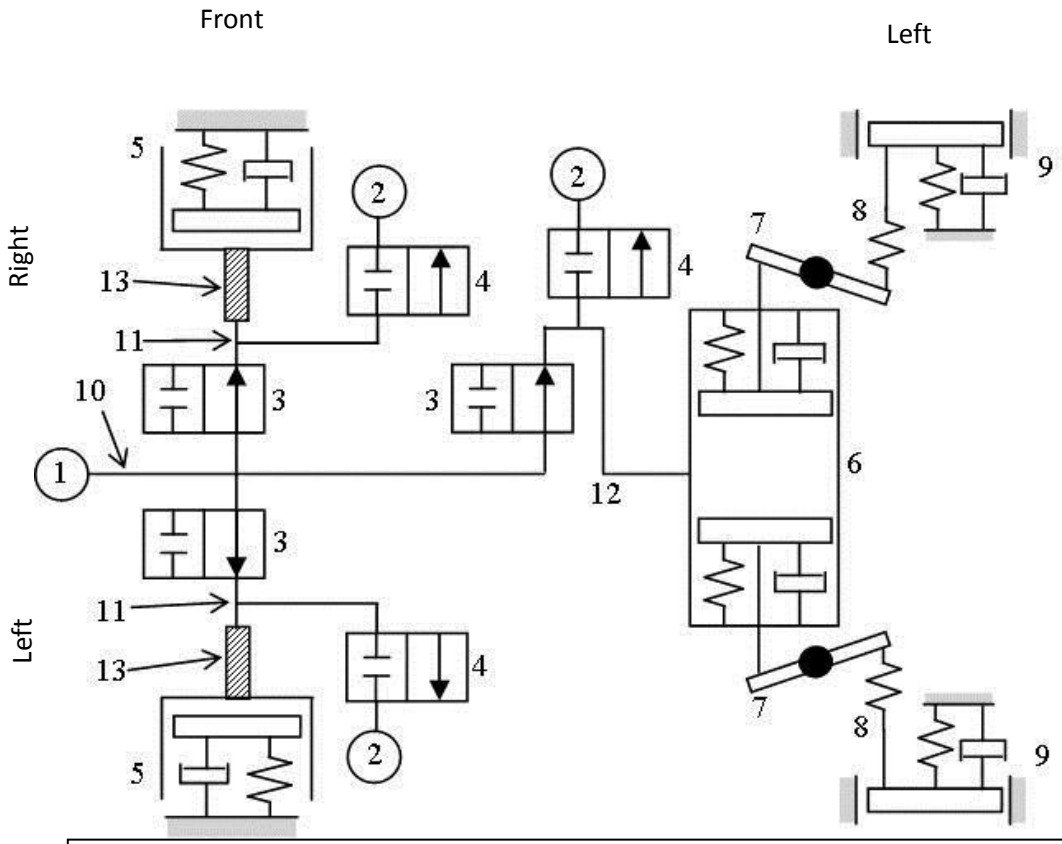

1:Master cylinder	2:Low pressure source	3:IN valve	4:OUT valve
5:Front drum brake	6:Power cylinder	7:Link	8:Wire
9:Rear drum brake	10:Master cylinder line	11:Front hydraulic line	
12:Rear hydraulic line	13:Front brake hose		

Figure 3-4 Hydraulic-mechanical hybrid brake system with ABS

3.2.2 Calculation procedures

Figure 3-5 shows the flow hart of the calculation procedures in the simulation. When a braking torque T_B is applied to the tire, a corresponding torque friction of the tire T_f is developed on the tire ground contact patch, which acts in the opposite direction of the applied braking torque T_B. The difference between T_B and T_F causes an angular acceleration $\dot{\omega}$ of the tire:

$$\begin{cases} T_{ffr} - T_{Bfr} = I_{\omega fr}\frac{d\omega_{fr}}{dt} \\ T_{frr} - T_{Brr} = I_{\omega rr}\frac{d\omega_{rr}}{dt} \end{cases}, \quad \begin{cases} T_{ffl} - T_{Bfl} = I_{\omega fl}\frac{d\omega_{fl}}{dt} \\ T_{frl} - T_{Brl} = I_{\omega rl}\frac{d\omega_{rl}}{dt} \end{cases} \tag{3-2}$$

Where I_ω is the inertia moment of the tire. The inertia moment of front tire is 0.43 kgm^2 and the inertia moment of rear tire is 2.53 kgm^2 [3-4].

In the numerical calculation, we consider that in-wheel motor will produce the regenerative braking torque. Then, the total braking torque for a rear tire is the sum of the mechanical braking torque and the regenerative braking torque. On the other hand, the braking torque for a front tire is only the hydraulic braking torque. Equation (3-3) shows the braking torque at each front and rear tire.

$$\begin{cases} T_{Bfr} = BEF_{fr} \times R_{fr}B_{Ffr} \\ T_{Brr} = (BEF_{rr} \times R_{rr}B_{Frr}) + T_{Rr} \end{cases}, \quad \begin{cases} T_{Bfl} = BEF_{fl} \times R_{fl}B_{Ffl} \\ T_{Brl} = (BEF_{rl} \times R_{rl}B_{Frl}) + T_{Rl} \end{cases} \tag{3-3}$$

Where R is the radius of the brake shoe and BEF is the braking efficiency factor. In the numerical analysis, the value of BEF is set to 1.5.

From Eq. (3-2), we can measure the angular speed of the tire, ω by differentiating $\dot{\boldsymbol{\omega}}$. Then, by using Eq. (3-1a) and Eq. (3-1b), the slip ratio, ρ of the tire can be known. If ρ is not in the optimum range (0.2 to 0.3), the ABS control unit will start to operate to control the braking pressure at the master cylinder. The braking pressure from the master cylinder will be directed to the front wheel cylinder and rear power cylinder.

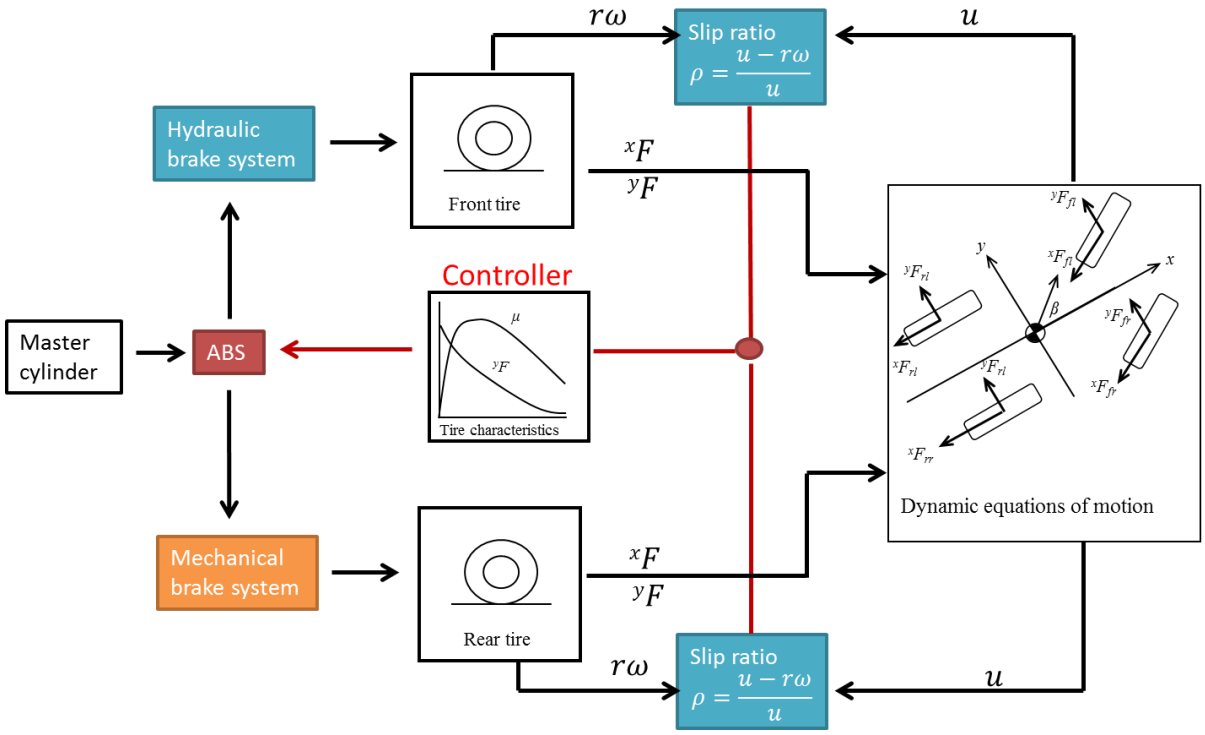

Figure 3-5 Flow chart of the calculation procedures in the numerical analysis

3.5 Results and Discussion

3.5.1 Effect of the hydraulic-mechanical hybrid brake system on an icy road

In the first part of the simulation, the effect of the hydraulic-mechanical hybrid brake system on an icy road is examined. The simulation conditions are as below:

i. Road condition: Icy road
ii. Initial velocity: 30 km/h
iii. Initial braking pressure: 1.8 MPa
iv. Steering angle: 0 degrees
v. Brake system: Hydraulic-mechanical hybrid brake system
vi. ABS: Off

The simulation results are shown from Figure 3-6 to Figure 3-9.

Figure 3-6 shows the effect of the hydraulic-mechanical hybrid brake system to the vehicle velocity and rotational speed of the front and rear tires. From Figure 3-6, during braking on an icy road, the vehicle took 13.2 seconds to completely stop. Although the vehicle took 13.2 seconds to completely stop, the rotational speed of the front and rear tires decreased rapidly. The rotational speed of the front tire decreased rapidly from 8.3 m/s to 0 m/s in 0.3 seconds, while the rotational speed of the rear tire decreased from 8.3 m/s to 0.5 m/s in 2 seconds.

The slip ratios of the front and rear tires are shown in Figure 3-7. From Figure 3-7, the slip ratio of the front tire increased rapidly to 1.0 in 0.3 seconds, while the slip ratio of the rear tire increased to 0.9 in 2 seconds. In this situation, the front and rear tires are locked and the vehicle is skidding. This phenomenon can be explained by examining the braking force and friction force at the front and rear tires.

Figure 3-8 shows the braking force at the front and rear tires. The braking force on the front tire is constant at 1100 N from the beginning until the end. The front brake system is a hydraulic brake system. The braking pressure generated from the master cylinder is directed to the front wheel cylinder. As a result, the braking force at the front tire is high and constant. On the other hand, the rear brake system is the mechanical brake system. Due to the rigidness and low response performance of the mechanical brake system, the mechanical braking force is very small. Although the mechanical braking force is small, the in-wheel motor at the rear

tire produced regenerative braking force during braking. The regenerative braking force is parallel to the rotational speed of the tire. Without regenerative brake control, the regenerative braking force is decreased from 4700 N to 300 N in 2 seconds.

The friction forces of the front and rear tires are shown in Figure 3-9. From Figure 3-9, it can be seen that the friction force on the front and rear tires is small. In general, compared to the dry asphalt, the friction coefficient of the icy road is very small. As a result, the friction force produced between the tire and the contact patch is very small.

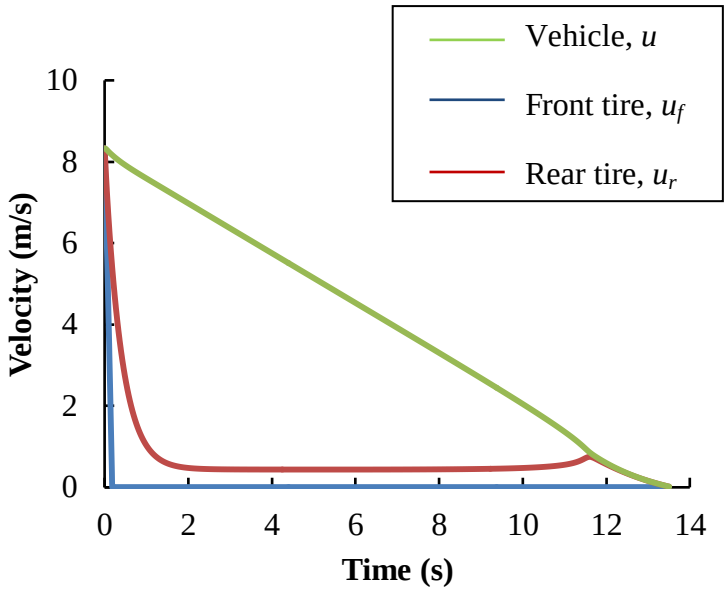

Figure 3-6 Change of vehicle velocity and rotational speed of front and rear tires

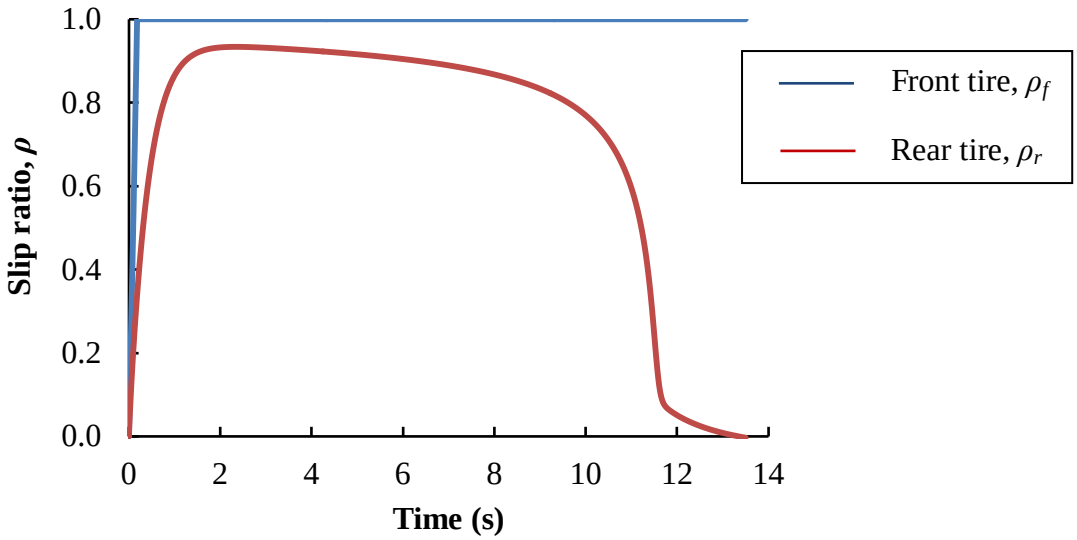

Figure 3-7 Slip ratio of the front and rear tires

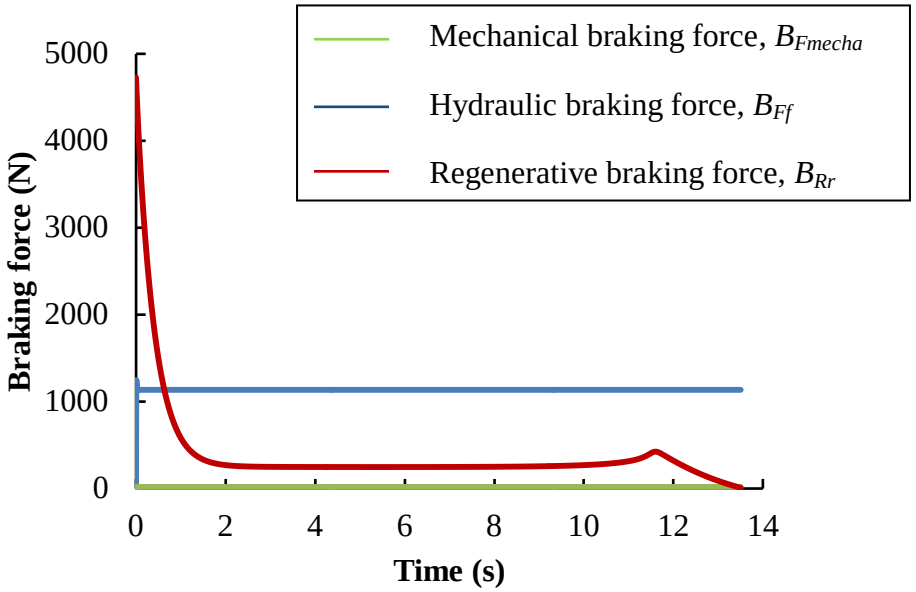

Figure 3-8 Change of braking force at the front and rear tires

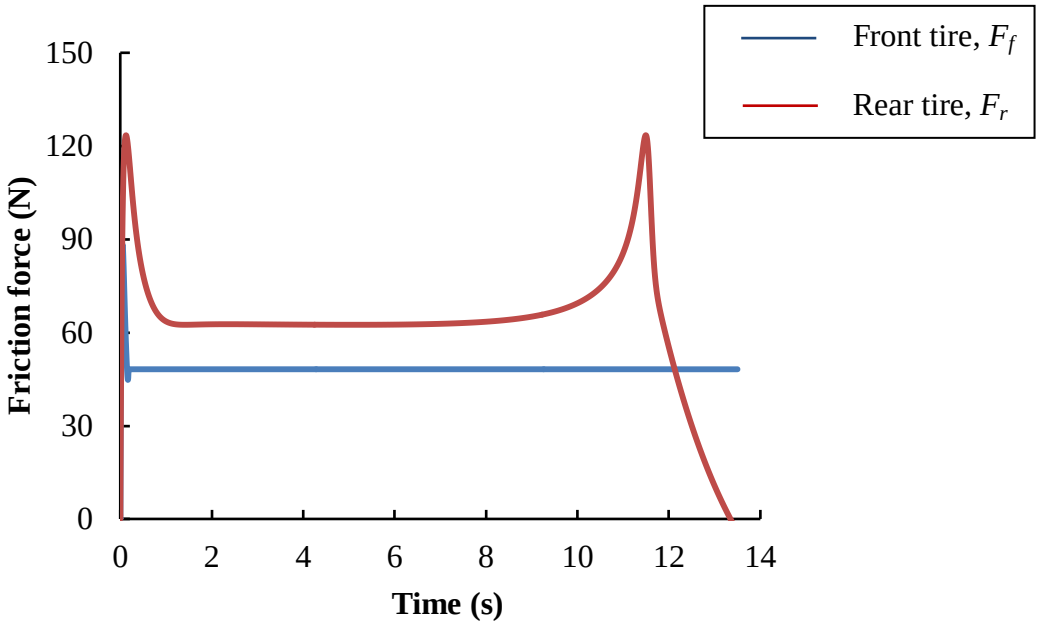

Figure 3-9 Change of friction force at the front and rear tires

3.5.2 Effect of the hydraulic-mechanical hybrid brake system with ABS on an icy road

In the second part of our simulation, the effect of the hydraulic-mechanical hybrid brake system with ABS on an icy road is examined. The simulation conditions are as below:

i. Road condition: Icy road
ii. Initial velocity: 30 km/h
iii. Steering angle: 0 degrees
iv. Brake system: Hydraulic-mechanical hybrid brake system
v. ABS: ON

The simulation results are shown from Figure 3-10 to Figure 3-13.

Figure 3-10 shows the vehicle velocity and rotational speed of the front and rear tires. From Figure 3-10, the vehicle took 10 seconds to a complete stop, which is 3.2 seconds shorter than without ABS. Due to the operational of ABS, the rotational speed of the front tire was fluctuated. Although the hydraulic unit of ABS was installed between the master cylinder and rear power cylinder, the rotational speed of the rear tire decreased rapidly due to the rigidness of the mechanical system between the power cylinder and rear drum brake.

The slip ratio of the front and rear tires are shown in Figure 3-11. From Figure 3-11, during braking on an icy road and ABS ON, the slip ratio of the front tire is fluctuating in the optimum range. On the other hand, the slip ratio of the rear tire is increased rapidly to 0.9 in 2 seconds. In this situation, the front tire was not locked, but the rear tire was almost locked.

The effect of the hydraulic-mechanical hybrid brake system with ABS to the braking force is shown in Figure 3-12. During braking on an icy road and with ABS, the braking force at the front tire is fluctuating. Based on the slip ratio of the front tire, the IN valve and OUT valve will open and close to obtain the optimum braking force. As a result, the braking force at the front tire is fluctuating during braking on an icy road. However, the optimum braking force on the rear tire cannot be obtained due to the rigidness of the mechanical brake system.

Figure 3-13 shows the effect of the hydraulic-mechanical hybrid brake system with ABS to the friction force. From Figure 3-13, it can be seen that the friction force of the front tire is 2 times higher than the friction force without ABS. Although the friction coefficient of the icy road is very small, ABS can maximize the braking force at the front tire and as a result, the

friction force between the tire and the contact patch is increased. On the other hand, the friction force of the rear tire is similar to the one with ABS disabled.

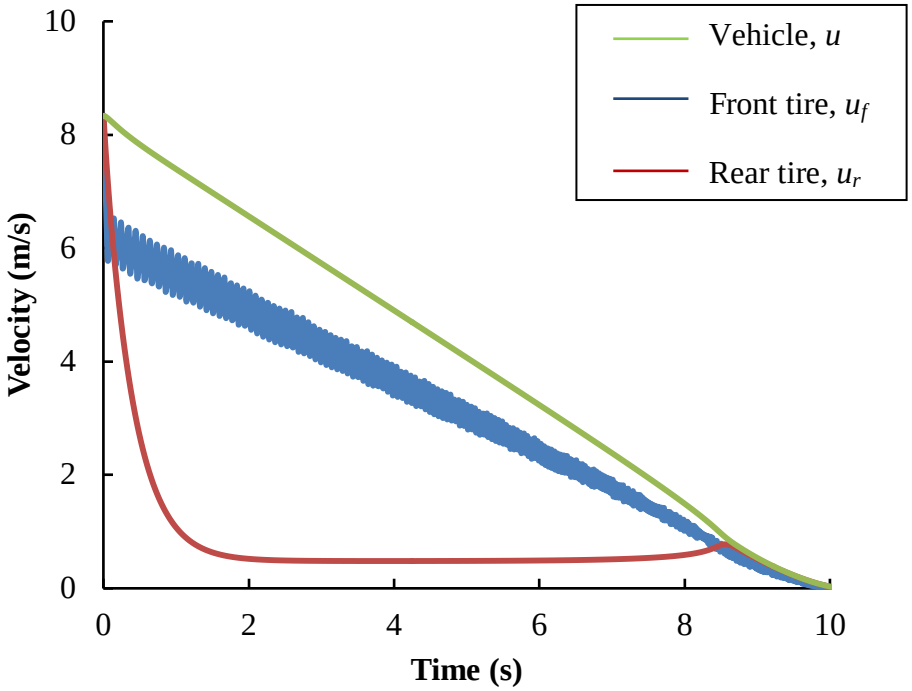

Figure 3-10 Change of vehicle velocity and rotational speed of the tire

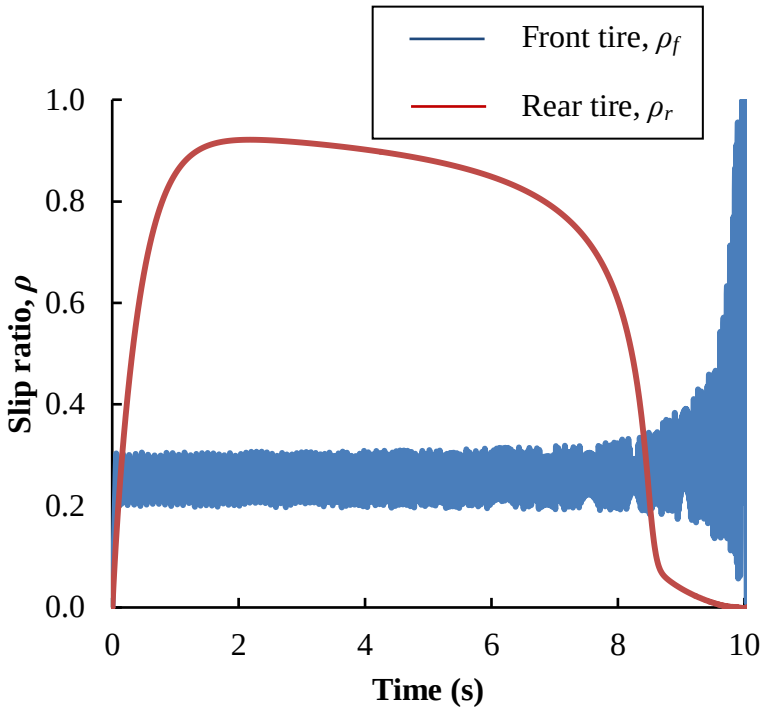

Figure 3-11 Slip ratio of front and rear tires

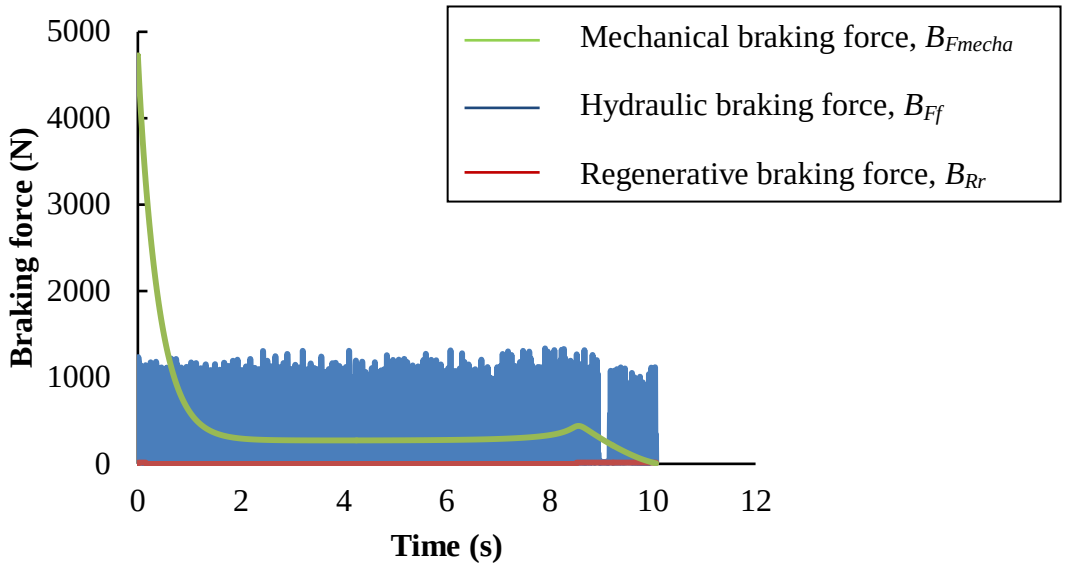

Figure 3-12 Braking force at the front and rear tires

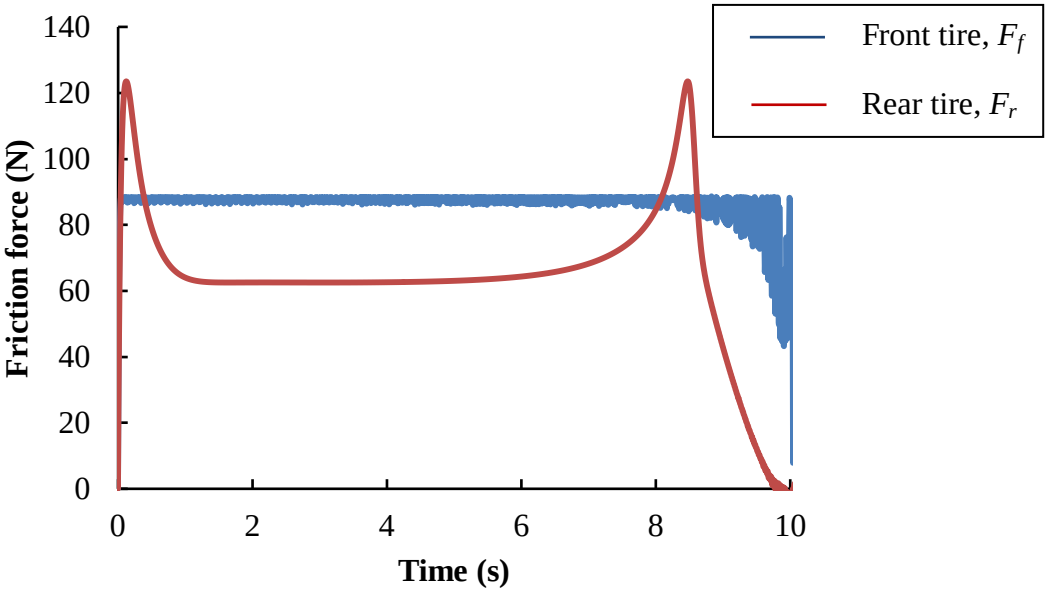

Figure 3-13 Friction force at the front and rear tires

3.6 Summary

In this chapter, the simulation model of hydraulic-mechanical hybrid brake system with ABS has been developed. The findings from the simulation results are as below:

1. During braking on icy road, without ABS, the tire locked-up occured and caused skidding of the vehicle.
2. The combination of hydraulic-mechanical hybrid brake system with ABS can prevent the front tire from being locked-up and have the slip ratio of front tire always kept in the optimum range.
3. Although the hydraulic unit of ABS was installed between the master cylinder and rear power cylinder, due to the rigidness of the mechanical brake system, the rear tire was locked-up and the slip ratio was over the optimum range.
4. The regenerative brake torque produced from the in-wheel motor is needed to control to prevent rear tire from locking-up during braking on an icy road.

Chapter 4

HYDRAULIC-MECHANICAL HYBRID BRAKE SYSTEM WITH ABS AND REGENERATIVE BRAKE CONTROL

4.1 Introduction

In this chapter, the combination of hydraulic-mechanical hybrid brake system with ABS and regenerative brake control is developed. First, the theory and the mechanism of the regenerative brake are described. From the theory of the regenerative brake, it is necessary to measure the optimum value of the regenerative brake coefficient. The experiment is developed to measure the optimum value of the regenerative brake coefficient. By using the optimum value of the regenerative brake coefficient, the simulation model of the hydraulic-mechanical hybrid brake system with ABS and regenerative brake control is constructed. The simulation results are presented and discussed. Lastly, the findings from the simulation results are described in the summary.

4.2 Fundamentals of the regenerative brake

One of the most important features of electric vehicles (EVs) is their ability to recover significant amounts of braking energy. The electric motor can be controlled to operate as a generator during braking to convert the kinetic energy of the vehicle into electrical energy that can be stored in the energy storage system and reused. Generally, there are two basic regenerative braking methods used today, which are parallel regenerative braking and series regenerative braking.

- Parallel regenerative braking

During parallel regenerative braking, both the electric motor and mechanical braking system always work in parallel to decrease the rotational speed of the tire [4-1]. Figure 4-1shows the parallel regenerative braking strategy. During braking, the mechanical braking cannot be controlled independently and some of the kinetic energy is converted into heat energy instead of electrical energy. The parallel regenerative braking does have the advantages of being simple and cost effective. This method also has the added advantage of always having the mechanical braking system as a back-up in case of a failure of the regenerative braking system.

- Series regenerative braking

During series regenerative braking, the electric motor is solely used for braking. It only operates when the motor or energy storage system can no longer accept more energy from the electric motor [4-1]. This method requires that the mechanical braking torque be controlled independently of the brake pedal force. Figure 4-2 shows the series regenerative braking strategy. The downfall of this method is that it brings a high cost and complexities into systems. For this method to function properly, a brake-by-wire has to be developed which either uses an electro-hydraulic brake (EHB) or an electro-mechanical brake (EMB). Both of these types require brake pedal simulators and redesigned brake systems which can become costly. Since these systems are brake-by-wire, there are also many redundancies required with sensors, processors and wiring for safety which will add more complexity of the system.

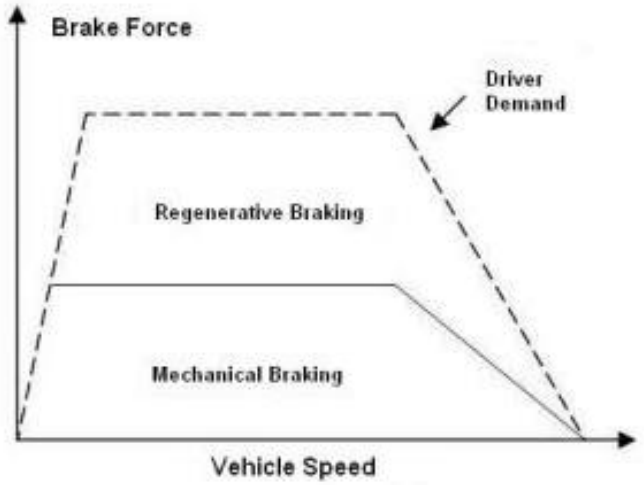

Figure 4-1 Parallel regenerative braking strategy

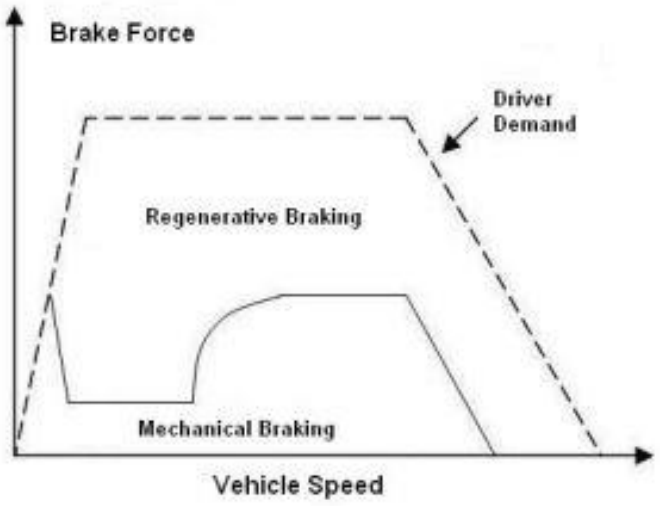

Figure 4-2 Series regenerative braking strategy

4.3 Numerical Analysis

4.3.1 Regenerative braking torque

Figure 4-3 shows the ideal braking force distribution used to determine the percentage of regenerative brake force and mechanical brake force. From the actual brake curve, by taking the front brake force produced when the coefficient of friction is in maximum value, the maximum value of rear brake force can be calculated. The equation of ideal braking force at the rear tire is shown in Eq. (4-1):

$$B_{Fmecha} + B_{Freg} = B_{Fideal} \tag{4-1}$$

where, B_{Fmecha} is a mechanical brake force, B_{Freg} is a regenerative brake force and B_{Fideal} is an ideal brake force for the rear tire. During ABS operation, due to the rigidity of the mechanical brake system, a response performance of the mechanical braking system is low and the time delay occurs. To compensate the lost friction force at the mechanical braking system, we proposed the regenerative brake control timing. The regenerative brake control timing operates similarly to ABS, which is based on the slip ratio. If $\rho > \rho_{dn}$, the regenerative brake turns off and the current produced is transferred to charge the battery. However, if $\rho < \rho_{up}$, the regenerative brake is turned back on to regain the ideal brake force.

In general, the regenerative braking torque that an in-wheel motor can produce is proportional to a wheel speed. Then, the regenerative braking torque and the regenerative brake force can be calculated by using Eq. (4-2) and Eq. (4-3).

$$T_{Rr} = C_R r \omega_r \quad , \quad T_{Rl} = C_R r \omega_l \tag{4-2}$$

$$B_{Rrr} = \frac{T_{Rr}}{R_{rr}} \quad , \quad B_{Rrl} = \frac{T_{Rl}}{R_{rl}} \tag{4-3}$$

where, T_R is the regenerative brake torque, C_R is the regenerative brake coefficient, r is the wheel radius, ω is the tire angular velocity, and B_R is the regenerative brake force.

4.3.2 Regenerative brake control

In general, an in-wheel motor on each wheel provides the possibility of enhanced vehicle motion control [4-2]. However, the excessive regenerative braking torque can result in the locked-up of the EV's wheel especially during braking on an icy road and emergency braking. On the other hand, the introduction of the ABS has contributed to improve the safety of the vehicles decisively by automatically controlling the brake force during braking in potentially dangerous conditions [4-3]. Due to the characteristics of the in-wheel motor, which is the torque response is fast and accurate, the in-wheel motor can be an actuator of ABS to control the regenerative braking torque on the driving tire.

Figure 4-4 illustrates the typical friction coefficient and slip ratio curves for the dry asphalt and icy road [4-4]. This figure is used as a reference in the regenerative brake control. Wheel skid will occur when the large regenerative braking torque is rapidly generated at the wheel. This will cause the wheel to lock-up and the vehicle to skid. The slip ratio is used to check if the wheel is locked or not and the equation of slip ratio during braking is [4-5] ~ [4-9]:

$$\rho = \frac{u - r\omega}{r\omega} \tag{4-4}$$

where u is the wheel absolute velocity or vehicle chassis velocity in the longitudinal direction. r and ω are the wheel radius and tire angular velocity respectively. When the slip ratio rapidly increases towards 1.0, the braking force and the side force generation on the wheel will be disappeared. This causes unstable vehicle motion and can be a dangerous spin motion.

In this study, based on the Figure 4-4, the regenerative brake control timing is proposed [4-10]-[4-11]. The regenerative brake control timing operates similarly to ABS, which is based on the slip ratio. If $\rho > \rho_{dn}$, the regenerative brake turns off and the current produced is transferred to charge the battery. However, if $\rho < \rho_{up}$, the regenerative brake is turned back on to regain the ideal brake force. From this mechanism, the braking force on the rear tire can be maximized and prevent wheel from being locked during braking on an icy road or under emergency braking.

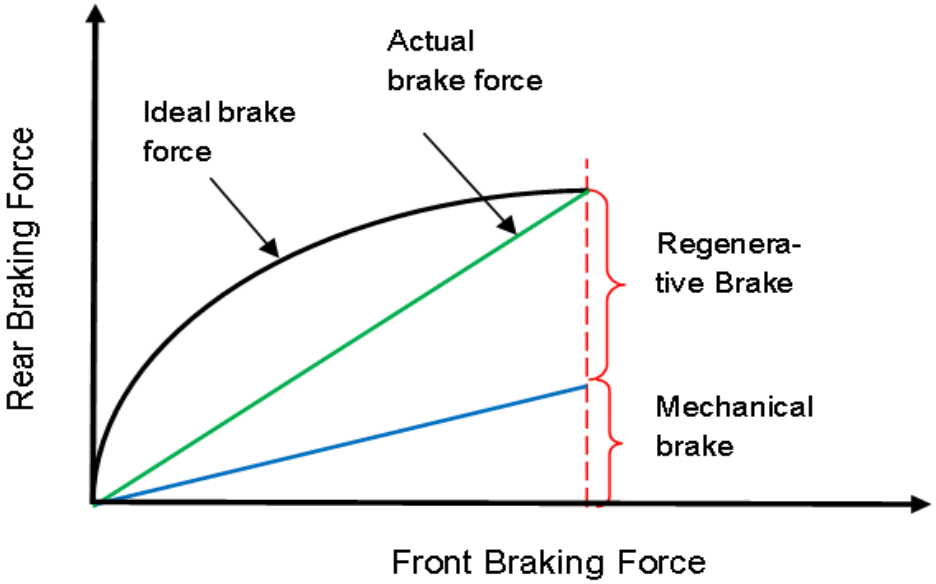

Figure 4-3 Ideal braking force distribution

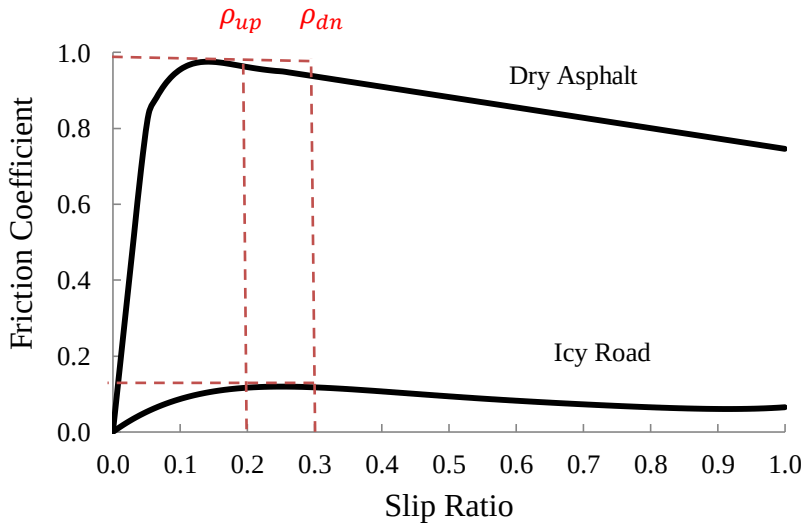

Figure 4-4 Typical friction coefficient and slip ratio curves for icy road and dry asphalt

4.3.3 Calculation procedures

Figure 4-5 shows the calculation flow chart for hydraulic-mechanical hybrid brake system with ABS and regenerative brake control. When a braking was applied, an in-wheel motor produced the regenerative braking torque. During braking on an icy road, when slip ratio, ρ is not in the optimum range (0.2 to 0.3), ABS will start to operate. The solenoid valves in the hydraulic unit of ABS were open or close to obtain the optimum braking pressure in the front wheel cylinder. On the other hand, the regenerative brake control timing operates similarly to ABS, which is based on the slip ratio. If slip ratio, $\rho > \rho_{dn}$, the regenerative brake turns off and the current produced is transferred to charge the battery. However, if the slip ratio, $\rho < \rho_{up}$, the regenerative brake is turned back on to regain the ideal brake force.

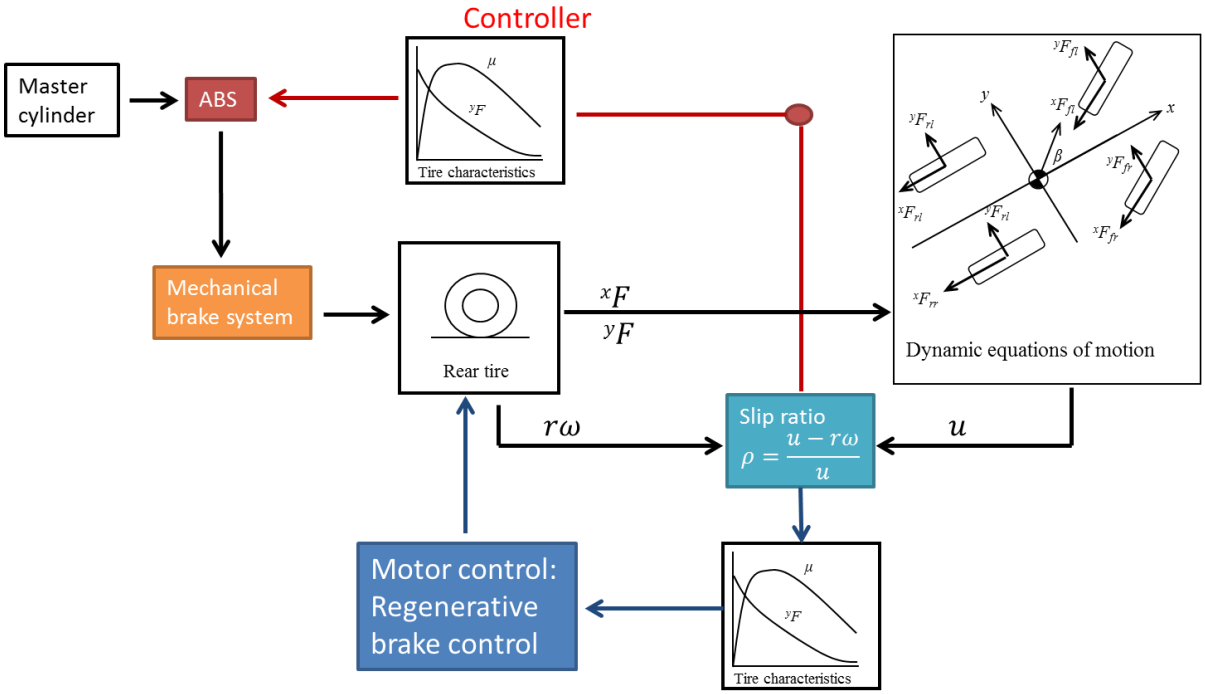

Figure 4-5 Calculation flow chart of the hydraulic-mechanical hybrid brake system with ABS and regenerative brake control

4.4 Analysis of the Regenerative Brake Coefficient

In this study, the experiment and simulation have been developed to measure the optimum value of the regenerative brake coefficient. This value is needed to be measured because it can affect the regenerative braking torque. The experimental results are compared to the simulation results to obtain the optimum value of the regenerative brake coefficient.

4.4.1 Experimental equipments and methods

Figure 4-6 shows the brake pedal force generator. The function of the brake force generator is to obtain the constant braking pressure in the master cylinder. From Figure 4-6 (a), the brake force generator consists of first lever (i), second lever (ii), brake pedal force stopper (iii) and brake pedal (iv). As shown in Figure 4-6 (b), the bolt (v) was installed on the brake pedal force stopper (iii). The function of the bolt (v) is to hold the first lever (i) and second lever (ii) at the certain degrees. This will allow the constant force on the brake pedal (iv). The constant force from the brake pedal (iv) will generate the constant braking pressure in the master cylinder. By using this mechanism, the constant braking pressure can be obtained.

Figure 4-7 shows the schematic figure of the sensors that were installed on the experimental vehicle, while Table 4-1 shows the function of each sensor. In the experiment, we have set several parameters such as a dry asphalt road and a steering angle at 0 degree. During braking, we assume that an in-wheel motor will continuously produce the regenerative braking force. First, the driver will push an accelerator pedal until the speed meter reaches 30 km/h. When the speed meter is 30 km/h, the driver will push a lever of the brake force generator until the vehicle completely stop. The experiment with the same condition was repeated in three times and the experimental data have been summarized into minimum value, average value and maximum value.

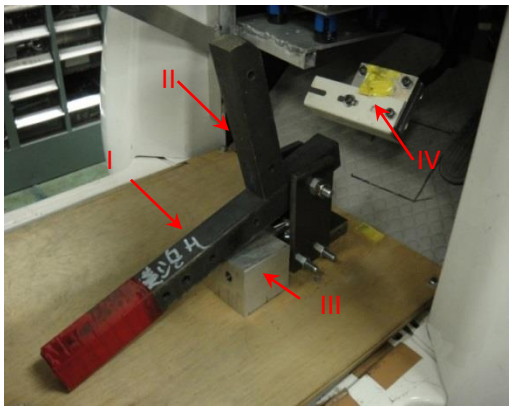

(a) Brake pedal force generator

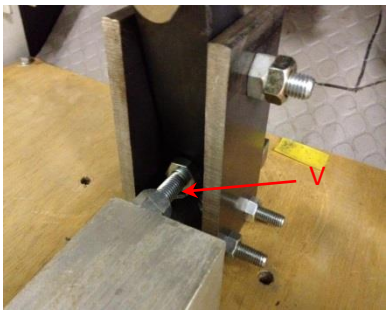

(b) Brake pedal force stopper

I: First lever
II:Second lever
III:Brake pedal force stopper
IV:Brake pedal
V: Bolt

Figure 4-6 Experimental setup. The brake force generator contains three components, which are first lever, second lever and brake pedal force stopper. The bolt was installed in the brake pedal force stopper to obtain the constant force.

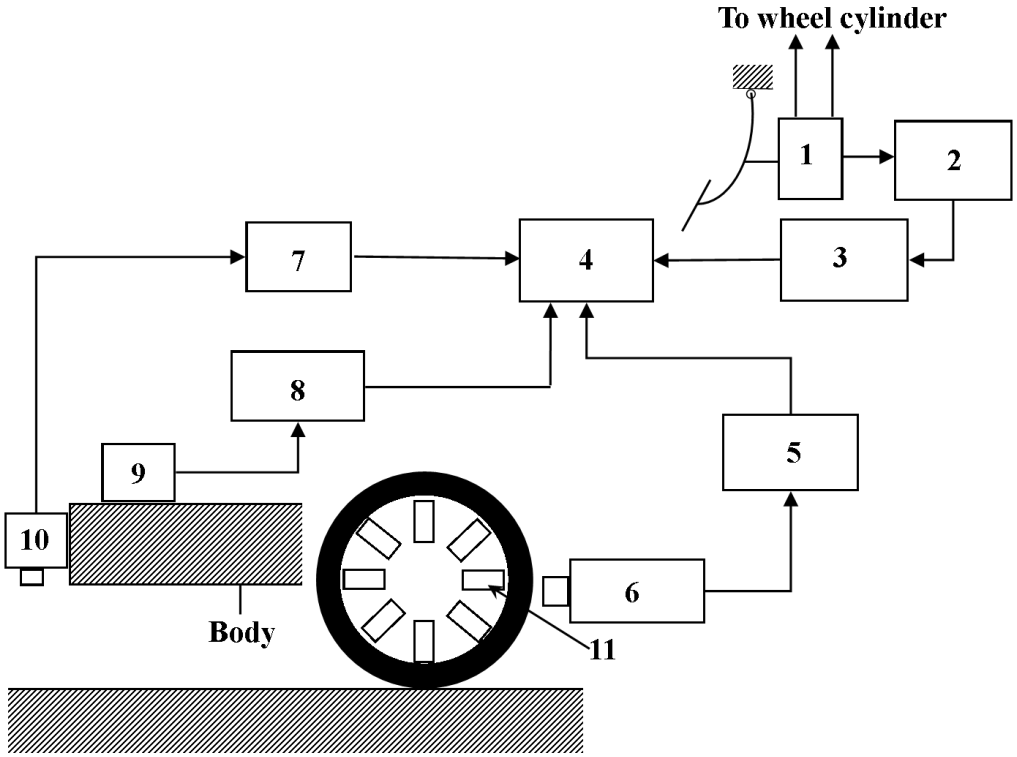

1: Master cylinder (NISSIN 11/16) 2: Fluid pressure sensor (KYOWA PGM-500KD)

3: Strain amplifier (KYOWA DPM-713B) 4: Data logger (KEYENCE NR-2000)

5: Digital rotation recorder (ONO SOKKI TM-3130)

6: Photoelectric rotation detector meter (ONO SOKKI LG-916)

7: Converter box 8: Strain amplifier (KYOWA DPM-601B)

9: Acceleration sensor (KYOWA AS-10B)

10: Photoelectric longitudinal speed detector meter (ONO SOKKI LC-3110)

11: Reflection tape

Figure 4-7 Experimental devices

4.5 Results and Discussion

4.5.1 Optimum value of the regenerative brake coefficient

The first part of this study is to measure the optimum value of the regenerative brake coefficient, C_R. Figure 4-7 shows the experimental result of the braking pressure in the master cylinder. As shown in Fig. 4-8 (a), during braking, due to the roughness of the road, the vehicle was vibrating. This causes the lever at the brake force generator to vibrate. As a result, the constant braking pressure cannot be obtained. However, from Fig. 4-8 (a), the experimental average value is close to the driver's desired braking pressure, which is 1.5 MPa. In the numerical analysis, the experimental average value is used as an input of the braking pressure. Then, from the experimental average value, we can compare the experimental result with the simulation result to measure the optimum value of the regenerative brake coefficient.

The effect of the braking pressure to the stopping distance is shown in Fig. 4-8 (b). From this result, the stopping distance for the minimum braking pressure is longer than the average and the maximum braking pressure. The minimum braking pressure took 8.7 m, while the average and the maximum braking pressure took 8.4 m and 7.9 m respectively. This result shows that the stopping distance of the vehicle is decreased when the braking pressure generated in the master cylinder is increased.

Then, to obtain the optimum value of the regenerative brake coefficient, we have compared the experimental results with the simulation results. In the simulation, three values of the regenerative brake coefficient have been used, which are 15, 20 and 25. Figure 4-9, 4-10 and 4-11 shows the experimental result and the simulation result of the vehicle velocity, rotational speed of the front tire and rotational speed of the rear tire respectively. As shown in Fig. 4-9, 4-10 and 4-11, when the regenerative brake coefficient is 20, the vehicle speed and the rotational speed of the front and rear tire always near to the experimental minimum, average and maximum value. However, when the regenerative brake coefficient is 15, starting from 1 second until the end, the vehicle speed is more than the experimental maximum value and when the regenerative brake coefficient is 25, starting from 0.1 second, the vehicle speed and the rotational speed of the front and rear tire is always less than experimental minimum value. From these results, we can say that the optimum value of the regenerative brake coefficient is 20. This value will be used in our numerical analysis to recognize the effect of the HMBS with ABS and regenerative brake control.

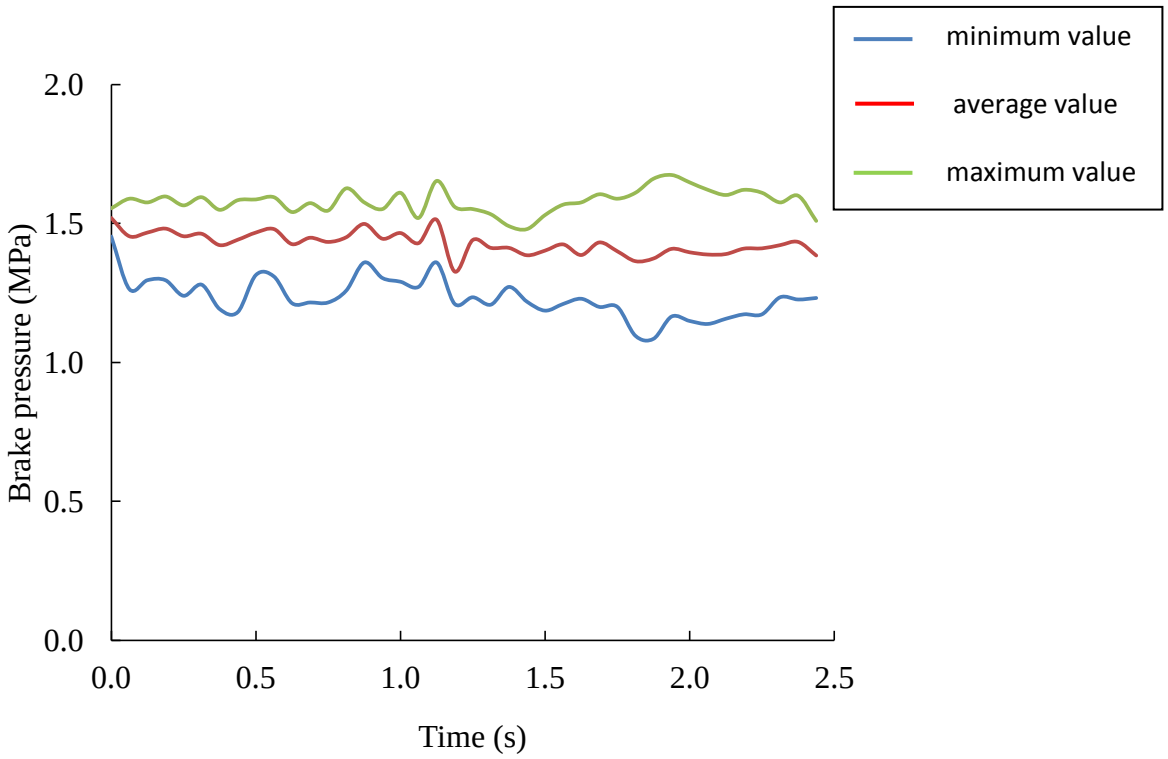

(a) Effect of the braking pressure to the stopping time

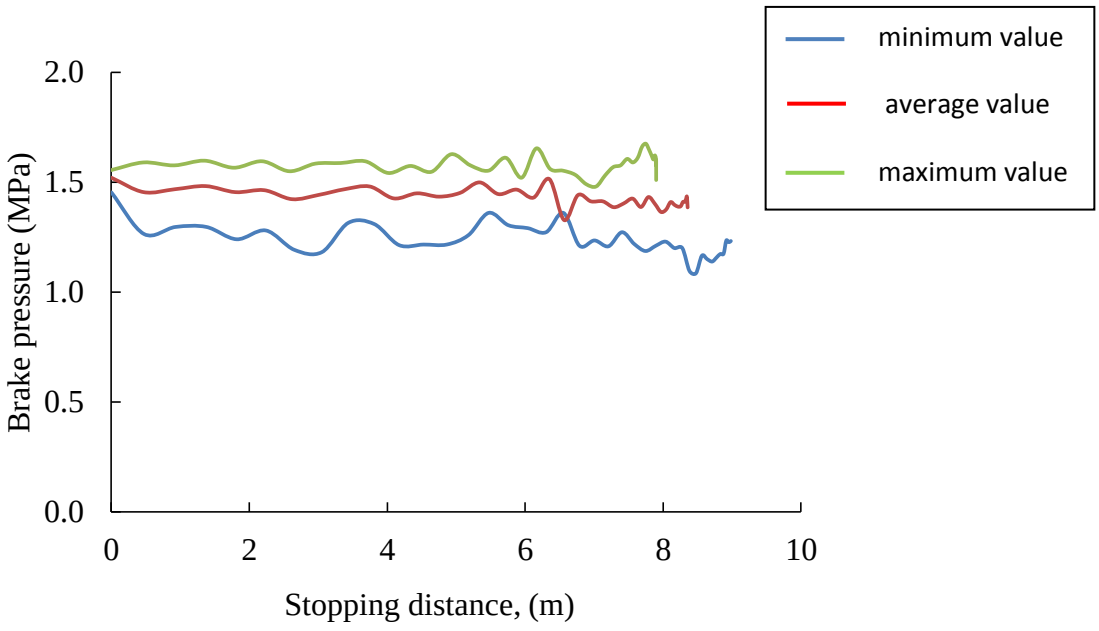

(b) Effect of the braking pressure to the stopping distance

Figure 4-8 Braking pressure in the master cylinder

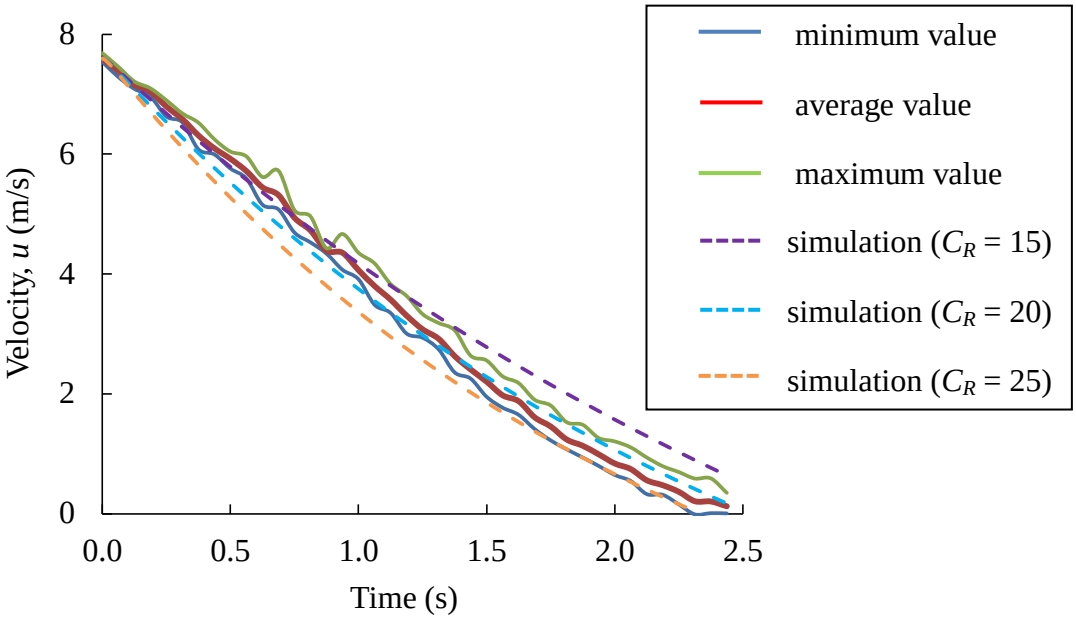

Figure 4-9 Change of the vehicle velocity

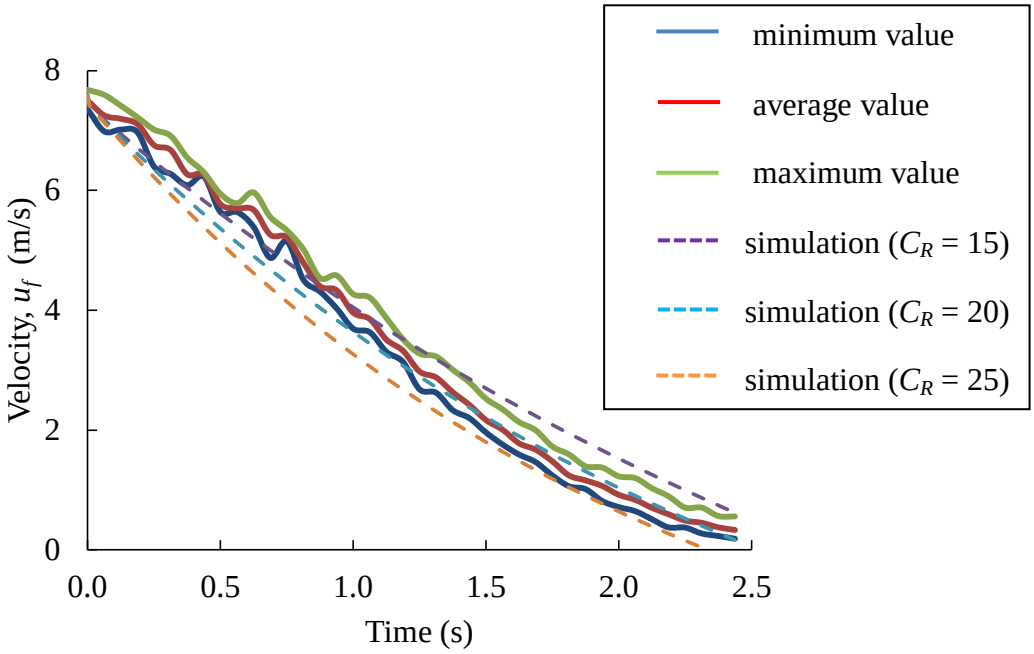

Figure 4-10 Change of the front tire rotational speed

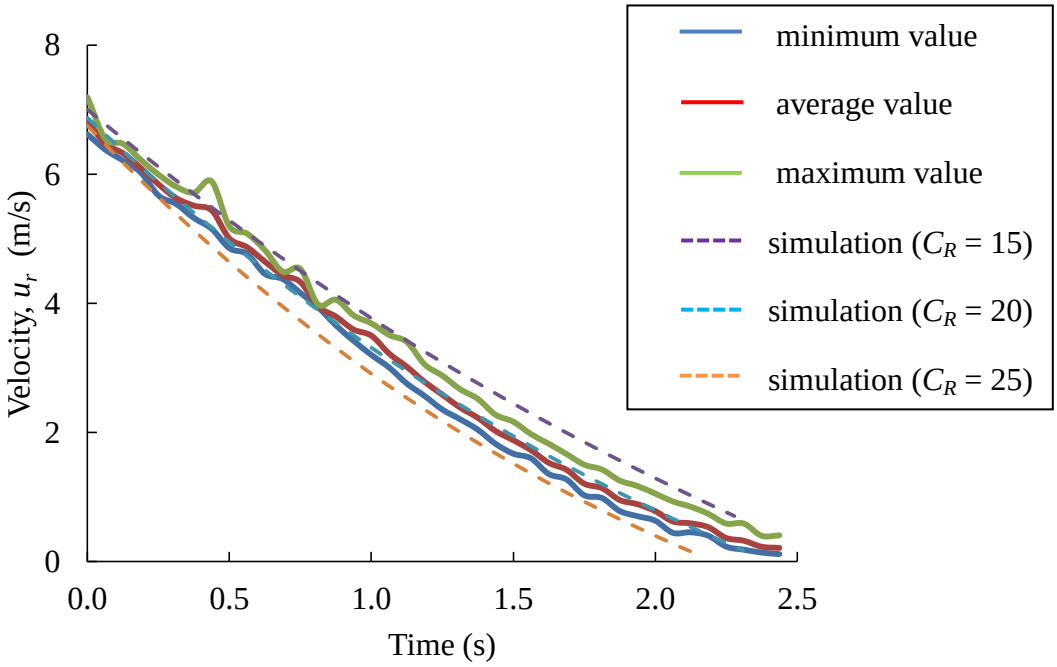

Figure 4-11 Change of the rear tire rotational speed

4.5.2 Effect of the hydraulic-mechanical hybrid brake system to the ABS and regenerative brake control

In this part, the effect of the ABS and regenerative brake control to the vehicle motion have been done in a simulation with two conditions; ABS and regenerative brake control OFF, and ABS and regenerative brake control ON. In the simulation, we have set several parameters which are, the initial vehicle velocity is 30 km/h, the initial braking pressure is 1.5 MPa, the steering angle is 30 degrees and the road condition is icy road. Figure 14 illustrates the vehicle trajectory in X and Y axis. From Fig. 4-11, in case of ABS and regenerative brake control OFF, a farther stopping distance and an under steering was produced. However, in case of ABS and regenerative brake control ON, a shorter stopping distance and more control over steering was produced.

The result of the vehicle speed, tire rotational speed and slip ratio can be used to describe the effectiveness of the ABS and regenerative brake control on the turning motion. Figure 4-12 shows the deceleration of the vehicle speed and tire rotational speed in case of ABS and regenerative brake control is OFF, while Fig. 16 shows the deceleration of the vehicle speed and tire rotational speed in case of ABS and regenerative brake control ON. From Fig. 4-12, the vehicle velocity, u took 13 seconds to a complete stop on an icy road, but the rotational speed of the front and rear tire, u_{fr}, u_{fl}, u_{rr}, u_{rl} were decreased rapidly. However, in case of ABS and regenerative brake control ON (Fig. 4-13), the vehicle velocity, u took 9 seconds to a complete stop and all of the tires were decreased gradually.

The result of slip ratio in case of ABS and regenerative brake control OFF was shown in Fig. 4-14, while the result of slip ratio in case of ABS and regenerative brake control ON was shown in Fig. 4-15. From Fig. 4-14, it can be seen that the slip ratio of front tire, ρ_{fr}, ρ_{fl} are rapidly become to 1.0, while the slip ratio of rear tire, ρ_{rr}, ρ_{rl} are increase rapidly to to 0.9 before decrease rapidly from 0.8 to 0 on 9 seconds.This result means that the tire is locked and the vehicle is skidding. In this situation, although the driver pushes a steering with the certain angle, the vehicle cannot turn with the driver desired direction. However, in case of ABS and regenerative brake control ON, from Fig. 4-15, we can see that the slip ratio of the front and rear tire, ρ_{fr} ,ρ_{fl}, ρ_{rr} ,ρ_{rl} are fluctuating and in the optimum range. In this situation, the vehicle was not skidding and the vehicle can be turned better than without ABS and regenerative brake control. The result in this section approved that when a small electric vehicle was braking on an icy road, ABS and regenerative brake control can improve the steering performance and the stability of the vehicle.

The next step of this study is to observe the effect of the ABS and regenerative brake control to the braking force at the front and rear tire. Figure 4-16 shows the braking force in case of ABS and regenerative brake control OFF while Fig. 4-17 shows the braking force in case of ABS and regenerative brake control ON. From Fig. 14-16, during braking, the braking pressure from the master cylinder is directed to the front wheel cylinder. In case of ABS OFF, the braking force at the front tire, B_{fr}, B_{fl} are very large. However, for a rear braking force, due to the rigidness of the mechanical brake system, the mechanical braking force B_{rr}, B_{rl} are very small. At the same time, an in-wheel motor produces the regenerative braking force, B_{Rrr}, B_{Rrl} which are proportional to the rotational speed of the tire. In case of regenerative brake control OFF, the regenerative braking force was decreased rapidly. On the other hand, from Fig. 4-17, in case of ABS and regenerative brake control ON, we can see the fluctuation at the front braking force, B_{fr}, B_{fl} and at the regenerative braking force, B_{Rrr}, B_{Rrl}. To keep the slip ratio in the optimum range, the IN valve and OUT valve will open and close to control the braking pressure at the front wheel cylinder, then the optimum braking force at the front tire, B_{fr}, B_{fl} are achieved. Similar to ABS, in case of regenerative brake control ON, when slip ratio increased more than the optimum value, the regenerative brake is turned off and the excessive energy is used to charge the battery. When the slip ratio decreased below than the optimum value, the regenerative brake force is again restored.

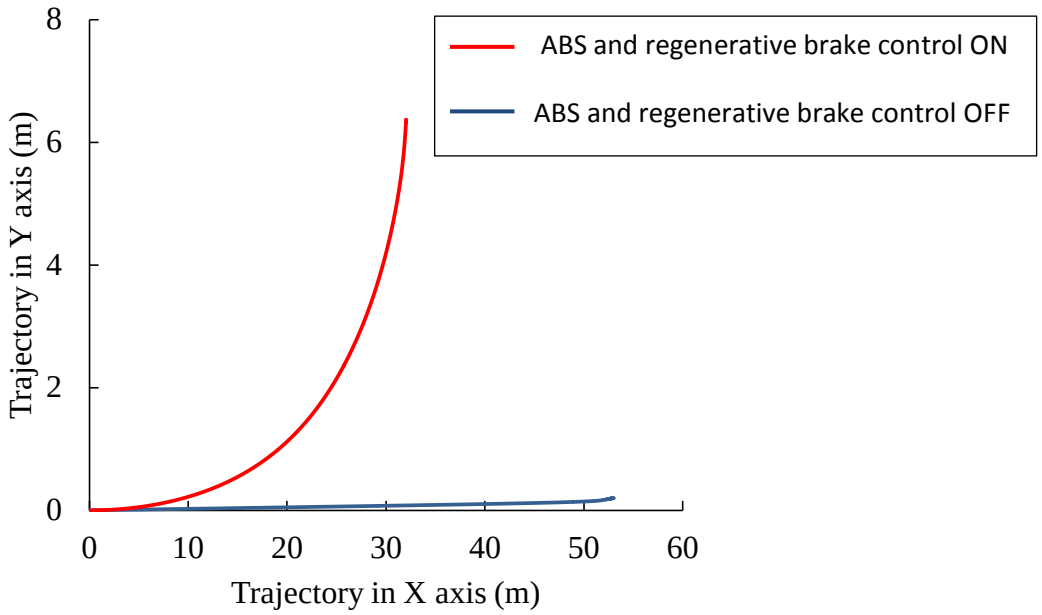

Figure 4-11 Effect of the hydraulic-mechanical hybrid brake system with ABS and regenerative brake control to the vehicle motion

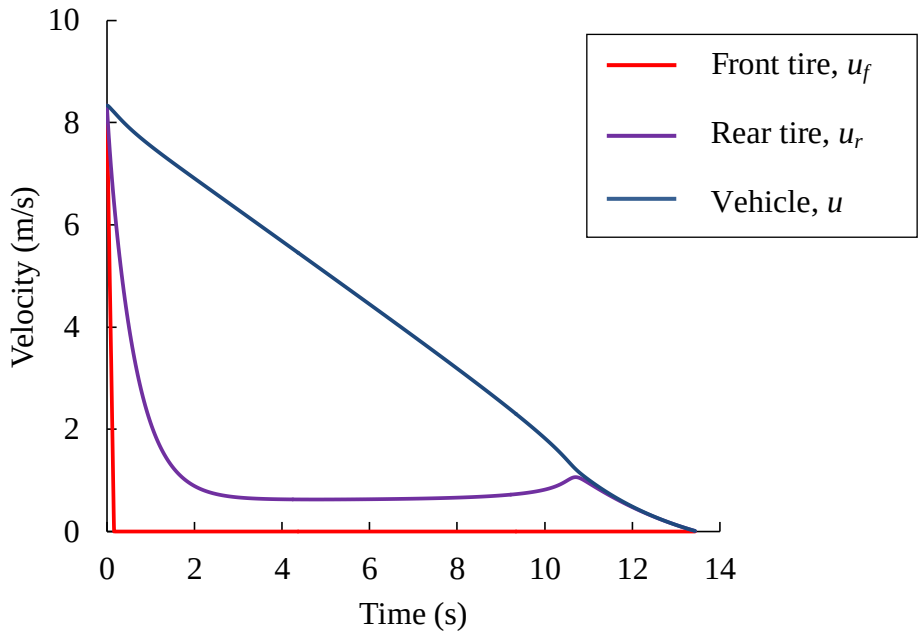

Figure 4-12 Change of vehicle velocity and rotational speed of the front and rear tires without ABS and regenerative brake control

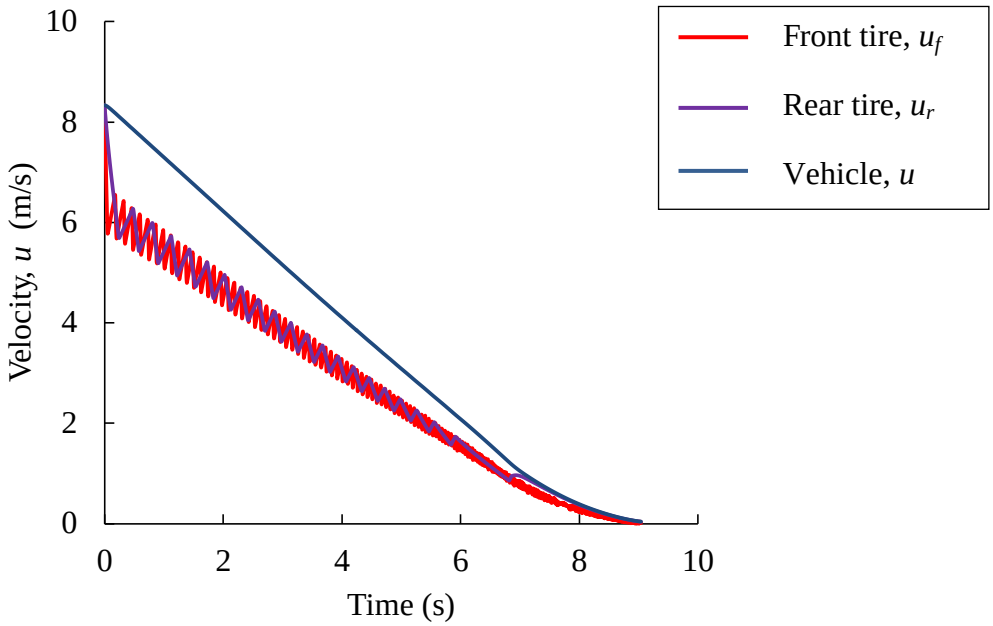

Figure 4-13 Change of vehicle velocity and rotational speed of the front and rear tires with ABS and regenerative brake control

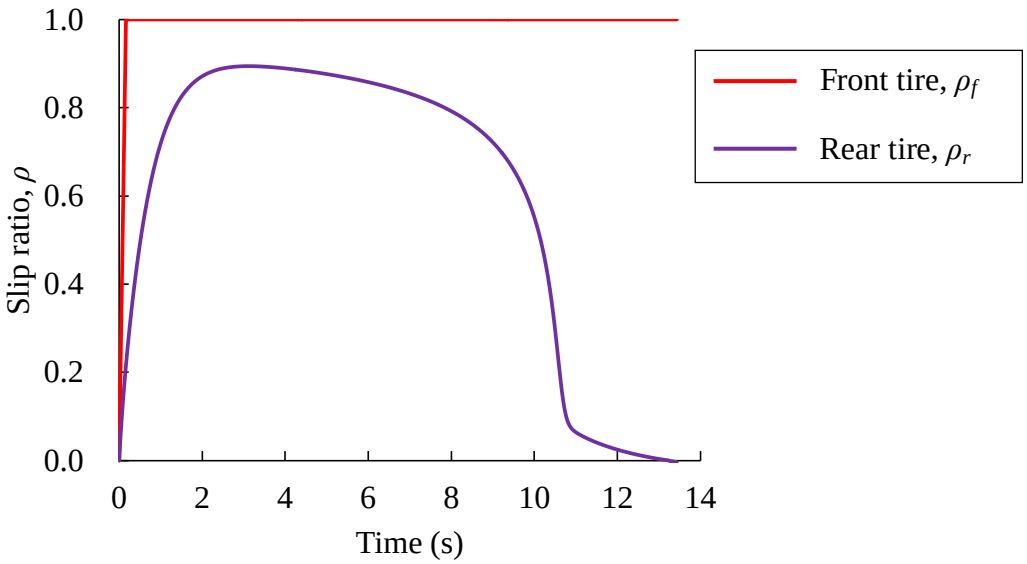

Figure 4-14 Change of slip ratio of the front and rear tires without ABS and regenerative brake control

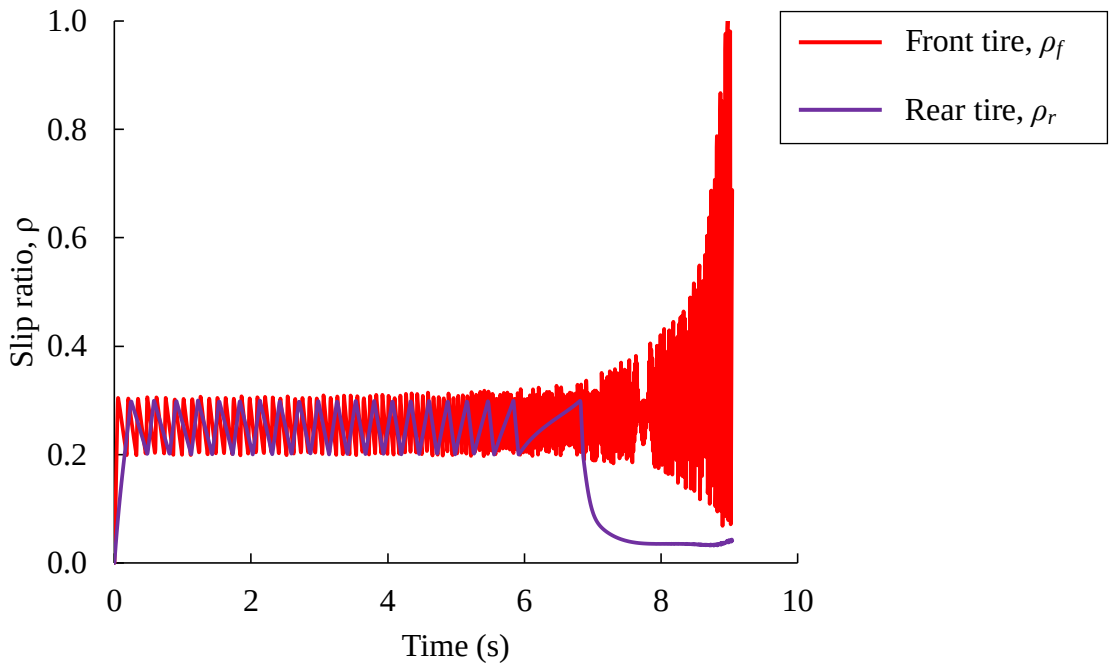

Figure 4-15 Change of slip ratio of the front and rear tires with ABS and regenerative brake control

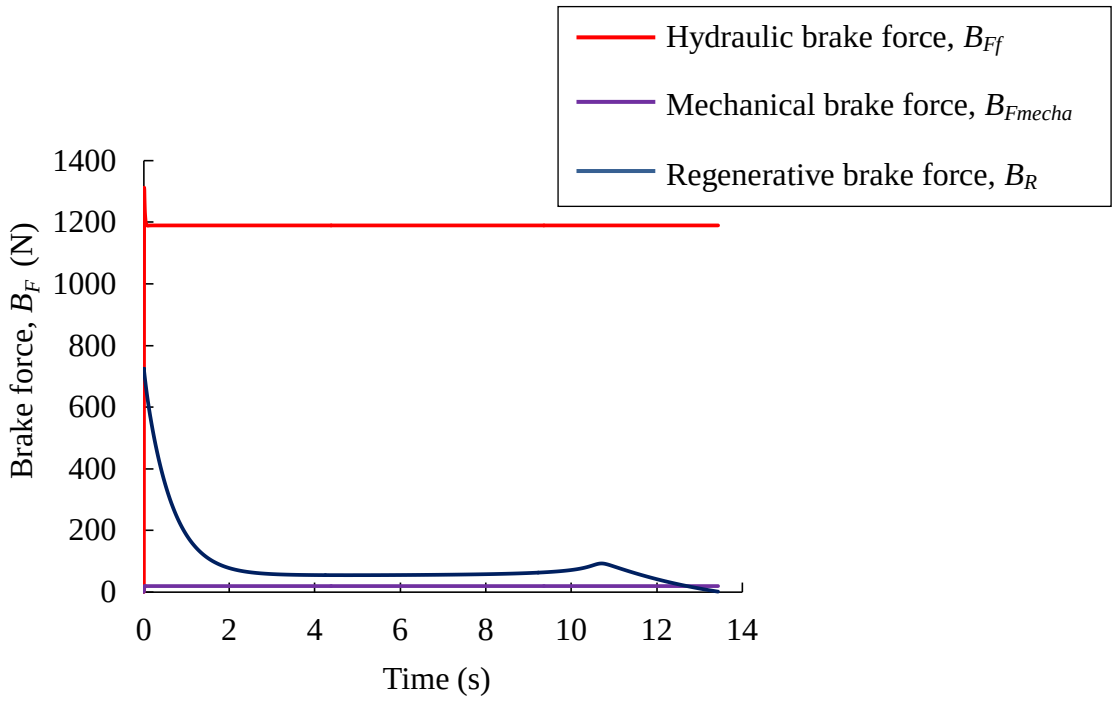

Figure 4-16 Change of braking force on the front and rear tires without ABS and regenerative brake control

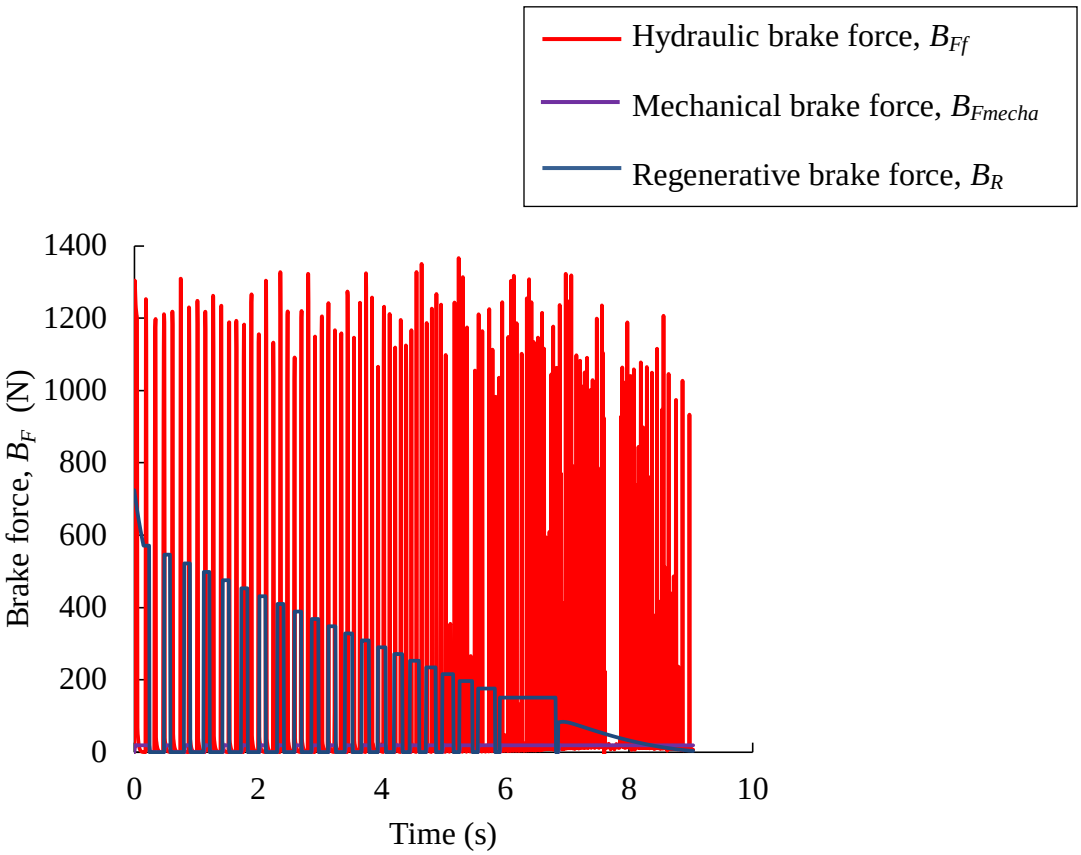

Figure 4-17 Change of braking force on the front and rear tires without ABS and regenerative brake control

4.6 Summary

In this chapter, the simulation model of hydraulic-mechanical hybrid brake system with ABS and regenerative brake control was developed. To determine the efficiency of the simulation model, the experiment to measure the optimum value of the regenerative brake coefficient has been done. The findings from the experiment and simulation results are as below:

1. From the experiment results, the optimum value of the regenerative brake coefficient is 20.
2. During braking on an icy road, the in-wheel motor can be an actuator of ABS to control the regenerative braking torque.
3. The combination of hydraulic-mechanical hybrid brake system with ABS and regenerative brake control can prevent tire locked during braking on an icy road.
4. During braking on an icy road and in the cornering condition, the combination of hydraulic-mechanical hybrid brake system with ABS and regenerative brake control can increase the steer performance of the vehicle.

Chapter 5

CONCLUSIONS

In this research, to increase the safety and stability of the small EVs with hydraulic-mechanical hybrid brake system, the combination model of hydraulic-mechanical hybrid brake system with ABS and regenerative brake control is proposed. The outcome of each chapter is described as below.

Chapter 1 Introduction

In recent years, small EVs have given public attention. Compared with the internal combustion engine vehicles (ICEVs), small EVs have great advantages on its propulsion system, which is in-wheel motor. Past research has proven that the advantages of in-wheel motor is a fast torque response, easiness in obtaining accurate torque feedback, capable of generating both traction and braking forces and small size but powerful output.

Although in-wheel motor has advantages to enhance motion control of small EVs, the safety system of the small EVs are not sufficient because it only contains seat belt as safety system. Due to the space limitation on the driving tire, an anti-lock brake system (ABS) which is a basic skid control method is difficult to install on the driving tire. For the same reason, some of the small EVs employ the mechanical brake system on the driving tire. Even though the mechanical brake system is compact, the rigidness and the response performance of the mechanical brake system is lower than hydraulic brake system.

Based on the disadvantages of the braking system of the small EVs, several methods of ABS and regenerative brake control have been reviewed. From the literature review, many methods have been proposed to improve the efficiency of ABS and regenerative brake. However, there is no research on the combination of ABS and regenerative brake control. On the other hand, there are few research on the electric motor to be an actuator of ABS.

Chapter 2 Braking Performance of the Hydraulic-Mechanical Hybrid Brake System

The experiment on small EVs from Toyota COMS model AK 10E-PC has been done to analysis the braking performance of the small EVs with hydraulic-mechanical hybrid brake system. In the experiment, two conditions of the braking system have been set, which are hydraulic-mechanical hybrid brake system without regenerative brake system, and hydraulic-

mechanical hybrid brake system with the regenerative brake system. The experimental results are concluded as below:

1. During braking on dry asphalt road, without regenerative brake operational, the hydraulic-mechanical hybrid brake system can stop the vehicle smoothly.
2. In case of hydraulic-mechanical hybrid brake system with regenerative brake operational, the stopping time is shorter than without regenerative brake operational.
3. The experiment results proved that the regenerative brake can improve the braking performance of the small EVs with hydraulic-mechanical hybrid brake system.

Chapter 3 Hydraulic-Mechanical Hybrid Brake System with ABS

To improve the braking performance of the small EVs, the simulation model of hydraulic-mechanical hybrid brake system with ABS has been developed. The hydraulic unit of ABS was installed at each front tire, and it is located between the master cylinder and the front wheel cylinder. For the rear tire, only one set hydraulic unit of ABS was installed for the both rear tires and it is located between the master cylinder and rear power cylinder. From the simulation results, several findings can be concluded as below:

1. During braking on an icy road, without ABS, the tire was locked and the vehicle was skidding.
2. The combination of hydraulic-mechanical hybrid brake system with ABS can prevent the front tire from locked.
3. Due to the rigidness of the mechanical brake system, the time delay was occurring during ABS operational. The rear tire was locked and the slip ratio is more than the optimum value.
4. The regenerative brake torque produce from the in-wheel motor is needed to control to prevent the rear tire from locked during braking on an icy road.

Chapter 4 Hydraulic-Mechanical Hybrid Brake System with ABS and Regenerative Brake Control

Due to the characteristics of in-wheel motor, which are fast torque response and easiness in obtaining an accurate torque feedback, the regenerative brake timing control has been

developed. The regenerative brake control is working together with the ABS during braking on an icy road. To determine the effectiveness of the simulation model, the experiment to measure the optimum value of the regenerative brake coefficient has been developed. The findings from the experimental results and simulation results are as below:

1. From the experiment, the optimum value of the regenerative brake coefficient is considered as 20.
2. During braking on an icy road, the combination of ABS and regenerative brake control can prevent the front and rear tires from locked and the vehicle from skidding.
3. The hydraulic-mechanical hybrid brake system with ABS and regenerative brake control can increase the steer performance of the vehicle during braking on an icy road and cornering.

REFERENCES

Chapter 1 Introduction

[1-1] S J Clegg : A review of Regenerative Braking Systems, Transaction of Institute for Transport Studies, University of Leeds, April 1996.

[1-2] Z.Ding, L.He and Z.Dong : Modeling and Testing of Low-Speed Electric Vehicle, Proceedings of the International Conference on Electric Information and Control Engineering (ICEICE), (2011), pp. 2355-2357

[1-3] M.I.Ishak, H.Koduki and H.Ogino: Research on anti-lock braking system of a 2 wheel small electric vehicle with hydraulic-mechanical hybrid brake system, Proceeding of the 2010 JSAE kanto International Conference of Automotive Technology for Young Engineers (ICATYE), 2010, CD-ROM.

[1-4] Z.Cai, C.Ma and Q.Zhao: Acceleration to Torque Ratio Based Anti-kid Control for Electric Vehicles, International Conference on Mechatronics and Embedded System and Appalications, 2010.

[1-5] K.Fuji and H.Fujimoto: Traction control based on slip ratio estimation without detecting vehicle speed for electric vehicle, Proceedings of the 2007 Power Conversion Conference, pp. 688-693, 2007.

[1-6] X.Wu, C.Ma, M.Xu, Q.Zhao and Z.Cai : Single-Parameter Skidding Detection and Control Specified for Electric Vehicles, Transactions of the Journal of the Franklin Istitute, (2014), pp.1-16

[1-7] Pill-Soo Kim : Cost Modelling of Battery Electric Vehicle and Hybrid Vehicle based on Major Parts Cost, Proceedings of The 5th International Conference on Power Electronics and Drive Systems (PAEDS), (2003), pp. 1295-1300

[1-8] K.Cakir and A.Sabanovic : In-wheel Motor Design for Electric Vehciles, Proceedings of the 2006 9th International Workshop on Advanced Motion Control (AMC 2006), (2006), pp. 613-618

[1-9] Y.Hori : Future Vehicle Driven by Electricity and Control – Research on Four-Wheel-Motored “UOT Electric March II” , IEEE Transactions on Industrial Electronics, Vol.51, No.5, (2004), pp 954-962

[1-10] S.Sakai, H.Sado and Y.Hori : Motion Control in an Electric Vehicle with Four Independently Driven In-Wheel Motors, IEEE/ASME Transactions on Mechatronics, Vol.4, No.1, (2009), pp. 9-16.

[1-11] H.Ogino, S.Kobayashi and S.Hasegawa: Research on Skid Control of Small Lectric Vehicle with Hydraulic-mechanical Hybrid Brake System (Effect of Regenerative Braking System in Skidding Condition), Transaction of The Japan Society of Mechanical Engineers Journal, Vol.77 No. 784, (2012), pp. 282-294. (in Japanese)

[1-12] S.Kobayashi and H.Ogino: Research on skid control of small electric vehicle with hydraulic-mechanical hybrid brake system (Simulation of 4 wheel brake model), Proceedings of the 2010 JSME Conference, Vol.5, pp.165-166, 2010. (in Japanese).

[1-13] S.Hasegawa and H.Ogino: Research on skid control of small electric vehicle with hydraulic-mechanical hybrid brake system (1st Report: Simulation of 2 wheel model of anti-lock braking system), Transaction of the School of Engineering, Tokai University Bulletin, Vol.49, No.2, pp. 89094, (2009). (in Japanese).

[1-14] M.K.Yoong, G.D.Gan, C.K.Leong, Z.Y.Phuan, B.K.Cheah and K.W.Chew : Studies of Regenerative Braking in Electric Vehicle, Proceedings of the 2010 IEEE Conference on Sustainable Utilization and Development in Engineering and Technology, (2010), pp. 40-45

[1-15] M.Ehsani, Y.Gao, S.E.Gay and A.Emadi : Modern Electric, Hybrid Electric and Fuel Cell Vehicles – Fundamentals, Theory and Design, CRC Press, Ltd., Boca Raton, Florida, (2003).

[1-16]M.A.Mollenjauer, T.A.Dingus, C.Carney, J.M.Hankey and S.Jahns : Anti-lock Brake Systems –An Assessment of Training on Driver Effectiveness, Transactions of the Accident Analysis and Prevention, Vol.29, No.1, (1997), pp. 97-108.

[1-17] N.Patra and K.Datta : Sliding Mode Controller for Wheel-Slip Control of Anti-lock Braking System, Proceedings of the 2012 IEEE International Conference on Advanced Communication Control and Computing Technologies (ICACCT), (2012), pp. 385-391

[1-18] J. Larminie and J. Lowry : Electric Vehicle Technology Explained, John Wiley and Sons, Ltd., (2003), pp. 23-29.

[1-19] E. Nakamura, M. Soga, A. Sakai, A. Otomo, and T. Kobayashi : Development of Electronically Controlled Brake System for Hybrid Vehicle, SAE Technical Paper, (2002), Paper 2002-01-0300.

[1-20] A.Lorico, J.Taiber and T.Yanni : Effect of Inductive Power Technology Systems on Battery-Electri Vehicle Design, Proceedings of The 37th Annual Conference on IEEE Industrial Electronic Society (IECON), (2011), pp. 4563-4569

[1-21] Mark S. Duvall : Battery Evaluation for Plug-In Hybrid Electric Vehicles, Proceedings of The 2005 IEEE Conference on Vehicle Power and Propulsion (VPCC), (2005), pp. 338-343

[1-22] K.M. Rahman, S. Jurkovic, S.Hawkins, S.Tarnowsky and P.Savagian : Propulsion System Design of a Battery Electric Vehicle, Transaction of the IEEE Electrification Magazine, Vol.2, No.2, (2014), pp. 14-24

[1-23] J.V.Byrne, and J.G.Lacy : Compatible Controller-Motor System for Battery-Electric Vehicle, Proceedings of The Institution of Electrical Engineers, Vol.117, No.2, pp. 369-376

[1-24] J.Weng, J.Li,G.Xiao and S.Biller : Virtual Battery: A battery Simulation Framework or Electric Vehicles, IEEE Transactions on Automated Science and Engineering, Vol.10, No.1, (2013), pp. 5-15

[1-25] A.Kuperman, U.Levy, J.Goren, A.Zafransky an A.Savernin : Battery Charger for Electric Vehicle Traction Battery Switch Station, IEEE Transactions on Industrial Electronics, Vol. 60, No.12, (2013), pp. 5391-399

[1-26] S.Greaves, H.Backman and A.B.Ellison : An empirical Assessment of the Feasibility of Batery Electric Vehicles for Day-to-Day Driving, Transactions of the Transportation Research Part A: Policy and Practice, Vol.66, (2014), pp. 226-237

[1-27] L.Ahmad, A.Yip, M.Fowler, S.B.Young and R.A.Fraser : Environmental Feasibility of re-use of Electric Vehicle Bateries, Transactions of the Sustainable Energy Technologies and Assessment, Vol.6, (2014), pp. 64-74

[1-28] J.Speirs, M.Contestabile, Y.Houari and R.Gross : The Future of Lithium Availability for Electric Vehicle Batteries, Transactions of The Renewable and Sustainable Energy Reviews, Vol.35, (2014), pp. 183-193

[1-29] K.Nam, H.Fujimoto and Y.Hori : Advanced Motion Control of Electric Vehicles Based on Robust Lateral Tire Force Control via Active Front Steering, IEEE/ASME Transactions on Mechatronics, Vol.19, No.1, (2014), pp. 289-299

[1-30] Y.Hori : Future Vehicle Driven by Electricity and Control –Research on Four Wheel Motored "UOT Electric March II-, Proceedings of The 7th International Workshop on Advanced Motion Control (AMC), (2002), pp. 1-14

[1-31] L.Feiqiang, W.Jun and L.Zhaodu : Fuzzy-logic-based Controller Design for Four-wheel-drive Electric Vehicle Yaw Stability Enhancement, Proceedings of the 2009 6th International Conference on Fuzzy Systems and Knowledge Discovery (FSKD), (2009), pp. 116-120

[1-32] K.Nam, H.Fujimoto and Y.Hori : Motion Control of Electric Vehicles Based on Robust Lateral Tire Force Control Using Lateral Tire Force Sensors, Proceedings of The 2012 IEEE/ASME International Conference on Advanced Intelligent Mchatronics, (2012), pp. 526-531

[1-33] Z.Shuai, H.Zhang, J.Wang, J.Liu and M,Quyang : Lateral Motion for Four-wheel-independent-drive electric vehicles using optimal torque allocation and Dynamic Message Priority Scheduling, Transactions of The Control Engineering Practice, Vol.24, (2014), pp. 55-66

[1-34] J.Hu, D.Yin and Y.Hori : Fault-tolerant Traction Control of Electric Vehicles, Transactions of the Control Engineering Practice, Vol.19, (2011), pp. 204-213

[1-35] Z.Guirong, L.Houyu and H.Fei : Propulsion Control of Fuel Cell Electric Vehicle, Proceedings of the 2011 3rd International Conference on Environmental Cience and Information Application Technology (ESIAT 201), (2011), pp. 439-443

[1-36] S.Caglar Baslamisli, I.E.Koe and G.Alas : Robust Control of Anti-lock Brake System, Transactions of the Vehicle System Dynamics, Vol.45, No.3, (2007), pp. 217-232.

[1-37] J.S.Lin and W.E.Ting : Nonlinear Control Design of Anti-lock Braking Systems with Assistance of Active Suspension, Proceedings of the Fourth International Conference on Fuzzy Systems and Knowledge Discovery, (2007), pp. 343-348

[1-38] M.Corno, M.Gerard, M.Verhaegen and E.Holweg : Hybrid ABS Control using Force Measurement, IEEE Transactions on Control Systems Technology, Vol.20, No.5, (2012), pp. 1223-1235

[1-39] C.Y.Lu and M.C.Shih : Application of the Pacejka Magic Formula Tyre Model on a Study of a Hydraulic Anti-Lock Braking System for a Light Motorcycle, Transactions of the Vehicle System dynamics, Vol.41, No.6, (2004), pp. 431-448.

[1-40] M.Tanelli, G.Osorio, M.Bernardo, S.M.Savaresi and A.Astolfi : Existence, Stability and Robustness Analysis of Limit Cycles in Hybrid Anti-lock Braking Systems, Transactions of the International Journal on Vehicle Control, Vol.82, No.4, (2009), pp. 659-678.

[1-41] H.Mirzaeinejad and M.Mirzaei : A Novel Method for Non-linear Control of Wheel Slip in Anti-lock Braking Systems, Transactions of the Control Engineering Practice, Vol.18, (2010), pp. 918-926.

[1-42] C.Xu, K.W.E.Cheng,L.Sha,W.Ting and K.Ding : Simulation of the Integrated Controller of the Anti-lock Braking System, Proceedings of the 2009 3rd International Conference on Power Electronics Systems and Applications, (2009), pp. 1-3

[1-43] W.Weidong and Y.Yongsan : Road Identification for Anti-Lock Brake Systems Equipped with Only Wheel Speed Sensors, Transaction of Tsinghua Science and Technology, Vol.6. No.4, (2001), pp. 383-385

[1-44] E.Dincmen, B.A.Guvenc and T.Acarman : Extremum-Seeking Control of ABS Braking in Road Vehicles with Lateral Force Improvement, IEEE Transactions on Control Systems Technology, Vol.22, No.1, (2014), pp. 230-237

[1-45] R.Bhandari, S.Patil and R.K.Singh : Surface Prediction ad Control Algorithm for Anti-lock Brake System, Transactions of the Transportation Research Part C, Vol.21, (2012), pp. 181-195.

[1-46] A.Petersen, R.Barrett and S.Morrison : Driver-training and Emergency Brake Perfromance in Cars with Antilock Braking Systems, Transactions of the Safety Science, Vol.44, No.10, (2006), pp. 905-917.

[1-47] J.Broughton and C.Baughan : The Effectiveness of Antilock Braking Systems in Reducing Accidents in Great Britain, Transactions of the Accident Analysis and Prevention, Vol.34, (2002), pp. 347-355.

[1-48] Y.Tang, X.Zhang, D.Zhang, G.Zhao and X.Guan : Fractional Order Sliding Mode Controller Design for Antilock Braking Systems, Transactions of the Neurocomputing, Vol.111, (2013), pp.122-130.

[1-49] M.Turki, S.Bouzaida, A.Sakly and F.M.Sahli : Adaptive Control of Nonlinear System Using Neuro-Fuzzy Learning by PSO Algorithm, Proceedings of the 2012 IEEE Mediterranean Electrotechnical Conference (MELECON), (2012), pp. 519-523.

[1-50] A.M.El-Garhy, G.A.El-Sheikh and M.H.El-Saify Fuzzy Life-Extending Control of Anti-Lock Braking System, Transaction of Ain Shams Engineering Journal,Vol.4, (2013), pp. 735-751.

[1-51] H.Chaoui and P.Sicard : Adaptive Fuzzy Logic Control of Permanent Magnet Synchronous Machines with Nonlinear Friction, IEEE Transactions on Industrial Electronics, Vol.59, No.2, (2012), pp. 1123-1133.

[1-52] N.Raesian, N.Khajehpour and M.Yaghoobi : A New Approach in Anti-lock Braking System (ABS) Based on Adaptive Neuro-Fuzzy Self-turning PID Controller, Proceedings of the 2011 2nd International Conference on Control, Instremnt and Automation (ICCIA), (2011), pp. 530-535

[1-53] P.Naderi, A.Farhadi, M.Mirsalim and T.Mohammadi : Anti-Lock and Anti-Slip Braking System, Using Fuzzy Logic and Sliding Mode Controllers, Proceedings of the 2010 IEEE Vehicle Power and Propulsion Conference (VPCC), (2010), pp. 1-6

[1-54] W.Wang, M.Chen, Y.Chien and T.Lee : Control of Uncertain Active Suspension System with Anti-lock Braking System using Fuzzy Neural Controller, Proceedings of the 2009 IEEE International Conference on System, and Cybernetics, (2009), pp. 3371-3376

[1-55] W.Wang, K.Hsu, T.Lee and G.Chen : Robust Sliding Mode-Like Fuzzy Logic Control for Anti-lock Braking Systems with Uncertainties and Disturbances, Proceedings of the Second International Conference on Machine Learning and Cybernetics, (2003), pp. 633-638.

[1-56] A.Harifi, A.Aghagolzadeh, G.Alizadeh and M.Sadeghi : Designing a Sliding Mode Controller for Slip Control of Antilock Brake Systems, Transactions of the Transportation Research Part C Emerging Technologies, Vol.16, No.6, (2008), pp. 731-741.

[1-57] Z.Junzhi, L.Yutong, L.Chen an Y.Ye : New Regenerative Braking Control Strategy for Rear-Driven Electrified Minivans, Transactions of the Energy Conversion and Management, Vol.82, (2014), pp. 135-145.

[1-58] D.B.Antanaitis : Effect of Regenerative Braking on Foundation Brake Performance, Transaction of the SAE International Journal of Passenger Cars –Mechanical Systems, Vol.3, No.2, (2010), pp. 14-30.

[1-59] M.A.Hannan, F.A.Azidin and A.Mohamed : Multi-Sources Model and Control of an Energy Management System for Light Electric Vehicles, Transactions of the Energy Conversion and Management, Vol.62, (2012), pp.123-130.

[1-60] Y.Gao, L.Chen and M.Ehsani : Investigation of the Effectiveness of Regenerative Braking for EV and HEV, SAE Technical Paper 1990-01-2910, (1999).

[1-61] X.Huang and J.Wang : Model Predictive Regenerative Braking Control for Lightweight Vehicles with In-wheel Motors, Proceedings of the Institute of Mechanical Engineering, Part D: Journal Automobile Engineering, Vol.226, No.9, (2012), pp. 1220-1232.

[1-62] A.Walker, M.Laperth and S.Wilkins : On Friction Braking Demand with Regenerative Braking, SAE Technical Paper, Paper 2002-01-2581, (2002).

[1-63] H.Yeo, S.Hwang and H.Kim : Regenerative Braking Algorithm for a Hybrid Electric Vehicle with CVT Ratio Control, Proceedings of the Institute Mechanical Engineering, Part D: Journal Automobile Engineering, Vol.226, No.4, (2012), pp. 494-506.

[1-64] W.J.B.Midgley, H.Cathcart and D.Cebon : Modelling of Hydraulic Regenerative Braking Systems for Heavy Vehicles, Proceedings of the Institute of Mechanical Engineering, Part D: Journal Automobile Engineering, (2013), pp. 1-13.

[1-65] P.Cocron, F.Buhler, T.Franke, I.Neumann, B.Dielmann and J.F.Krems : Energy Recapture through Deceleration –Regenerative Braking in Electric Vehicles from a User Perspective, Transactions of the Ergonomics Journal, Vol.56, No.8, (2013), pp. 1203-1215.

[1-66] B.Wang, X.Huang, J.Wang, X.Guo and X.Zhu : A Robust Wheel Slip Ratio Control Design Combining Hydraulic and Regenerative Braking System for In-wheel-motors-driven Electric Vehicles, Transactions of the Journal of the Franklin Institute, (2014), pp. 1-26.

[1-67] S.A.Oleksowicz, K.J.Burnham, A.Southgate, C.McCoy, G.Waite, G.Hardwick, C.Harrington and R.McMurran : Regenerative Braking Strategies, Vehicle Safety and Stability Control Systems –Critical Use-Case Proposals, Transactions of the International Journal of Mechanics and Mobility, Vol.51, No.5, (2013), pp. 684-699.

[1-68] Drakunov, S., U.Ozguner, P.Dix, and B. Ashra (1995) : ABS Control using Optimum Search Via Sliding Modes, IEEE Transactions Control Systems Technology, Vol 3, No.1, pp. 79-85.

[1-69] Kawabe, T., M. Nakazawa, I. Notsu, and Y. Watanabe : A Sliding Mode Controller for Wheel Slip Ratio Control System, Vehicle System Dynamic, (1997), pp. 393-408.

[1-70] Choi, S. and D.W. Cho : Control of Wheel Slip Ratio using Sliding Mode Controller with Pulse Width Modulation, Proceedings of the 4th International Symposium on Advanced vehicle Control, (1998), pp. 629-635.

[1-71] Freeman, R. : Robust Slip Control for a Single Wheel, Research report CCeC 95-403 (1995), University of California.

[1-72] Yu, J.S. : A Robust Adaptive Wheel-slip Controller for Antilock Brake System, Proceedings of the 36th IEEE Conference on Decision and Control, Vol.3, pp. 2545-2546.

[1-73] Sontag, E.D. : Mathematical Control Theory, Springer-Verlag (1998).

[1-74] Liu, Y. and J. Sun : Target Slip Tracking using Gain-scheduling for Braking Systems, Proceedings of the American Control Conference (1996), pp. 1178-1182.

[1-75] Tsiotras, P. and C. Canudas de Wit : On the Optimal Braking of Wheeleed Vehicles, Proceedings of the American Control Conference (2000), Vol.1, pp. 569-573.

[1-76] Wellstead, P.E. and N. Pettit : Analysis and Redesign of Antilock Brake System Controller, IEE proceedings of Control Theory Apalication, Vol. 144 (1997), pp. 413-426.

[1-77] Taheri, S. and E. Law : Slip Control Braking of an Automobile During Braking and Steering Maneuvers, Transactions of the Avanced Automotive Technologies, Vol. 40 (1991), pp. 209-227.

[1-78] CIKANEK S.R., BAILEY K.E.: 'Regenerative braking system for a hybrid electric vehicle'. Proceedings of the ACC'2002, Anchorage, USA, 8– 10 May 2002, pp. 3129– 3134

[1-79] MI C., LIN H., ZHANG Y.: 'Iterative learning control of antilock braking of electric and hybrid vehicles', IEEE Transactions on Vehicular Technol., 2005, 54, (2), pp. 486– 494

[1-80] PATERSON J., RAMSAY M.: 'Electric vehicle braking by fuzzy logic control'. Proceedings of the IEEE IASAM'93, Orlando, USA, 1993, pp. 2200– 2204.

[1-81] GAO H.W., GAO Y.M., EHSANI M.: 'A neural network based SRM drive control strategy for regenerative braking in EV and HEV'. Proceedings of the IEEE IEMDC'2001, Cambridge, USA, 2001, pp. 571–575.

[1-82] YEO H., KIM H.: 'Hardware in the loop simulation of regenerative braking for a hybrid electric vehicle', Proceedings of the Inst. Mechanical Engineering, Volume D, Journal of Automobile Engineering, 2002, 216, (11), pp. 855–864.

[1-83] WU H.X., CHENG S.K., CUI S.M.: 'A controller of burshless DC motor for electric vehicle', IEEE Trans. Magn., 2005, 41, (1), pp. 509– 513.

[1-84] LEE J., NELSON D.J.: 'Rotating inertia impact on propulsion and regenerative braking for electric motor driven vehicles'. Proceedings of the IEEE VPPC'2005, Chicago, USA, 2005, pp. 308– 314.

Chapter 2 Braking Performance of the Hydraulic-Mechanical Hybrid Brake System

[2-1] M.H. Peeie, H.Ogino and Y.Oshinoya : Skid Control of Small Electric Vehicle with Hydraulic-Mechanical Hybrid Brake System, Proceedings of the MJIIT-JUC Joint International Symposium 2013, (2013), pp. 1-4.

[2-2] M.Abe : Vehicle Handling Dynamics, (2009), pp. 30-37.

[2-3] R. Rajamani : Vehicle Dynamics and Control, Mechanical Engineering Series, (2012) pp. 93- 95.

[2-4] Toyota Auto Body Company Handbooks.

[2-5] H.Ogino, S.Kobayashi and S.Hasegawa : Research on Skid Control f Small Electric Vehicle (Effect of Regenerative Braking System in Skidding Condition), Transactions of the Japan Society of Mechanical Engineers, Vol.77, No.78, (2011), pp. 282-295. (in Japanese)

[2-6] S.Kobayashi and H.Ogino : Research on Skid Control of Small Electric Vehicle with Hydraulic-Mechanical Hybrid Brake System (Simulation of 4 Wheel Model), Proceedings of the 2010 Annual Congress of the Japan Society of Mechanical Engineers, (2010), CD-ROM. (in Japanese).

[2-7] S.Hasegawa and H.Ogino : Research on Skid Control of Small Electric Vehicle with Hydraulic-Mechanical Hybrid Brake System (3rd Report: Effect of the ABS on the Disturbance), Proceedings of the 2010 Annual Congress of the Japan Society of Mechanical Engineers, (2010), CD-ROM. (in Japanese)

[2-8] M.I.Ishak, H.Koduki and H.Ogino: Research on anti-lock braking system of a 2 wheel small electric vehicle with hydraulic-mechanical hybrid brake system, Proceeding of the 2010 JSAE Kanto International Conference of Automotive Technology for Young Engineers (ICATYE), 2010, CD-ROM.

[2-9] M.I.Ishak, H.Ogino and Y.Oshinoya: Research on Motion Control of 4 Wheel Steering Vehicles (Effect of Regenerative Brake on Vehicle's Motion), Proceedings of the School of Engineering, Tokai University, Vol.53, No.2, (2013), pp. 99-103. (in Japanese)

Chapter 3 Hydraulic-Mechanical Hybrid Brake System with ABS

[3-1] E.F.Kececi and G.Tao : Adaptive Vehicle Skid Control, Transactions of the Mechatronics, Vol. 16, (2006), pp. 291-301.

[3-2] S.Kobayashi and H.Ogino : Research on Skid Control of Small Electric Vehicle with Hydraulic-mechanical Hybrid Brake System (Simulation of 4 Wheel Brake Model, Proceedings of the 2010 JSME Annual Congress, (2010), pp. 165-166. (in Japanese)

[3-3] H.Leiber and A.Czinezel : Antiskid System for Passenger Cars with a Digital Electronics Control Unit, Society of Automotive Engineers, (1979), paper 790458.

[3-4] H.Ogino, M.I.Ishak and Y.Oshinoya : Stability Analysis of Small Electric Vehicle – Effect of Hystresis of Friction Brake Force for Regeenrativ Braking Force, Proceedings of the School of Engineering, Tokai University, Vol. 52, No.1, (2012), pp. 55-64. (in Japanese)

[3-5] H.Lin and Y.Zhang : Iterative Learning Control of Antilock Braking of Electric and Hybrid Vehicles, Proceedings of the IEEE Transactions on Vehicular Technology, (2005), pp. 486-487.

[3-6] T.Suzuki and H.Fujimoto : Slip Ratio Estimation and Regenerative Brake Control without Detection of Vehicle Velocity and Acceleration for Electric Vehicle at Urgent Brake Turning, Proceedings of the 11th IEEE International Workshop on Advanced Motion Control, (2010), pp.273.

[3-7] Y.Hori : Future Vehicle Driven by Electricity and Control (Research on Four Wheel Motored “UOT Electric March II), Proceedings of the 7th International Workshop on Advanced Motion Control, (2002), pp. 27.

Chapter 4 Hydraulic-Mechanical Hybrid Brake System with ABS and Regenerative Brake Control

[4-1] M.Abe : Vehicle Handling Dynamics (Theory and Aplication), (2009), pp. 30-37.

[4-2] Z.Cai, Z.Ma and Q.Zhao : Acceleration to Torque Ratio Based Anti-Skid for Electric Vehicle, Proceedings of the 2010 IEEE International Conference on Mechatronics and Embedded Systems and Applications, (2010), pp. 577-581.

[4-3] M.Ehsani, Y.Gao and S.Gay : Characterization of Electric Motor Drives for Traction Applications, Proceedings of the Industrial Electronics Society, (2003), pp. 891-896.

[4-4] K.Fujii and H.Fujimoto : Traction Control Based on Slip Ratio Estimation without Detecting Vehicle Speed for Electric Vehicle, Proceedings of the 2007 Power Conversion Conference, (2007), pp. 688-693.

[4-5] A.Harifi, A.Aghagolzadeh, G.Alizadeh and M.Sadeghi : Designing a Sliding Mode Controller for Slip Ratio of Antilock Brake Systems, Transactions of the 2008 Transportation Research Part C, Vol. 16, (2008), pp. 731-741.

[4-6] J.Hellgren and E.Jonasson : Maximization of Brake Energy Regeneration in a Hybrid Electric Paraller Car, Transactions of the International Journal of Electric and Hybrid Vehicle, Vol. 1, No.1, (2007), pp. 95-121.

[4-7] M.I.Ishak, H.Ogino and Y.Oshinoya : Research on Motion of 4 Wheel Steering Vehicles (Effect of Regeneratve Brake on Vehicle's Motion, Proceedings of the School of Engineering, Tokai University, Vol. 53, No.2,(2013), pp. 99-103.

[4-8] S.Kodama, L.Li and Y.Hori : Skid prevention for EVs based on the emulation of torque characteristics of separately-wound DC motor, Proceedings of the 8th IEEE International Workshop on Advanced Motion Control (2004), pp.75-80.

[4-9] Ogino, H., Kobayashi, S. and Hasegawa, S., Research on skid control of small electric vehicle (Effect of the regenerative braking system in skidding condition), Transactions of the Japan Society of Mechanical Engineers, Series C, Vol.77, No.784 (2011), pp.282-295.

[4-10] M.H.Peeie, H.Ogino, and Y. Oshinoya : Skid control of small electric vehicle with hybrid brake system (Effect of the PID control), Proceedings of the 21st Transportation and Logistics Conference 2012 (2012), pp.145-148.

[4-11] D.Peng, Y.Zhang, C.L.Yin and Zhang : Combined control of a regenerative braking and antilock braking system for hybrid electric vehicles, Transactions of the International Journal of Automotive Technology, Vol.9, No.6 (2008), pp.749-757.